AD-A115 445 GOULDING (MERRILL K) AND ASSOCIATES GLENDALE CA F/G 1/5
STUDY OF THE DE-ICING PROPERTIES OF THE ASDE-3 ROTODOME.(U)
APR 82 M K GOULDING DOT-TS-15950

UNCLASSIFIED DOT-FAA/RD-81-112 NL

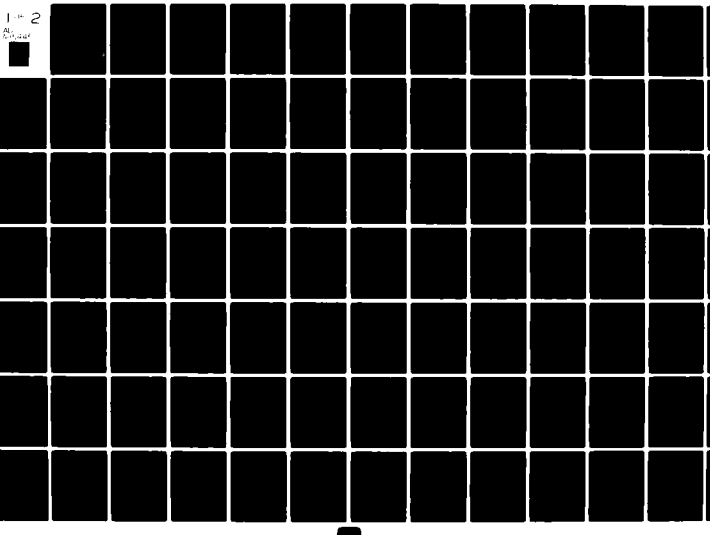

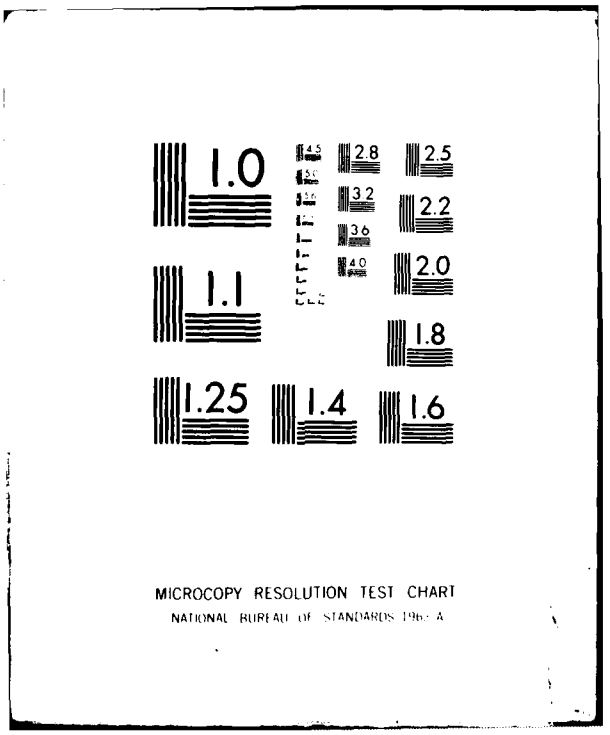
1.0
1.1
1.25
1.4
1.6
1.8
2.0
2.2
2.5
2.8
3.2
3.6
4.0
4.5
MICROCOPY RESOLUTION TEST CHART
NATIONAL BUREAU OF STANDARDS 1963-A

DOT-FAA-RD-81-112
DOT-TSC-FAA-81-24

Systems Research and
Development Service
Washington DC 20590

Study of the De-icing Properties of the ASDE-3 Rotodome

Merrill K. Goulding

Merrill K. Goulding and Associates
Consulting Engineers
Glendale CA 90033

April 1982
Final Report

U.S. Department of Transportation
Federal Aviation Administration

NOTICE

This document is disseminated under the sponsorship of the Department of Transportation in the interest of information exchange. The United States Government assumes no liability for its contents or use thereof.

NOTICE

The United States Government does not endorse products or manufacturers. Trade or manufacturers' names appear herein solely because they are considered essential to the object of this report.

Technical Report Documentation Page

1. Report No.	2. Government Accession No.	3. Recipient's Catalog No.
DOT-FAA-RD-81-112	AD-A115 445	

4. Title and Subtitle	5. Report Date
STUDY OF THE DE-ICING PROPERTIES OF THE ASDE-3 ROTODOME	April 1982
	6. Performing Organization Code: DTS-541
7. Author(s): Merrill K. Goulding	8. Performing Organization Report No.: DOT-TSC-FAA-81-24
9. Performing Organization Name and Address: Merrill K. Goulding & Associates* Consulting Engineers Glendale CA 90033	10. Work Unit No. (TRAIS): FA 121/R1135
	11. Contract or Grant No.: TS-15950
12. Sponsoring Agency Name and Address: U.S. Department of Transportation Federal Aviation Administration Systems Research & Development Service Washington DC 20590	13. Type of Report and Period Covered: FINAL REPORT Sept 1978-Sept 1980
	14. Sponsoring Agency Code: ARD-100

15. Supplementary Notes

*Under Contract To U.S. DEPARTMENT OF TRANSPORTATION
Research and Special Programs Administration
Transportation Systems Center
Cambridge MA 02142

16. Abstract

A study was conducted of the thermal characteristics of the ASDE-3 system's rotating radome (rotodome), a spheri-toroidal thin wall structure, approximately 18 feet in diameter and 6 feet in height. The purpose of the study was to determine the thermal transmissivities of the various regions of the design, discover "hot spots," determine the need for insulation, heater exhaust deflectors and other enhancements, and to make a prediction of the ability of its heaters to prevent system outages due to ice accretion on the rotodome.

An analysis made using test data to predict the ability of the rotodome to resist icing conditions was very encouraging, demonstrating that convection becomes the dominant mode of heat loss during high wind conditions. A conservative analysis was made with winds applied at full velocity across all regions of the rotodome. The results indicate that the goal of de-icing the rotodome appears achievable using 30 kW of power. Although there are hot spots about the rotodome, the de-icing function using the hot air blower system is satisfactory. To reduce hot spots near the blower assembly, a deflector is recommended at the output of the blower.

17. Key Words	18. Distribution Statement
Airport Surface Detection Equipment, ASDE, Rotodome, Thermal Analysis	DOCUMENT IS AVAILABLE TO THE PUBLIC THROUGH THE NATIONAL TECHNICAL INFORMATION SERVICE, SPRINGFIELD, VIRGINIA 22161

19. Security Classif. (of this report)	20. Security Classif. (of this page)	21. No. of Pages	22. Price
Unclassified	Unclassified	132	

Form DOT F 1700.7 (8-72) Reproduction of completed page authorized

PREFACE

This report covers work done under contract to the U.S. Department of Transportation, Transportation Systems Center. In the course of its final preparation, Mr. Philip J. Bloom of the TSC was the Technical Editor.

METRIC CONVERSION FACTORS

Approximate Conversions to Metric Measures

Symbol	When You Know	Multiply by	To Find	Symbol
		LENGTH		
in	inches	2.5	centimeters	cm
ft	feet	30	centimeters	cm
yd	yards	0.9	meters	m
mi	miles	1.6	kilometers	km
		AREA		
in^2	square inches	6.5	square centimeters	cm^2
ft^2	square feet	0.09	square meters	m^2
yd^2	square yards	0.8	square meters	m^2
mi^2	square miles	2.6	square kilometers	km^2
	acres	0.4	hectares	ha
		MASS (weight)		
oz	ounces	28	grams	g
lb	pounds	0.45	kilograms	kg
	short tons (2000 lb)	0.9	tonnes	t
		VOLUME		
tsp	teaspoons	5	milliliters	ml
Tbsp	tablespoons	15	milliliters	ml
fl oz	fluid ounces	30	milliliters	ml
c	cups	0.24	liters	l
pt	pints	0.47	liters	l
qt	quarts	0.95	liters	l
gal	gallons	3.8	liters	l
ft^3	cubic feet	0.03	cubic meters	m^3
yd^3	cubic yards	0.76	cubic meters	m^3
		TEMPERATURE (exact)		
°F	Fahrenheit temperature	5/9 (after subtracting 32)	Celsius temperature	°C

Approximate Conversions from Metric Measures

Symbol	When You Know	Multiply by	To Find	Symbol
		LENGTH		
mm	millimeters	0.04	inches	in
cm	centimeters	0.4	inches	in
m	meters	3.3	feet	ft
m	meters	1.1	yards	yd
km	kilometers	0.6	miles	mi
		AREA		
cm^2	square centimeters	0.16	square inches	in^2
m^2	square meters	1.2	square yards	yd^2
km^2	square kilometers	0.4	square miles	mi^2
ha	hectares (10,000 m^2)	2.5	acres	
		MASS (weight)		
g	grams	0.035	ounces	oz
kg	kilograms	2.2	pounds	lb
t	tonnes (1000 kg)	1.1	short tons	
		VOLUME		
ml	milliliters	0.03	fluid ounces	fl oz
l	liters	2.1	pints	pt
l	liters	1.06	quarts	qt
l	liters	0.26	gallons	gal
m^3	cubic meters	35	cubic feet	ft^3
m^3	cubic meters	1.3	cubic yards	yd^3
		TEMPERATURE (exact)		
°C	Celsius temperature	9/5 (then add 32)	Fahrenheit temperature	°F

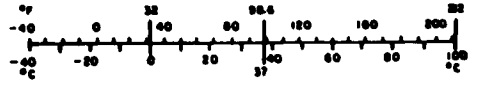

TABLE OF CONTENTS

TABLE OF CONTENTS (CONTINUED)

TABLE OF CONTENTS (CONTINUED)

LIST OF ILLUSTRATIONS

EXECUTIVE SUMMARY

A study was conducted of the thermal characteristics of the ASDE-3 system's rotating radome (rotodome). The purpose of the study was to determine the thermal transmissivities of the various regions of the design, discover "hot spots," determine the need for insulation, heater exhaust deflectors and other enhancements and finally make a prediction of the ability of its heaters to prevent system outages due to ice accretion on the rotodome.

First, a review of the literature on icing was made to determine under what meterological conditions ice accretion was possible. It was learned that temperatures between 1.4° and 30.5°F were the most probable in combination with winds less than 37 MPH. The third and fourth gating parameters were water droplet sizes less than 52 microns in diameter and liquid water content of the air of less than 0.89 grams per cubic meter.

Tests were then conducted in San Diego, California on a clear windless night in September, 1979 to corroborate theoretical predictions of conductive, convective and radiative heat losses from the rotodome. The results of those tests were very close to the values theoretically predicted in an earlier analysis conducted during the design phase of the ASDE-3 development program. It was found that in the absence of winds the heat lost via convection was one-half the amount via radiation. With a 50-percent duty cycle the interior-to-exterior temperature differentials were found to be 54°F. Therefore, with full heater power applied continuously, the maximum interior temperature would be less than 105°F for the lowest icing temperature of 1°F. Published values for the conductances of the various materials for the rotodome construction were compared with the test values, and differences on the order of 6 percent were found.

An analysis was then made using the test data to predict the ability of the rotodome to resist icing conditions. The analysis was very encouraging, demonstrating that convection becomes the

dominant mode of heat loss during high wind conditions. A conservative analysis was made with winds applied across all regions of the rotodome, including the floor. The results were negative. Actually, the floor of the rotodome is in a stagnation region created by the pedestal; consequently, if the floor is ignored the rotodome would be adequate as designed. If the stagnation region below the pedestal was considered, the design would be marginal and insulation on the floor would be in order. "Hot spots" were also discovered in the design. It can be demonstrated that savings on heating bills of from 9 percent to 26 percent could be achieved if a 0.060" thick insulating cover weighing approximately 10 pounds were employed on the floor of the rotodome where icing is not a problem. During an average of 46 icing alerts lasting an average of 15 hours at airports, this could amount to as much as $1,635 per airport with icing climatology in 15 years, based on average wind speeds of 15 MPH and constant energy costs of $0.057 per kW-hour.

A recommendation is made for future study of the climatology of various sites to determine which rotodomes will require heaters and which could get by on only 1 or 2 heater elements (10 and 20 KVA) per heater blower. This could be accomplished by computerizing the 20-some parameters ranging from air viscosity to height above ground for the installation to get a readily solvable equation for each individual situation.

SUMMARY AND CONCLUSION

Trying to predict the de-icing capability of the rotodome is not an easy task considering the many variables involved, not the least of which are:

1. The heaters are distributing heat unevenly about the rotodome.
2. There are consequently "hot spots" about the rotodome which make averaging readings difficult.
3. There are dead zones, i.e., like in the roof where the "boiling action" of the internal turbulence is less and consequently heat transfer in those regions is less.
4. There is a "lossy" area just below each heater which has been ignored.

The analysis, however, demonstrates that it is possible to prevent ice accretion on the rotodome if the floor is insulated. If it is not, there will be situations where the convective heat loss alone would be greater than 30 kW. The analysis was done for a 10-year, worst-case icing wind, but with larger than realistic cases of extreme temperature, water droplet size and liquid water content in the incident air stream. If nothing is done to the existing design, it will probably prevent outages in more that 99 percent of the icing conditions it is exposed to. Because of conservatism in the analysis, the worst case analyzed will undoubtedly never exist at altitudes less than 5,280 feet, and the design should be adequate for the continental United States.

The goal of de-icing the rotodome appears achievable using 30 kW of power and no insulation on the roof or window of the rotodome. However, consideration should be given to insulation of the botton (floor). From the wind tunnel "tufting" tests it appears that there is a counter flow in the stagnation area of the

flow, in the vicinity of the floor. Since the water content of the incident air stream has considerable kinetic energy, it is most probable that it will not make the counter flow regime, but instead impinge on the pedestal. Therefore, ignoring de-icing of the floor may be in order. However, a 0.06" layer of insulation on the floor, weighing less than 10 lbs, would enhance de-icing of the balance of the rotodome, and conserve power.

Although there are hot spots about the rotodome, the de-icing function using the hot air blower system is satisfactory. To reduce hot spots near the blower assembly, a deflector is recommended at the output of the blower.

RECOMMENDATION

An insulating blanket for the floor of the rotodome would help to achieve better thermal balance and would reduce electric bills between 9 and 26 percent. This blanket is highly recommended.

A simple plastic deflector is recommended which would direct the exhaust air upwards, rather than directly into a "hot spot" on the rotodome windows.

Insulating the heaters from the structure is recommended to prevent conductive heat loss paths in the areas beneath the heaters. It should be pointed out, however, that such insulation would raise the inside temperature slightly on an extremely hot day.

SECTION 1. REVIEW OF ICING RESEARCH

1.1 SYNOPSIS

From the literature search it is apparent that there has been much work done on aircraft wing icing and de-icing but little on the icing and de-icing of radomes. Some work has been done on the icing and de-icing of ships by the Russians, Japanese, and the U.S.A., while some work has been done on icing of buildings by the Canadians and Russians. There is almost no research on the conditions under which icing occurs. Part of the reason for this is the large number of variables which bear upon the nature of icing; meterological, actinometric, geophysical, chronographic, barometric, height above ground level, geometric parameters of the body under consideration, and surface properties of the body under consideration.

1.2 AN EVALUATION OF PASSIVE DE-ICING MECHANICAL DE-ICING, AND ICE DETECTION

From 1971 to 1973 the U.S. Army Cold Region Research and Engineering Laboratory at Hanover, New Hampshire conducted tests on Mt. Washington for the FAA[1] to evaluate methods of de-icing and ice detection. It was determined that passive ice removal was ineffectual in operational situations and that they depended on the geometry or on waste energy not usually available at radome installations. Mechanical de-icers such as induced vibration, inflatable covers and a deformable substrate were more effective. Turning heaters on at the proper time was essential for keeping radomes clear. In a dry snowstorm, heaters melted snow which was susceptible to freezing, especially on the top back side of radomes where a turbulence regime deposits slow moving air and snow back against the radome.

[1] FAA Report AD-777-947 by S.F. Ackley, et al.

The phobic coatings were unsuccessful, however, five-fold decreases in ice build-up were noted on Teflon over bare metal, due to the lower adhesion of ice to Teflon. Nevertheless, ice was intolerable without another means to dislodge it. Typical greases were rain eroded, and they picked up dirt particles which were ice nuclei. In addition, greases had to be reapplied regularly.

Sponge rubber substrates were found to break up ice loads unequally, creating greater imbalance than undistributed ice and was consequently ruled out. Rotational forces (centrifugal) were found to be very effective in releasing ice as were vibrations induced by the rotation. The Gullberg de-icer (which deforms the iced surface) was found effective except against wet snow.

The time of outage from that onset of icing was found to be approximately 10 minutes. Therefore, any method which will operate satisfactorily in 10 minutes will be most reliable and economical, such as heaters.

The range of water droplet sizes encountered during testing was 10 to 100 microns. It was found that high wind speeds caused turbulence which could shed ice. Meltwater which ran off onto unheated areas caused secondary problems.

For the TACAN antenna which is 7 feet high and 4'8" in diameter, it was found that a 10-kW heater was required for ice prevention and to offset radiation, wind, and low temperature losses. This is all the energy normally required to operate a VORTAC facility. It was found that after melting only 1 mm of ice, gravity would cause the ice to be shed from vertical surfaces. Mechanical means of displacing the ice were found to be much more energy efficient (0.43 joules) than those necessary (30.2 joules per square centimeter) to melt ice; an effectiveness ratio of 70:1. (This supposes the ice to already be at 32°F.)

They found that the most effective system for removing ice was to deliver the energy to the point where it would do the most good. The ice build-up was asymmetric, with the largest build-up on the leading edge of the structure.

Ice detectors were found to be the key to a successful ice clearing system. Heaters operated only 3 percent of the time when triggered at an air temperature of 35°F and were shut down by a time delay relay 15 minutes after the last icing signal was received. Thermostatically controlled heaters caused more outages than they prevented because they operated during dry snow conditions. The incident snow caused a greater than the normal icing rate on the radomes. It was recognized that if the heaters were turned off when the air temperature dropped below 25°F the system operated better since heaters were found to operate unnecessarily 90 percent of the time they were on.[2]

Hygrodynamic's ice detector was tested and found to be erratic or nonfunctioning at temperatures below 30°F and winds over 30 MPH or if ice accumulation increased. A second detector (from Technology Incorporated) was also found to be unreliable because of icing on the tip of the probe. A third device, supplied by Rosemont Engineering Co., was accurate in monitoring the duration of icing conditions.

1.3 CALCULATION OF GLAZE WIND LOADS ON HIGH INSTALLATIONS

From 1963 to 1965 the Russians observed icing conditions at the Obninskaya Tower in Siberia.[3] They compared their data with 5- and 10-year expectancies across Russia's cold region and deduced the 5- and 10-year maximum wind-speed below which icing occurred. These velocities are one-half the peak observations over a period of several years, which compares with other countries.[4]

At heights of 25 to 100 meters during the 2-year period frost was encountered 21 times and crust ice 46 times; build-up

---

[2] See Minutes of FAA Task Force on Weather Outages, 11-13 Sept. 1973.

[3] Army Technical Translation FSTC-HT-23-486-69.

[4] G. Gleanomi, L'ellettrodoto, 220/230 kv Constr. Metal, No. 5, Rome, Italy 1963.

was less than 20 mm. Two percent of the time the maximum wind was 10-12 meters/second (22-27 MPH). The data corroborated the deduction that wind during icing was one-half the peak velocity during non-icing periods. Extrapolating their data to a 5-year wind/ice condition, they arrived at 20-60 mm of ice build-up with a 16.2 meter/second (36.5 miles/hour) wind. This compared favorably with ground level wind velocities calculated for the Kaluga Station[5] of 21 m/sec for once in 5 years and 22 m/sec for once in 10 years. For the Zhidra Station corresponding values are 22 and 23 m/sec. Again dividing by two to obtain the peak crusting velocity, one receives 11 m/sec once in 5 years. The ratio for 100 meters altitude vs. ground level is

$$V_H = V_{Ho} \frac{\ln \frac{H}{Zo}}{\ln \frac{Ho}{Zo}} \text{ or } 1.5$$

Therefore, the maximum crusting velocity on a 330-foot tower would be 1.5 x 11 = 16.5 m/sec, or 37.2 MPH.

Other observations made on the coefficient of scope, found to be 0.4 for a hemisphere.

1.4 ICING INTENSITY DATA FOR THE 1954-55 SEASON

The Aeronautical Icing Research Laboratory of Smith, Hinchman and Grylls, Inc. made 63 natural icing observations on Mt. Washington for the Air Force during 1954-55.[6] They measured liquid water content, mean effective droplet diameter, droplet size distribution, ambient air temperature, true air speed and, type of icing.

---

[5] L. Ye Anapol'skiy, Wind Velocities Over the Territory of USSR, Gidrometco izdat, 1961.

[6] WADC Technical Note 55-520.

The minimum ambient air temperature during icing encountered was -6°F. The maximum effective droplet diameter encountered was 31 microns. The maximum liquid water content encountered was 0.89 grams/cubic meter. The equipment used was a group of 5 cylinders; 1/8, 1/2, 1-1/4, 2 and 3 inches diameter.

1.5 CLIMATIC TESTS OF A RIGID RADOME FOR GROUND SYSTEMS

During 1954-55 Lincoln Laboratories conducted tests for the Air Force[7] on top of Mt. Washington. Two radomes were evaluated; each was a 3/4 sphere of 31-foot diameter and made from polyester and fiberglass. For a 13-year period the following weather is expectable: -20°F temperature every year, the lowest temperature -46°F, precipitation greater than 3 inches every month of the year, average wind speed in winter exceeds 40 MPH, the chill factor is greater than most polar regions, relative humidity averages 81 percent from September to February, and fog exists 23 days every month of the year.

Rime ice[8] and frost feathers[9] are the ice forms most often encountered. In mid-winter due to lower temperatures, icing was less prevalent; the average ice accumulation being 1/2" on each radome. In only 3 out of 22 observations did it reach 1-1/2" accumulation.

The theory of Langmuir & Blodgett[10] indicates virtually no collection for the droplet range up to 50-60 microns for radomes 31-55 feet in diameter. In three observations out of 22, glaze ice[11] was found to an average thickness of 3/8". Dry snow never accumulated on the unheated radomes.

---

[7] Presented in a Paper at the Radar Symposium, Ohio State Univ. June 28, 1955.

[8] Ice which forms upon impact without forming a liquid film.

[9] Frost feathers are rime ice which builds out into the wind.

[10] Langmuir, Irving & Blodgett, Kather, Mathematical Investigation of Water Droplet Trajectories, G.E. Research Laboratory, 12/44-7/45.

[11] Glaze ice is caused by freezing rain.

A 1/4" steel cable attached to the apex of the dome made a more effective whip than nylon in cleaning the radome of glaze ice which was more difficult to clear than rime ice.

In laboratory tests it was found that one watt per square inch for 20 minutes would clear 1/2" of ice. Infrared lamps were used as energy sources and the power consumption followed classical theory as regards precipitation rates, air temperatures, and wind speeds. A density of 1-3 watts/in.^{2} covered all situations.

It was found that liquid water content and droplet size were considerably in excess of those associated with fog over level ground surfaces. Large drops and a high liquid water content favored the formation of ice. Drop size and water content decreased with decreasing temperature. In view of the experience, it was predicted that rime ice would not be a problem at radome sites. Canadian meteorological data showed that freezing rain and drizzle paralleled the mean winter precipitation; and also that freezing rain and drizzle were rare phenomenona at inland stations of polar regions. The survey showed that precipitation rates were slight and frequency of occurrence decreased with increasing latitude. Freezing precipitation did occur at Gander, Newfoundland and in Labrador for many hours with moderate to strong winds and temperatures well below 32°F.

Icing rate was found to be a function of horizontal wind speed rather than precipitation rate on the top of the radome. From the precipitation rate, it is possible to estimate drop size, terminal velocity, and liquid water content.[12] The maximum ice accretion rate was found along Newfoundland coasts and was 1/4 inch per hour. Wet snow (above 25°F) did cause icing. This could amount to 1 inch per hour of precipitable water.

[12] Laws, J.O. 1943 The Relationship of Drop Size to Intensity, Transactions of the Am. Geophysical Union, 24, P.3, 452-459.

They found that the average wind with freezing precipitation was 20 MPH; and 30 MPH winds were extremely rare.

1.6 TEST AND EVALUATION OF 6 TACAN WIRE WOUND HEATED RADOMES

A field evaluation was made at 6 VORTAC facilities during the six months of 1974-75 winter;[13] at Mullan Pass, Idaho; Lakeview, Oregon; Elko, Nevada; Denver, Colorado; Rochester, Minnesota; and Clarion, Pennsylvania. The purpose was to determine effectiveness of the means of preventing outages caused by snow and ice. The units had a sophisticated servo system which drove a VARIAC to regulate temperature inside the radomes. In all, the servo system had to;

1) detect icing conditions,

2) turn power on to heat radome,

3) maintain radome temperature, and

4) safeguard overheating the radome.

The control monitored ambient air, relative humidity and radome temperature with servo sensors 8 feet above ground level near the radomes. The system was intended to turn on at 45°F and shut down when an interior temperature of 90°F was reached or the outside temperature went above 45°F with a 30-minute timer in the ambient shut-down circuit. Due to rapid cycling the servo made the system work on a 50-percent duty cycle, but this was only after a field modification made the servo operational. The servo system continually "hunted" above and below the nominal setting because of a 3-minute thermal time lag of the radome thermistor. Consequently, the system was ineffectual during extreme weather conditions. For example, the year 1973 yielded 13 outages without heaters at Mullan Pass, Idaho totalling 40 hours, while in 1974 with heaters, only 8 outages occurred totalling 23 hours.

---

[13] Report No. FAA-RD-76-130 Prepared for D.O.T.

At Lakeview, Oregon the heater "turn-on" was reset to 50°F to reduce outages after a heavy, "wet" snowfall.

At Elko, Nevada a near outage occurred with the radome setting at 50°F. A light snow was falling initially with winds gusting to 30 knots and 22°F ambient temperatures. A 1/2 inch build-up of snow occurred on the radome. Forty minutes later, the radome was clear. Their conclusion was that the heaters operated marginally in heavy, wet snowfalls.

In Denver, Colorado the heaters averted a 4-inch snow build-up while a nearby VOR antenna without heaters had to be shut down.

At Mullan Pass, Idaho the control setting was 45°F but the radome surface never rose above 28°F while the outside air temperature never went below 20°F. The optimum setting for the heater control could not be determined.

The field modification which prohibited the servo from becoming a "bang-bang servo" was determined to save approximately $40.00 per 15-hour day (at $0.6 per kW hour).[14]

1.7 MINIMIZE SNOW AND WEATHER EFFECTS--VORTAC TASK II TACAN ANTENNA

In 1971 a study was accomplished at FAATC for the FAA[15] of wire wound radomes, oversize radomes, ice-phobic treated radomes, and ones covered with a polyurethane shroud. The shroud showed the most promise of all. Previous FAA tests[16] showed that 1.25 watts/sq. in. of heater power was necessary to prevent outages. For the TACAN test it was found only 0.655 watts/sq. in. (0.1 watt/sq. cm.) were required. The subject test provided two radomes with 1 watt and 1.3 watts/sq. in. During a field

---

[14] By comparison, Los Angeles rates for October 1979 are $0.57 per kW hour.

[15] FAA Report FAA-RD-71-56, Sept. 1971.

[16] At Sconwell Laboratories for the FAA.

evaluation conducted in 1968-69, it was found that the modified radomes prevented outages that normally would have occurred. FAATC flight tests showed that the modified radomes were unacceptable in terms of radio frequencies at the low end of the low band, which verified anechoic chamber data.

The hydrophobic coatings were a failure, having no effect on the start of ice information. When combined with mild vibration during and after ice formation, it was still unsuccessful in preventing or removing ice.

A simulated larger radome was made using pine planks. These tests demonstrated that a larger radome would still cause outages, if ice built up on it.

The tests of a prototype poluyrethane shroud, designed and built by Gullberg Industries, Media, Pennsylvania did not prevent ice build-up. Mild vibration and high pressure caused cracks in the ice cover but no ice removal. Speculation by the observers was that perhaps enough wind would have shed some of the cracked ice.

1.8 SURVEY OF THE LITERATURE ON SHIPBOARD ICE FORMATION

N. Fein and A. Freiberg reviewed in the Naval Engineers Journal in 1965 the literature on shipboard icing. Their investigating showed that ice begins forming at -1.5°C and continued to -40°C (-40°F). The smaller and purer the droplets, the lower the temperature at which freezing began. Accretion of ice did not occur below -17.7°F (0°F) because then water hitting a ship would be in the form of small ice crystals which were dry and would not adhere.

A supercooled condition is always necessary for water to change to ice. In addition, a critical radius is necessary for nucleation to begin. The critical radius can be supplied by a flat surface (infinite radius). Thus, a very small crystal of ice will melt at 0°C because its radius of curvature is less than the temperature-dependent critical radius. An aggregation of

molecules must first be in the pattern they would be in solid ice before nucleation (crystal structure) can begin. Glaze ice was found most common at 0°C but existed down to -18°C.

No silicone surface treatments were found to be ice-phobic, rather they accelerated accretion. This was thought to be because treated surfaces tend to be rougher than smooth metal or painted surfaces, thus aiding nucleation. Tests were conducted on aluminum, lucite, and glass surfaces. An initial ice film was found to grow rapidly over a horizontal surface before any appreciable vertical growth began.

It was found from the literature that there was no accretion rate or quality-of-ice-accreted data versus weather conditions. Few studies on the accretion of ice on solid surfaces have been made.

1.9 RESEARCH ON PREVENTION OF SHIP ICING

At the Institute of Low Temperature Science in Sapporo, Japan studies were conducted from 1960-66 on artificial ice accretion, and on the character of icing and anti-icing surface materials such as mats, rubber coated canvas, and anti-icing paints.

Artificial icing was created in a wind tunnel at speeds from 5 to 20 meters/second and temperatures from -5 to -15°C. Fine brass rods 10 mm to 250 mm in diameter were used as collectors. These studies showed that higher temperatures and lower wind speeds yielded semi-transpanent ice. As the temperature was decreased and wind speed increased, the ice became gradually whiter. The whiter it became, the harder it was. For equal wind speeds the accreted ice increased as the air temperature decreased. This may not necessarily correlate in nature, because the liquid content would probably drop with temperature.

In vivo observations on the Kurile fishing boats noted no ice accretion above -2°C or wind velocities less than 5 m/sec. (11 MPH). The smaller the vessel, the lower the wind speed, and the higher the temperature, the sooner ice accretion commenced.

The application of mats to the fore decks, forward hull, stern, and masts of fishing boats proved helpful in shedding ice spontaneously due to compliance coupled with ships' motions, vibrations, and wind action. Moreover, it was found to be simpler to remove accreted ice by means of hard mallets on the mats. A problem was encountered when the mats eventually fell off due to wear and tear and wave action.

Rubber coated canvas was found to be the best means of spontaneoulsy removing ice and would probably by used for hatch and winch covers, henceforth.

1.10 INFLUENCE OF ICE UPON CONSTRUCTION AND METHODS OF COMBATING ICE PROBLEMS

The U.S. Army made a collection of Russian papers on icing in December, 1974.[17] dealing with ice cover effects, properties, pressure, and loads. These related to dams, building, and reservoirs.

Some interesting aspects gleaned from the Russian studies were:

1) As ice specimen size increases, strength decreases.

2) Mathematical methods for predicting the physical pattern of ice in nature were remote from reality, due to the anisotropy of ice.

3) The strength decreases by a factor of 3-4 prior to melting, due to solar radiation effects.

4) The adhesion force of ice was found to be on the average 8.2 kg/cm^2 (force/area).

5) They felt that there was as yet inadequate study, of the mechanical properties of ice.

6) Ice breakers employing "vibration devices" were able to travel 2-3 times faster than breakers not so equipped.

[17] TL 422 available from Nat'l Technical Information Service.

7) Dark pulverized substances sprinkled on ice were not very effective in enhancing melting because it was covered by subsequent snow fall and because the sun was not available continuously.

8) Sodium alginate and zinc stearate were effective when sprinkled on water in preventing ice formation, but had to be reapplied after passage of a ship. The French found the same true in their experiments.

9) The energy to keep a surface clear of ice is less than that necessary to melt it free of ice due to the insulating qualities of ice.

10) At a surface temperature of 1°C the ice will be cleared or when 3 mm of ice has melted.

11) The shear strength of ice is less than its adhesive force with metal, consequently scraping a surface often leaves a small residue.

12) Physiochemical methods of ice removal generally cause more corrosive damage than they are worth.

13) The hydraulic pressure necessary to cut ice from a surface is 800 or more atmospheres and requires complicated equipment.

14) Heating elements on the surface to be cleared were 1.5 to 2 times more efficient than tubular heat exhangers, and could conform to any shape much more readily.

15) At air temperature of -20°C 800 watts/m^2 (0.08 watts/cm^2 or 0.516 watts/in^2) were found to be sufficient to clear a surface of ice.

16) Optimal spacing of heater elements on the surface was found to be 0.1 to 0.2 meters.

17) Ice viscosity depends upon temperature, orientation of crystals, and the length of time the load is applied.

18) Plastic deformation of ice is not a linear function but rather a power function of the applied stress.

1.11 SUMMARY

It appears that although much study and effort has gone into studying icing and ice prevention, much is still unknown about the exact meteorological conditions which will create icing at the low end of the temperature regime. This regime exists only at higher elevations so it should not be a deterrent to the present study since the ASDE-3 system is primarily for use at elevations of 5,000 feet or less. From the body of knowledge extant, it appears that the choice of heaters for deicing the ASDE-3 rotodome is the best all-around method.

SECTION 2. RESEARCH METHODOLOGY OF THE SELECTED PROBLEM

2.1 GENERAL

The problem of efficiently de-icing the ASDE-3 rotodome is one of optimizing heat flow paths to the points where they do the most good. The leading edge presented to the wind stream is the most critical area with the roof following as a close second. Any loss through the floor, pedestal opening, or excessive losses through seams should be minimized. Preliminary design calculations ignored losses via the pedestal and considered the back of the rotodome as a second window. The first model which burned during a fire in Long Island, New York did have two windows each 180 degrees in azimuth (a front and a rear window). Some preliminary tests were conducted briefly on this prototype model in San Diego, California. These tests were exploratory in nature to prepare for actual icing conditions testing in Long Island.

2.2 EXPLORATORY TESTS

On January 10, 1979, some preliminary thermal tests were conducted after RF range testing concluded at 4:00 p.m. These tests were conducted with both heaters cycling on and off simultaneously not in cascade as they will be in the final configuration. These tests were conducted with virtually "no wind" conditions for about one hour until darkness set in. The rotodome was still at a 30 degree tilt from range testing and one "man way" was closed using the fabricated aluminum cover while the other on the lower side was covered with cardboard since it was necessary to run the wires through there rather than through the static slip rings. A standard household, Robert-Shaw thermostat was used and it cycled between 83° and 79°F when set at 80°F. It was not possible to confirm this, so there is no accurate, verifiable base on which to predicate this preliminary data. Figure 2-1 shows the test set-up during preliminary tests.

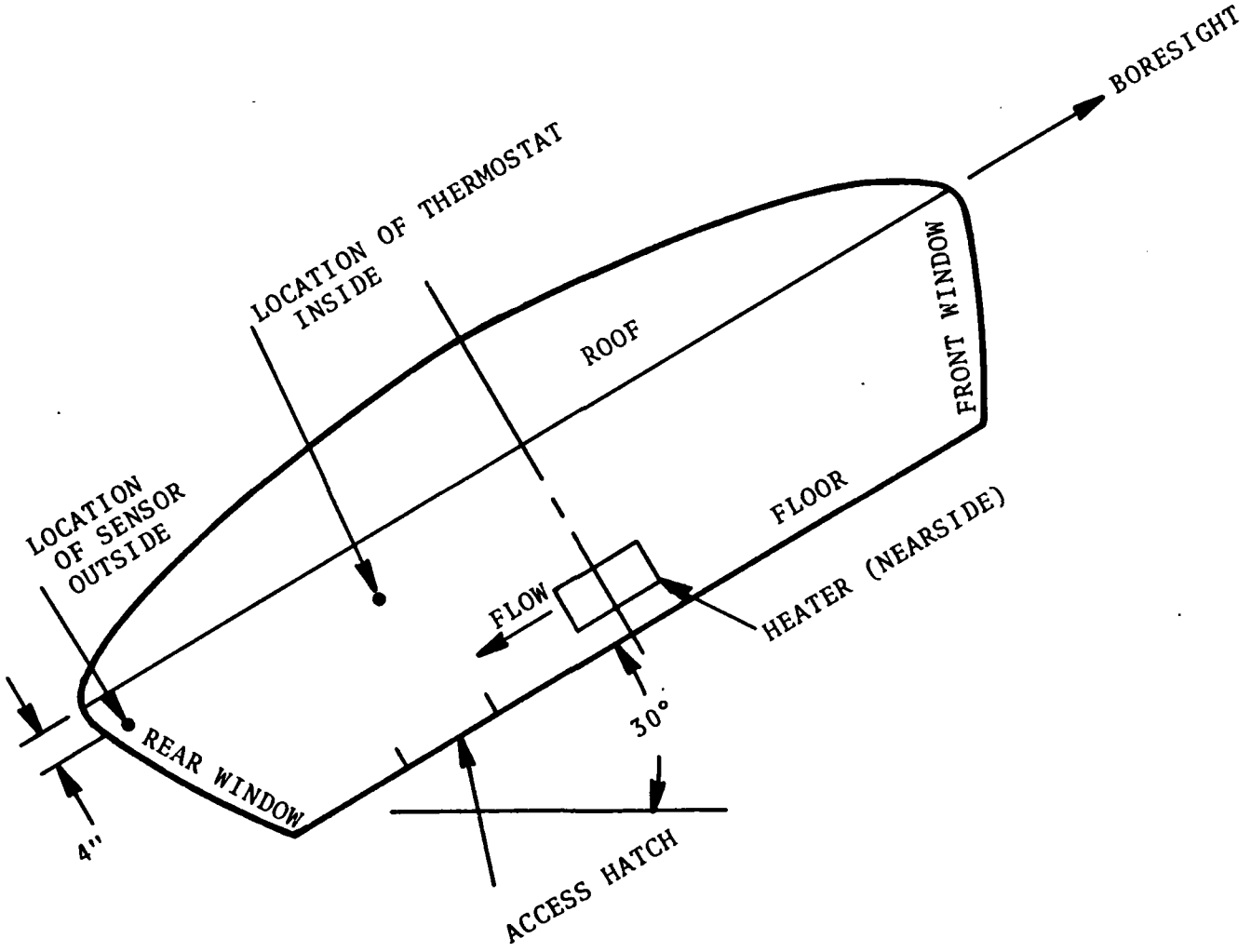

FIGURE 2-1. ORIENTATION OF ROTODOME DURING PRELIMINARY TEMPERATURE TESTS

Two conclusions can be drawn from the preliminary tests: a) Perhaps 240 V power should be supplied for the heaters unless a transformer is located in proximity to the ASDE-3 installation as the IR drop was 13.5 percent and would probably be similar in a remote tower installation; b) The rotodome floor should probably have an insulated floor to reduce energy consumption, increase heater life, and increase the efficiency of the system by providing more heat for the roof and window rather than for the floor.

2.3 A SECOND ROTODOME

Subsequent to fire destroying the first rotodome a second was built. The latter had a back side much like the roof, except it had a phenolic, honeycomb core instead of an aluminum core. The back side took the place of the original rear window which was incidentally not used as an R-F window, but rather was made identical to the real front window so that the better of the two might become the "front" (R-F) window.

The back side has markedly different heat transfer characteristics from a window. The back is more insulative being a honeycomb sandwich structure rather than a thin (0.19 inch) shell structure. The approximate dimensions for the back are 1 inch thick, 4 feet high and 180° in azimuth on a radius of about 8 feet. Due to the heat transfer characteristics of the back side, the original design calculations are "off" by that difference. The internal temperature for one thing will be higher.

Final Tests

On the evening of September 18-19, 1979, in San Diego, California, a test was implemented according to the procedure which follows.

2.4 ROTODOME THERMAL TESTS

2.4.1 Intent

The procedure was intended to be used to investigate the thermal properties of the ASDE-3 rotodome September 10-13, 1979

in San Diego, California at Teledyne Micronetics R-F antenna range, on a third-shift, noninterfering basis with respect to R-F testing of the ASDE-3 antenna.

2.4.2 Purpose

In order to verify earlier design calculations and to refine them to know when to turn on and off the auxiliary heaters, it was desirable to verify the coefficients of heat transfer for the various areas of the rotodome as well as the various coefficients of radiation and convection. Moreover, during the investigation, an attempt was made to find hot spots in the rotodome, as well as areas that could be shielded and/or insulated in order to conserve and better utilize the available heat. Finally, a prediction can be made from the data of the ice prevention capabilities of the current design and any further modifications to enhance those capabilities. The purposes then were:

1) Determine heat transfer coefficients of floor, window, seams, back, and roof of the rotodome.
2) Examine the design for the hot spots.
3) Experiment with various deflection angles for the heater exhaust.
4) Experiment with insulation on the floor of the rotodome.

2.4.3 Instrumentation

The following test equipment was available and set up before the start of testing:

1) A 24-channel strip recorder;
2) 24 electronic thermocouple Type T leads:
3) An ammeter;
4) A 35 mm camera with infrared film;
5) A quantity of insulation approximately 1/16 to 3/16 inch thick, sufficient to cover the entry holes in the floor;

6) Sufficient putty or tape to mount all of the thermocouples;

7) A voltmeter suitable for measuring up to 240 volts:

8) A bolometer

9) A humidistat

10) A wattmeter

2.4.4 First Night Test Set-Up

The rotodome was set up in its normal outdoor operational configuration with the exception of heater controls, humidistat and ice sensor. The antenna and back-up structure were in place and the man-access covers installed in the floor of the rotodome. The rotodome was installed on an operational pedestal. The heaters were installed in their operational configuration, one facing forward and one rearward. The heater exhaust deflectors were installed in their intended operational attitude. The rotodome was tested on a nearly windless night, in the middle of the night, so as to reduce ambient heating or cooling influences. In addition, the following additional preparations were made.

1) Hooked up the heaters to the 30 kVA input line;

2) Set up the bolometer approximately 30 feet from the rotodome along with the thermometer, and humidity meter;

3) Mounted 12 thermocouples on the inside of the rotodome window in a pattern of two rows of six each, equally spaced approximately 12 inches from the top and bottom of the window. The spacing within each row was approximately 60 inches with 12 inches left over on each end of the row;

4) Mounted another 12 thermocouples on the outside of the rotodome, each one in opposition to a corresponding one on the inside;

5) Set the 24-channel recorder and the electronic box associated with the thermocouples outside the rotodome;

6) Closed the access covers to the rotodome;

7) Turned the heaters on and allowed them to operate until the rotodome attained an inside constant temperature above outside ambient, by monitoring one thermocouple suspended inside radome airspace;

8) Accomplished the above by hooking up only one of the elements in each heater, (10 kVA); and

9) Allowed the unit to soak at this first night temperature for at least one hour.

2.4.5 Test Data Recording (First Night)

1) Took a complete set of readings of all thermocouples. Recorded the information on a strip chart from the 24-channel recorder.

2) Took a series of photographs of the rotodome from all four sides 0° (boresight) 90°, 180° and 270° clockwise in azimuth as viewed from above.

3) Did a complete survey of the rotodome to check for hot spots using thermocouples. Looked, in particular, at the following places:

   (a) floor

   (b) window in fromt of heater blowers

   (c) roof and back

   (d) floor in front of heater blowers.

   Recorded findings on Data Sheet #2.

2.4.6 Second Night Test Set-Up

Repeated the set-up from the first night above, except this time mounted the thermocouples in Steps 1 and 3 evenly about the front 1/2 of the rotodome floor, window, and roof.

2.4.7 Test Data Recording (Second Night)

1) Hooked up only the forward facing heater (5 kVA) and the second blower. Allowed unit to stabilize.

2) Repeated Step 1 from the first night.

3) Connected the second heater (one element only) for a total of 10 kVA. Allowed unit to stabilize.

4) Repeated Step 2.

5) Connected the forward facing heater's second element for a total of 15 kVA. (The rotodome was then operating at 1/2 capacity; the total capacity is 30 kVA.) Allowed the unit to stablize.

6) Repeated Step 2.

7) Took one 24-foot long thermocouple lead and took a temperature reading on the outside of the rotodome at the following places:

   (a) roof junction

   (b) floor junction

   (c) turntable top

   (d) pedestal (various locations)

   (e) back/window joint

   (f) back/roof joint

   (g) back/floor joint

   (h) ground.

SECTION 3. ANALYSIS OF THE DATA

3.1 INTRODUCTION

This section will first present the data taken during final rotodome thermal tests conducted September 18, 19 and 20, 1979. Then the data will be reduced and displayed as isothermal maps of the rotodome. Next, a few extrapolations will be made to predict maximum rotodome temperatures.

An analysis will then be made to correlate the data taken to some actual physical characteristics of the rotodome.

Finally, from the data taken an extrapolation will be made to some hypothetically severe icing conditions, and a statistical evaluation will be attempted for the ability of the rotodome to prevent outages.

3.1.1 Data Taken Sept. 18, 1979

Data was taken in a first attempt to measure temperatures inside and outside the window, the floor, roof and back wall. The data is somewhat unreliable because too much clay was used around the thermocouple tips actually causing a "hot house" effect in the immediate vicinity of data being recorded. See Figure 3-1, first night test isotherms.

3.1.2 Comments on First Night's Data

It was observed when the testing was being done that the Esterline-Angus recorder was reading properly while it was being connected to 12 thermocouple leads and indoors at 76°F, but when taken outdoors to a lower ambient, it immediately read too low. Data was taken anyway, with the intent that the unit would be checked against a well calibrated oven the next night. It was later learned that the Zener diode, temperature compensating circuit had a dead battery and was therefore not compensating for ambient changes in temperature.

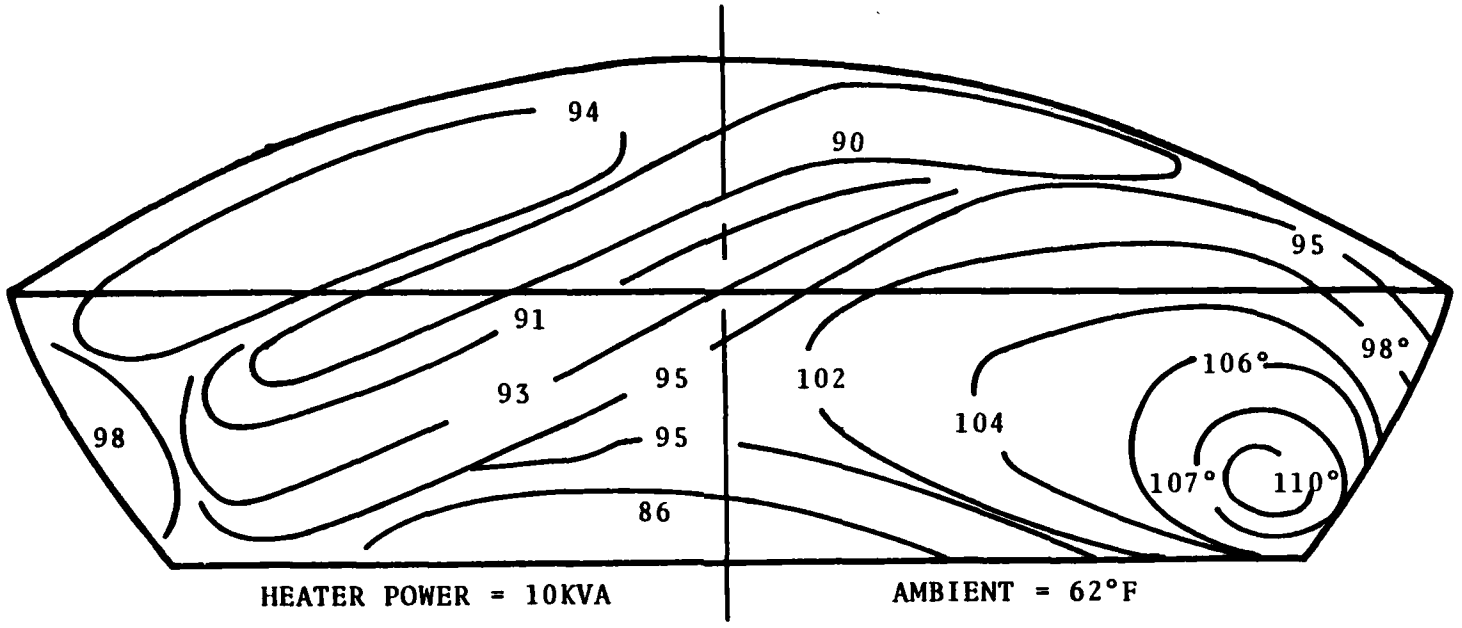

FIGURE 3-1. INSIDE ISOTHERMS, FIRST NIGHT'S TEST

The first night 12 thermocouple leads were wired to the recorder. This necessitated moving all the leads midway through the first night's test in order to take more recordings. The second night another 12 leads were connected to the recorder and a larger grid pattern was utilized on the rotodome window simultaneously with the roof and floor which meant the leads did not have to be moved during testing.

The first night 10 kVA continuous power was utilized for all readings while during the second night three sets of data were recorded at 5, 10, and 15 kVA continuous power consumption.

3.1.3 Chronology of Second Night's Test

9:00 p.m.	Turned on 5 kVA (front heater).
10:24 p.m.	Not stablized.
10:38 p.m.	Not stabilized.
11:14 p.m.	Stabilized Lead #24 = 80°F Thermo = 88°F. (Inside ambient) No wind.
11:28 p.m.	Turned on both heaters @ 10 kVA (9 kVA allowing for IR drop) 2-- V @ 23 A. max. 22 min.
12:20 a.m.	Took set of readings while readjusting Lead #1.
	#1 looked well set.
12:30 a.m.	Inside climbing 1°/10 minutes.
	Ambient = 66°F - no wind.
12:40 a.m.	Inside climbing 1°/10 minutes.
12:45 a.m.	Check on Lead #1 @ ambient #1 = 58.5, temperature = 66°F. Inside temperature still increasing 1-2°/5 minutes.
12:52 a.m.	Stabilized - ambient 65°F.
1:10 a.m.	Humidity/Thermo = 65°F. Thermometer = 62°F 15 kVA: 2 heaters front, 1 rearward turned on @ 1:00 a.m.

1:50 a.m. Took readings: 64°F humidity/thermo. 62°F, Lead #20 = 150°F.

2:02 a.m. Stablized.

2:10 a.m. Lead #19 on bottom of window support bracket, 45°clockwise from forward facing heater when viewed from above.

2:12 a.m. Lead #19 on window/back seam 1/2 height (open front hatch).

2:14 a.m. Lead #19 under heater on I-beam floor seam.

2:16 a.m. Lead #19 on roof band rear 315°.

2:18 a.m. Lead #19 of edge of floor 270°.

2:20 a.m. Lead #19 on roof seam 90° (boresight).

2:22 a.m. Lead #19 on floor beam 90° (boresight) 1/2 radius.

2:24 a.m. Lead #19 turntable 2nd ring.

2:26 a.m. Lead #19 AZ shaft just below the AZ indicator band - 90° (boresight).

2:28 a.m. Lead #19 bottom of AZ Hsg at junction to gear box.

2:30 a.m. Lead #19 end of gear box 90°.

2:32 a.m. Lead #19 on macadam 90° (boresight).

2:34 a.m. Lead #19 tip of leg 1/2 height 30°

End of Test

2:56 a.m. Thermometer = 60°F.

Humidity/Thermometer = 63-1/2°F.

See Figures 3-2, 3-3, 3-4 and 3-5.

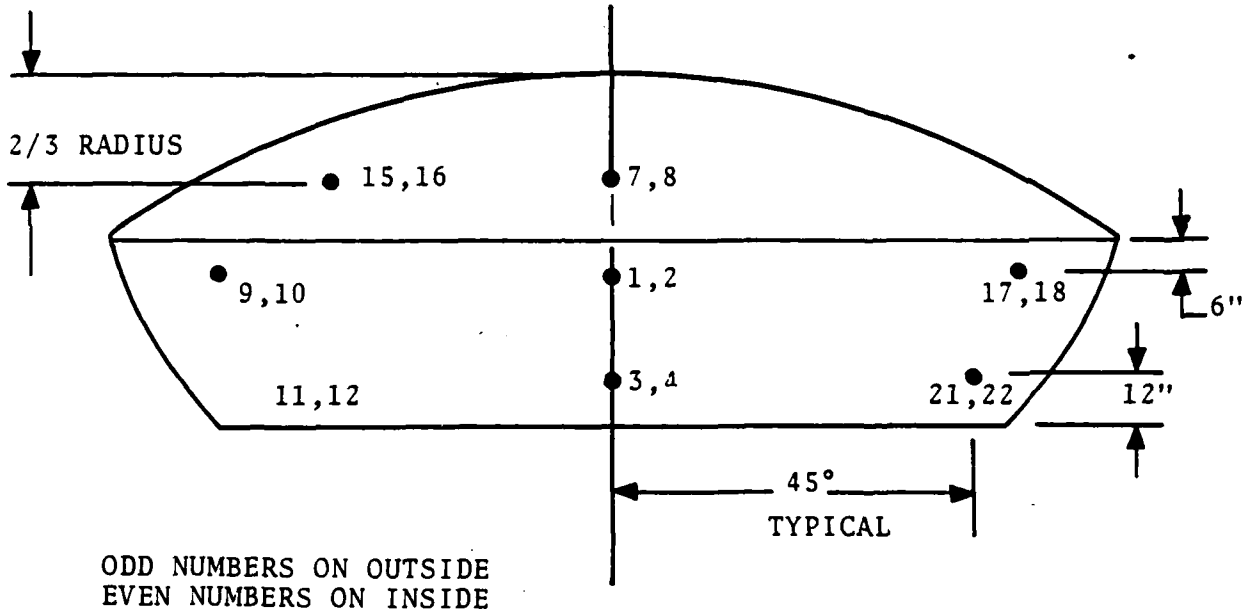

ODD NUMBERS ON OUTSIDE
EVEN NUMBERS ON INSIDE

#24 SUSPENDED IN AIR NEXT TO HEATER SENSOR

#23 NOT USED

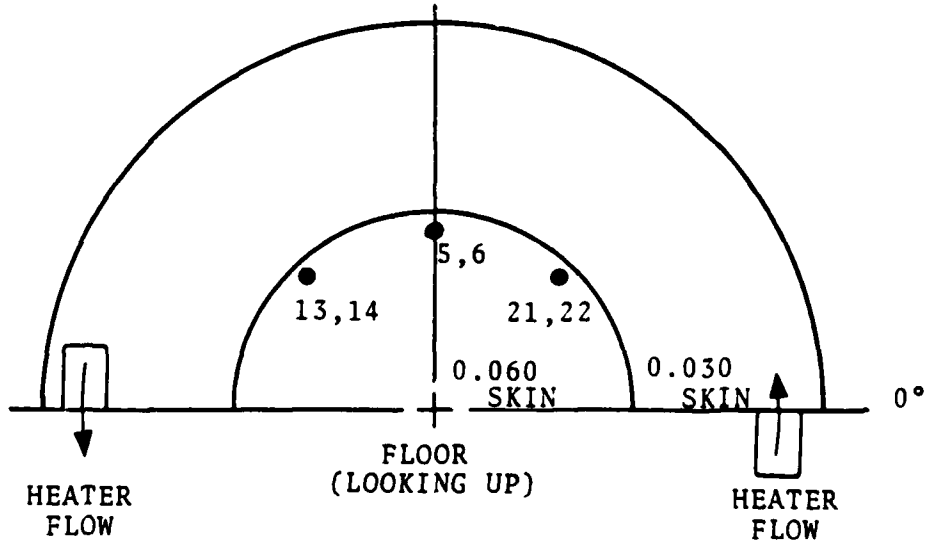

FIGURE 3-2. LOCATION OF THERMOCOUPLES, SECOND NIGHT'S TEST

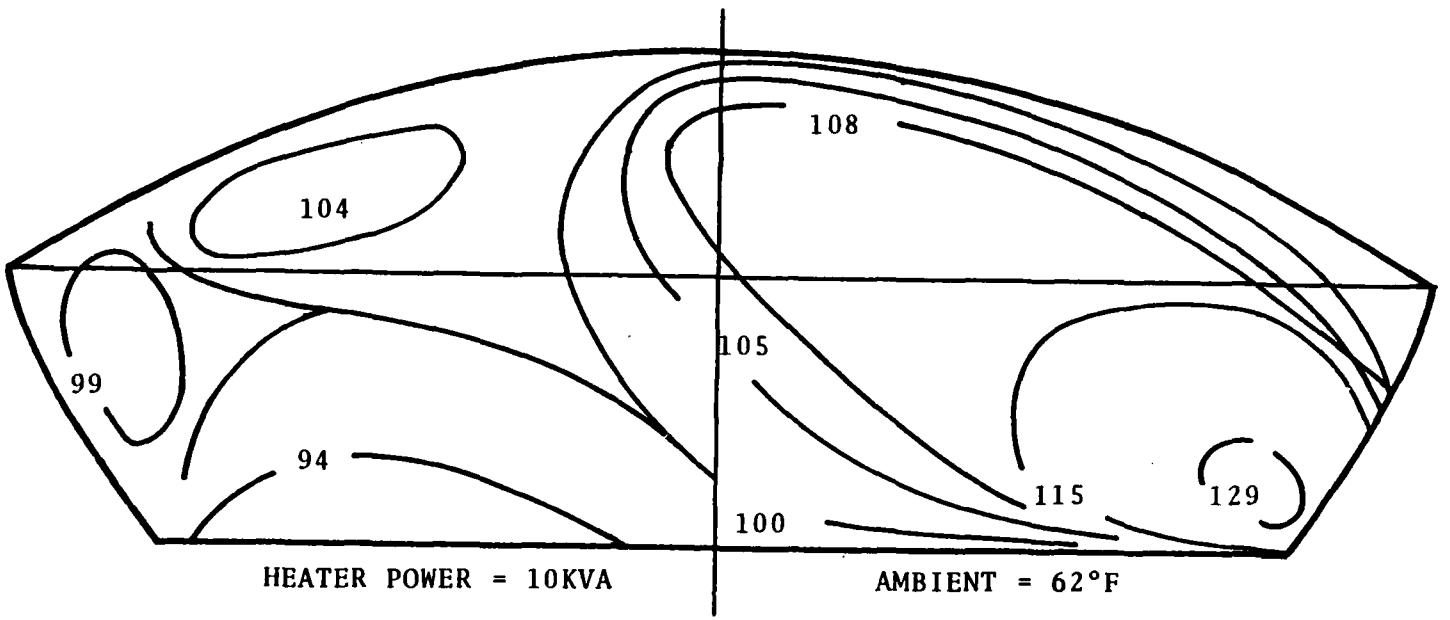

FIGURE 3-3. INSIDE ISOTHERMS SECOND NIGHT'S TEST

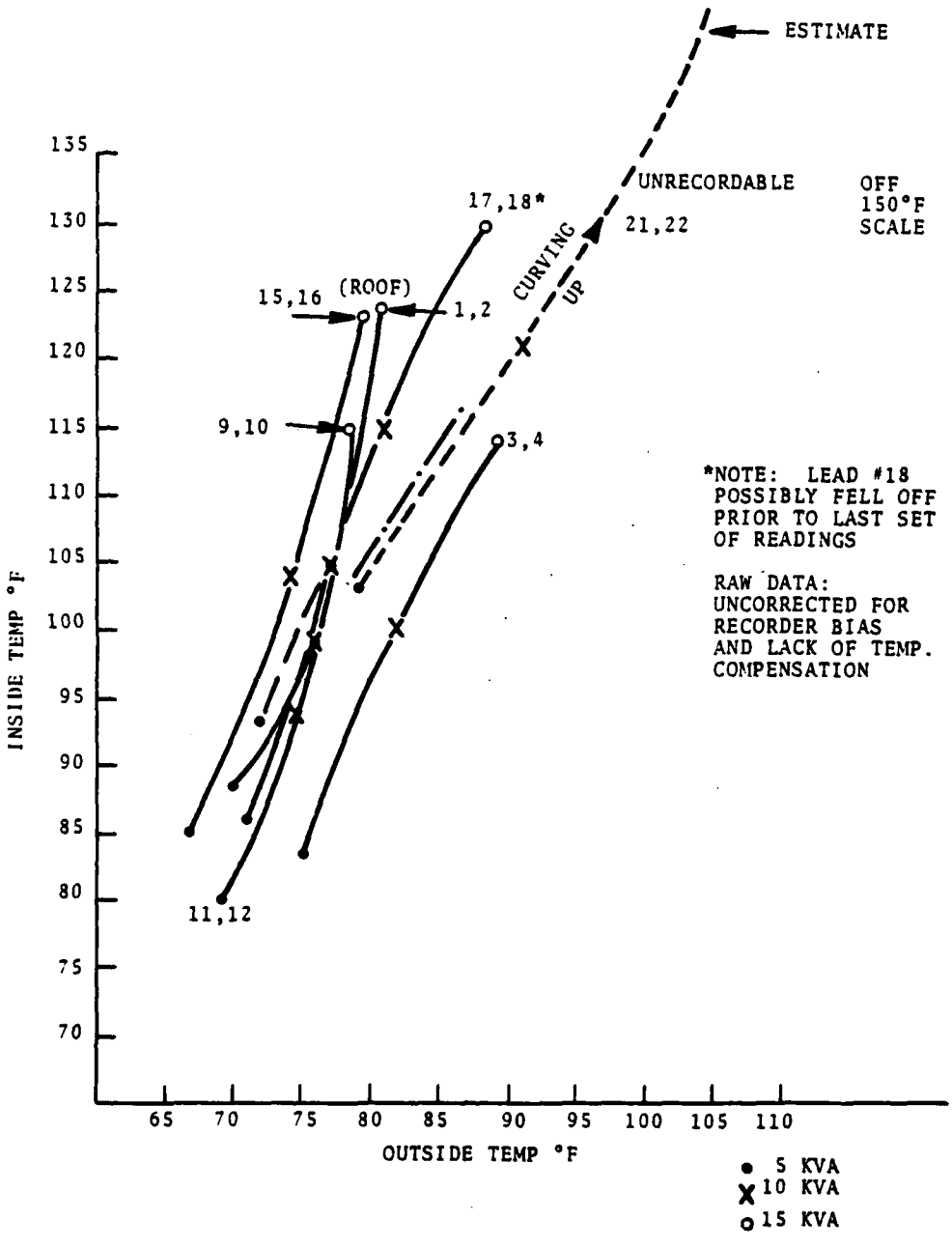

FIGURE 3-4. WINDOW INSIDE VS OUTSIDE TEMPERATURE, SECOND NIGHT'S TEST

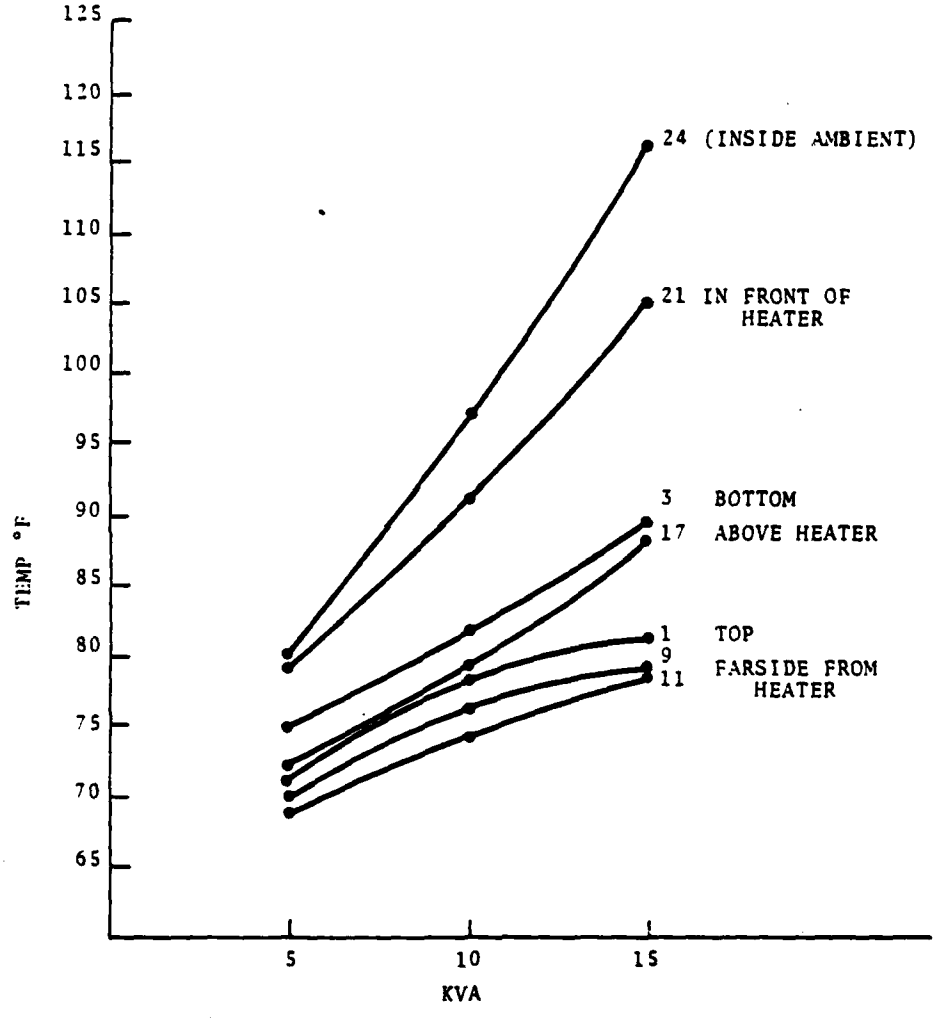

FIGURE 3-5. OUTSIDE TEMPERATURE OF WINDOW VS POWER CONSUMPTION

3.2 ICE PREVENTION ANALYSIS (See Appendices for Supporting Information)

3.2.1 Principal Modes of Heat Loss

There are three principal modes of heat loss from the rotodome:

1) conduction

2) radiation

3) convection

3.2.1.1 Conductive Mode

The conductive mode is a linear function with respect to temperature differential while the radiative transfer behaves according to the law of Stefan-Boltzmann which is a function of the fourth powers of the relative (absolute) temperatures and the convective transfer (ignoring winds) behaves somewhat as a function of the 1.25 power of the temperature differential.

The conductive mode is the simplest and at the same time the lowest mode of heat loss from the subject rotodome. The only path available for the conductive loss is through the azimuth drive shaft and therefrom it must be subsequently lost via the same 3 modes of heat transfer: conduction through the bearings, seals, radiation from the shaft to the inside of the pedestal housing, and finally to a small extent by convective transfer in the still air space inside the pedestal from shaft to housing exterior.

This conductive transfer through the azimuth shaft behaves according to the following formula:

$$Q = hA\Delta T$$

where h is a function of path length and the conductivity of the material, i.e.,

$$h = \frac{K}{L}$$

The shaft, see Figure 3-6, is composed of 4142H steel and has the thermal-physical characteristics as depicted in the following page.

$K = 27.8$ BTU/FT^{2}HR/°F/Ft Per Table 45, Handbook of Heat Transfer

$L = 1 - 1/3$ Ft

$A = 12.2$ In^2 $= .0847$ Ft^2

$Q = \frac{27.8}{1.33} \times (.0847)$ (77°-73°F) @ 13.5 kVA
at top of shaft / / at bottom of AZ shaft

$Q = 7.08$ BTU @ 13.5 kVA

$= 15.74$ BTU @ 30 kVA

1 BTU = .2931 watt-hour

$Q = 2.08$ watts @ 13.5 kVA

$= 4.61$ watts @ 30 kVA

Thus, it can be seen that conduction causes a very small heat loss for the rotodome and can virtually be ignored.

3.2.1.2 Radiative Mode

The radiative heat loss is a function of the sky and ground temperature, the roof, window and floor temperatures and their respective areas and surface emissivities as well as look angles.

Typically, the loss behaves according to the following formula:

$$Q = A_1 F_{12} \sigma (T_2^4 - F_1^4) \varepsilon_1 \varepsilon_2$$

where F is a shape factor which is the fraction of the total radiation from area A_1 which falls on area A_2 (the sky, ground, etc.). Calculation of the shape factor is a function of integrating the intensity over the two areas involved. This is a very complex factor because it is not only proportional to radiation intensity, but a function of the angle of incidence on the receptor body. For the sky it can be assumed normal as if the

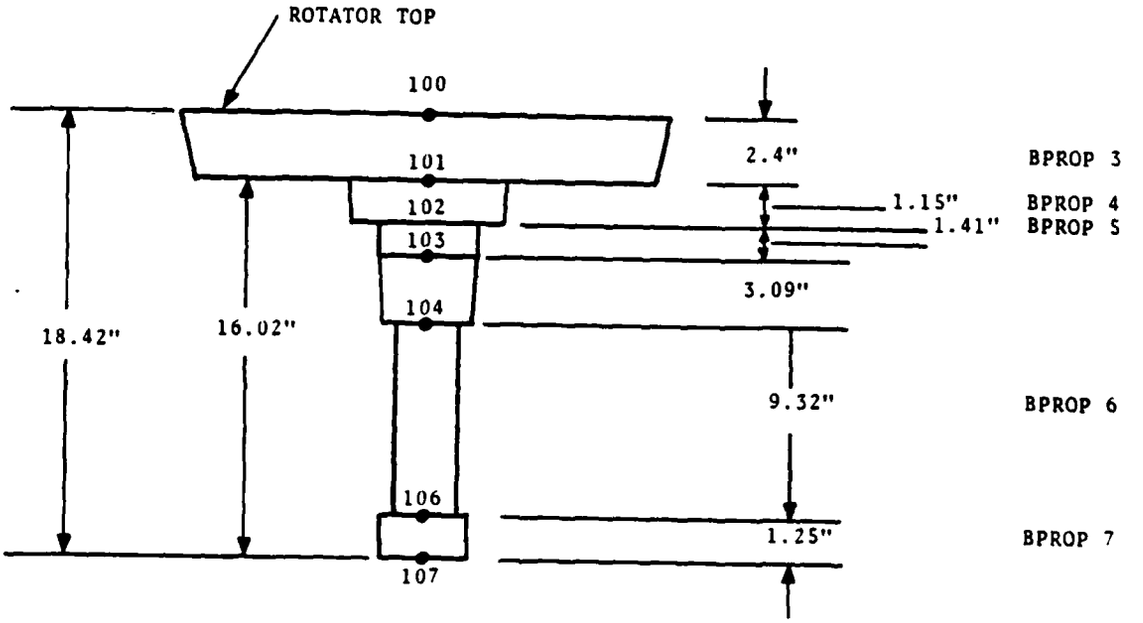

BEAM PROP	AREA	PATH LENGTH
4	25.8	1.5
5	14.13	4.5
6	10.31	9.32
7	12.2	1.25

AVG. AREA = 12.2 in^2

AVG. PATH LENGTH = 8 in.

FIGURE 3-6. AZIMUTH DRIVE SHAFT THERMAL-PHYSICAL CHARACTERISTICS FROM STARDYNE ANALYSIS

surfaces were parallel--in which case, the proportionality is called normal intensity I_n. The emissivity power is then a function of integration over a hemisphere of look angles from each unit area of the rotodome surface as follows:

$$E = \int_{\phi=0}^{\phi=\pi/2} I_n \pi \, S_{IN} \, 2\phi d\phi$$

and for the general case involving various areas, the following:

$$A_1 F_{12} = \frac{1}{\pi} \int_{A_1} \int_{A_2} \frac{\text{Cos}\phi_1 \, \text{Cos}\phi_2 \, d \, A_1 \, d \, A_2}{\gamma^2}$$

where r is the radial separation of the two surfaces, i.e., the density of radiation intensity decays with the square of the distance. Fortunately, copius empirical work has been done on the above relationship and the values of emissivity are well documented in the literature, as well as working handbooks. The problem then breaks down into one of summing the various areas, emissivities and temperature differentials for the several regions of the rotodome, i.e., roof, window, and floor. (See Figures 3-7 and 3-8.)

$$Q = \left[\sum \varepsilon_1 \varepsilon_2 \, A \, F_{12} (T^4 - t^4)\right] \, 0.171 \times 10^{-8}$$

The various areas are:

Roof = 269 ft^2

Window = 104.5 ft^2

Back = 104.5 ft^2

Floor = 153 ft^2

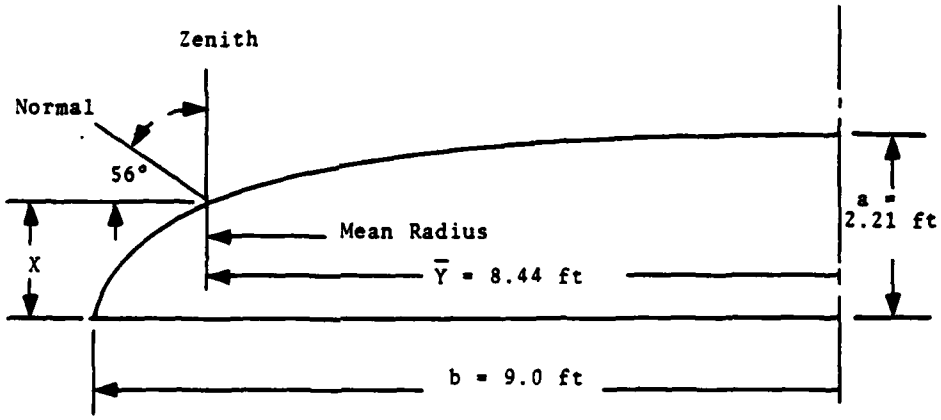

Mean R = 8.44 Ft

$$\frac{x^2}{a^2} + \frac{y^2}{b^2} = 1$$

a = 2.21 Ft.

b = 9 Ft.

$\alpha = \tan^{-1} \frac{\Delta x}{\Delta y} = 33.68°$

@ 8.44 Ft. = y

x = .77 Ft

Avg % Radiated to Sky = $100 \times \frac{146}{180} = 81\%$

Avg % Radiated to Ground = $100 \times \frac{34}{180} = 19\%$

FIGURE 3-7. ROOF EMISSIVITY LOOK ANGLES

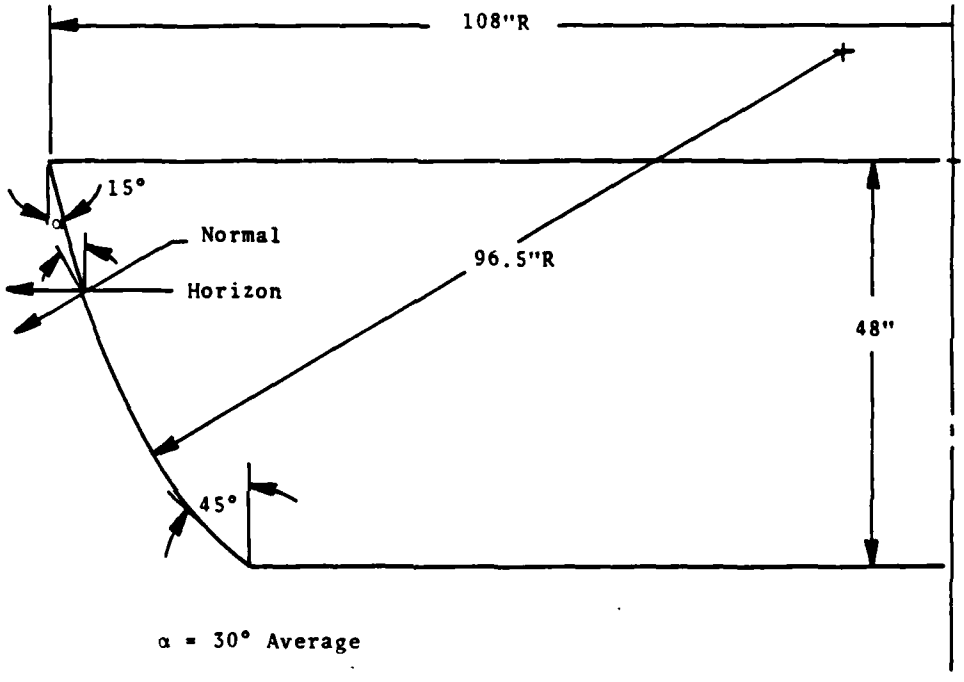

α = 30° Average

Avg % Radiated to Sky = $100 \times \frac{60}{180} = 33\%$

Avg % Radiated to Ground = $100 \times \frac{120}{180} = 67\%$

FIGURE 3-8. WINDOW EMISSIVITY LOOK ANGLES

The various temperatures are (@ 15 kVA constant)

Sky = -50°F = 410°R

Roof = 80°F Avg. = 540°F

Window = 85°F Avg. = 545°R

Back = 78°F = 538°R

Floor = 84°F Avg. = 544°R

Ground = 74°F = 534°R in vicinity of rotodome

Ground = 62°F = 522°R remote from rotodome

The various emissivities are:

Sky = 1.0

Roof = 0.91

Window = 0.91

Back = 0.91

Floor of rotodome - 0.882 (painted aluminum)

Macadam/concrete = 0.8 (under rotodome)

Ground = 0.8

At 13.5 kVA the radiative heat loss as tested was:

$$Q = 0.171 \times 10^{-8} \Big[0.91 \times 0.81 \times 269 \times (540^4 - 410^4) + \text{roof to sky}$$

$$0.8 \times 0.91 \times 0.19 \times 269 \times (540^4 - 524^4) + \text{roof to ground}$$

$$0.91 \times 0.33 \times 104.5 \times (545^4 - 410^4) + \text{window to sky}$$

$$0.8 \times 0.91 \times 0.67 \times 104.5 \times (545^4 - 524^4) + \text{window to ground}$$

$$0.91 \times 0.33 \times 104.5 \times (538^4 - 410^4) + \text{back to sky}$$

$$0.8 \times 0.81 \times 0.67 \times 104.5 \times (538^4 - 524^4) + \text{back to ground}$$

$$0.8 \times 0.882 \times 153 \times (544^4 - 534^4) \Big] \text{ floor to macadam}$$

Q = 29,065 BTU/HR

Q = 8.517 kW dissipated due to radiation during test conducted at San Diego.

3.2.1.3 Convective Mode

The third mode of heat loss is also a major mode. The convection loss is a function of a number of factors:

a) Physical orientation of the surface in question, i.e., vertical or horizontal, top or bottom;

b) Physical characteristics of surface in question, i.e., cylindrical, flat, spherical;

c) Length of path for convective boundary layer against surface in question;

d) Total surface area;

e) Surface roughness;

f) Wind;

g) Viscosity of air;

h) Coefficient of heat conductivity for air;

and other coefficients governed by combinations of the above factors, as well as boundary layer thickness and overall dimensions of the rotodome (diameter). These coefficients are Reynolds Number, Nusselt Number, Prandtl Number and Grashof Number.

For the case of the rotodome, as tested, on a windless night (or day) the convective heat loss is simply a function of the bouyancy effects and viscous forces due to the density change of the air in proximity to the rotodome caused by heating. The (Gr) Grashof Number may be considered as a ratio which mathematically characterizes this effect.

$$G_r = \frac{g\beta\Delta T d^3}{\nu^2}$$

where:

g = acceleration of gravity

β = coefficient of volumetric expansion

ΔT = difference in temp. of rotodome surface and the ambient air

d = a linear dimension

ν = the kinematic viscosity

or the Rayleigh Number could be used interchangeably:

$$R_a = \frac{g\beta\Delta T d^3 C\rho}{\nu K}$$

$$R_a = Gr\ Pr$$

From our case for the window: (in SI units)

$$R_a = \frac{9.81 \times (3.38\times10^{-3}) \times (28.33-16.67)(1.22)^3 \times 1.005 \times (1.18)^2}{1.81 \times 10^{-5} \times 2.82 \times 10^{-5}}$$

$= 1.94 \times 10^9$ which is in the turbulent regime

and for the roof

$$R_a = \frac{9.81 \times (3.38\times10^{-3})(26.91-16.67)(5.49)^3\ 1.005(1.18)^2}{(1.81\times10^{-5}) \quad \times \quad (2.82\times10^{-5})}$$

$= 154 \times 10^9$, which is in the turbulent regime and for the back side:

$$R_a = \frac{9.81 \times 3.38 \times 10^{-3}\ (23.33-16.67)(1.22)^3\ 1.005(1.18)^2}{510 \times 10^{-12}}$$

$R_a = 1.1 \times 10^9$, just turbulent.

Heat loss from Table 4-3 of ASHRAE Handbook.

for roof C = 1.63 BTU/Hr-Ft^2 - °F

for sides C = 1.60 BTU/Hr-Ft^2 - °F (45° slope)

for floor C = 1.08 BTU/Hr-Ft^2 - °F

Then Q = ΣhA T

= 1.63 x 269 x 18.5 + roof

1.60 x 104.5 x 12 + back

1.60 x 104.5 x 21 + window

1.08 x 152 x 18.3 + floor

Q = 16,633 BTU/hr

= 4.875 kW

3.2.1.4 Summation of Heat Losses

The sum of the heat losses then are:

Q = conductive + radiative + convective

= 0.002 + 8.517 + 4.875 = 13.4 kW
or 13.4 kVA

This agrees within 0.8 percent of the ammeter reading for power consumption.

3.2.2 Heat Loss-Verification of Heat Transfer Coefficients

The next problem is to verify the coefficients of heat transfer through the various regions of the rotodome.

From Appendix Hexcel data, we obtain the following values:

For the floor, at a mean temperature of 92°F:

U = 0.925 x 4.1 BTU/hr-ft^2 °F.

= 3.79 BTU/hr-ft^2 °F.

This should equate to that lost via convection and radiation for the same area:

$$\Sigma U = \frac{1}{\frac{1}{3.79} + \frac{1}{1.65}} = 1.15$$

/ inside film coefficient

$Q = \Sigma UA\Delta T + 1.15 \times 152 \times 24.67 = 4{,}310$ BTU/Hr:

vs $Q = hA\Delta T + 0.171 \times 10^{-8} A \times .882\ (544^4 - 534^4) \times 0.8$

$= 1.08 \times 152 \times 18.3 \times 0.171 \times 10^{-8} \times 153 \times 0.882 \times .8(4.93 \times 10^9)$

$= 3{,}004 + 1.157$

$+ 4{,}161$ BTU/hr

The comparison of 4,310 to 4.161 is within 4 percent. This was done using only the ΔT through the floor. Solving backwards to obtain a new ΔT we get 25.3°F for the total ΔT to inside ambient air.

A similar comparison can be made for the roof where the core is 1" thick aluminum Hexcel with fiberglass facing from Hexcel data for a mean temperature of 104°F, U = 3.3. Combining this U with the inside air film

$$\Sigma U = \frac{1}{\frac{1}{U_1} + \frac{1}{U_2}} = \frac{1}{\frac{1}{3.3} + \frac{1}{1.65}} = 1.1 \text{ BTU/hr-ft}^2\ ^\circ\text{F}$$

The heat flow is then:

$Q = UA\Delta T$

$= 1.1 \times 269 \times 46.5$

$= 13{,}800$ BTU/hr

This should equate to the convective and radiative loss:

$$Q = A\left\{h\Delta T + .171 \times 10^{-8} \times .91\left[.81 \times 540^4 - 410^4 + .8 \times .19\,(540^4 - 524^4)\right]\right\}$$

$$= 269\left\{1.63 \times 18.5 + .156 \times 10^{-8}\left[.81 \times 56.77 \times 10^9 + .152 \times 9.64 \times 10^9\right]\right\} = 269\,(30.16 + 73.84)$$

$$= 27{,}974 \text{ BTU/hr}$$

The comparison is off by 51 percent which can be accounted for by turbulence in the inside air which would increase the heat exchange. Solving backwards again and adding 0.7° for the ΔT through the inside boundary layer we get a new U of:

$$U = \frac{Q}{A\Delta T} = \frac{28{,}200}{269 \times 47.2} = 2.22$$

and an inside film coefficient of 6.8 which means the air near the roof is being stirred up quite a bit.

For the back which is a 1-inch thick phenolic core with fiber glass facings, from Hexcel data, the U= 0.8 BTU/hr-ft^2 °F for a mean temperature of 90°F.

$$U = \frac{1}{\frac{1}{.8} + \frac{1}{3.0}} = 0.632$$

then $Q = UA\Delta T$

$= 0.632 \times 104.5 \times (147-77)$ assumed inside temperature.

$= 4{,}620$ BTU.

From radiative and convective losses we calculate:

$$Q = A\left\{h\Delta T + 0.171 \times 10^{-8} \times 0.91 \left[0.8 \times 67\ (538^4-524^4) + 0.33\ (538^4-410^4\right]\right\}$$

$$= 104.5\left\{1.6 \times 12 + 0.156 \times 10^{-8}\left[4.49 \times 10^9 + 18.32 \times 10^9\right]\right\}$$

$$= 104.5\ (19.2+35.59)$$

$$= 5{,}726 \text{ BTU's.}$$

The difference here is 19 percent and is probably off because the inside back temperature is probably higher and also the U value of the sandwich is higher. Since the average back temperature is probably not greater than 157°F the actual U for the back is probably on the order of 0.85 for the Hexcel material faced with fiberglass rather than 0.5 chosen above. Note that the coefficient is very dependent upon cell size.

For the window a K value of 0.0975 $\frac{\text{BTU - ft}}{\text{hr - ft}^2\text{°F}}$

by ASHRAE for fiberglass @ 100°F. Extrapolating we obtain a value of 0.0997 for 105°F, the average temperature of the rear window. The heat flow then predicted would be:

$$Q = UA\Delta T$$

where $U = \frac{1}{\frac{L}{K} + \frac{1}{h}}$

where L = 0.19" window thickness = 0.16 ft.

K = 0.0997

h = 3.0 BTU/ft^2-hr °F

U = 2.02 BTU/ft^2-hr °F

$$Q = 2.02 \times 104.5 \times 37.67$$

$$= 7973 \text{ BTU/hr.}$$

The measured and calculated heat loss, however, was:

$$Q = A\left\{h\Delta T + 0.171 \times 10^{-8}\left[0.67 \times 0.8 \times 0.91\ (545^4-524^4)\right.\right.$$

$$\left.\left. + 0.33 \times 0.91 \times (545^4-410^4)\right]\right\}$$

$$= 104.5\left\{1.6 \times 21 + 0.171 \times 10^{-8}\left[6.26 \times 18\right] \times 10^9\right\}$$

$$= 104.5\ (33.6+41.5)$$

$$= 7{,}848\ \text{BTU/hr.}$$

Consequently, the more probable value of U above is 1.99, which yields a K of 0.0940 or an L of 0.19 inches average window thickness or some combination of the two.

Summing the various areas we see the following heat losses and percentages, as tested:

Roof	Q = 27,974 BTU/hr	= 8.20 kW	= 61%
Window	= 7,848 BTU/hr	= 2.30	= 17%
Back	= 5,726 BTU/hr	= 1.68	= 13%
Floor	= 4,161 BTU/hr	= 1.22	= 9%
		Σ 13.4 kW	100%

We see the comparative values of K's and U's from published data below:

	Published	As Tested	% Difference
Roof	3.3	3.3	-0-
Window	0.997	0.0940	-5.7
Back	0.5 to 0.8	0.85	+6.25
Floor	3.79	3.79	-0-

The differences noted can be attributed to a multiplicity of factors, such as material thickness, materials, bonding agents, measured data, film thickness of boundary layers and degree of momentum in the boundary layers. The entire calculation set also

ignored seams as they were not far different in temperature from the surrounding materials and contribute a rather small percentage of the total area.

3.2.3 Prediction of De-Icing Capability (Rotating Rotodome)

A worst case analysis will be made of the meteorological conditions contributing to the icing of the rotodome. The gating parameters will be determined from the research of Section 2 and the source data in the Appendices hereof.

Largest mean droplet diameter	= 52 microns
Maximum 10-year wind speed (icing)	= 37 MPH
Maximum liquid water content	= 0.89 gms/m^3
Lowest icing temperature	= -17°C = 1.4°F

The heat balance equation is:

$$Q_a = Q_{cond} + Q_r + Q_s + Q_e + Q_{conv} - Q_f - Q_k$$

where:

- Q_a = Heat from available power source
- Q_{cond} = Conductive heat loss
- Q_r = Radiant heat loss
- Q_s = Sensible heat loss to impinging water
- Q_e = Heat of evaporation of impinging water which is not flung off
- Q_{conv} = Convective heat loss
- Q_f = Skin friction heat gain
- Q_k = Kinetic energy of impinging water

Before proceeding it is informative to make an extrapolation of the test data to determine heat fluxes for the various regions of the rotodome. The 30 kW of available power is compared to 13.4 kVA from the test:

$$Q = 8.2 \text{ kW} \times \frac{30 \text{ kW}}{13.4 \text{ kVA}} = 18.36 \text{ kVA} \quad \text{Roof} = 61\%$$

$$Q = 2.3 \text{ kW} \times \frac{30 \text{ kW}}{13.4 \text{ kVA}} = 5.15 \quad \text{Window} = 17\%$$

$$Q = 1.68 \text{ kW} \times \frac{30 \text{ kW}}{13.4 \text{ kVA}} = 3.76 \quad \text{Back} = 13\%$$

$$Q = 1.22 \text{ kW} \times \frac{30 \text{ kW}}{13.4 \text{ kVA}} = 2.73 \quad \text{Floor} = 9\%$$

$$100\%$$

$$\Sigma = 30 \text{ kW}$$

It can readily be appreciated that the back of the rotodome is in the most trouble with only:

$$\frac{\text{watts}}{\text{unit area}} = \frac{3,760}{104.5 \times 144} = 0.25 \text{ watts/in}^2$$

Remember from Section 1 that the TACAN antenna required 0.655 watts/sq. in. to keep it clear.

By returning to the original design and insulating the floor, one could obtain:

$$18.36 + 2\ (5.15) = 28.66 \text{ kW}$$

Comparing this to 30 kW, the roof would receive 19.22 kW and the windows 10.78 kW for a new density of:

$$\frac{10780}{209 \times 144} = 0.36 \text{ watts/in}^2 \text{ for the windows}$$

and

$$\frac{19220}{269 \times 144} = 0.50 \text{ watts/in}^2 \text{ for the roof.}$$

In order to find the icing capability it is necessary to start with some basic assumptions:

1) That the rotodome is spinning at 60 RPM;

2) That the rotodome surface temperature is > 31°F;

3) That the rotodome rear window is as built from 1" thick phenolic core;

4) After conductive losses, sensible heat losses, evaporative losses and kinetic heat gains, the balance remaining of the heating budget is distributed through the rotodome in the same manner as during the test, and is lost via convection and radiation.

We will start by predicting the conductive losses using the above assumptions for a 37 mph wind.

$$Q_{cond} = 2 \text{ watts} \times \frac{30 \text{ kVA}}{13.4 \text{ kVA}} = 5 \text{ watts (negligible)}$$

Q_F = The skin friction heat gain

This is a function of drag coefficient for skin friction.

Drag= C_{fqS}

where

$C_f = 0.427/(\log R_e - 0.407)^{2.64}$

$R_e = \frac{VD}{\nu} = \frac{54 \times 18}{141 \times 10^{-6}} = 6.94 \times 10^6$

$q = 1/2\rho v^2$

$= 0.5 \times \frac{0.0818}{32.2} \times 54^2$

$= 3.70 \text{ lbs/ft}^2$

$S = 478 \text{ ft}^2$

$C_f = 3.13 \times 10^{-3}$

Drag $= 3.13 \times 10^{-3} \times 3.7 \times 478$

$= 5\ 54 \text{ lbs.}$

H.P. $= \frac{D \times \omega \times \bar{R}}{550 \text{ ft-lbs/sec}}$ $\omega = 2\pi$ $\bar{R}$ = 7.6 ft avg. for wetted surface area.

$= .48$

The recovery factor for turbulent flow is 0.92 (the balance is lost as noise).

Q_F = 0.92 x 0.48 H.P.

= 0.442 H.P. = 0.330 kW

Q_s = Sensible heat loss to impinging water.

In order to establish sensible heat loss, a capture rate must be determined for the rotodome.

Capture rate is a function of:

Scale Factor $\psi = \frac{9\ c(\rho a)}{a(\rho d)}$

and Reynolds modulus $R_u = \frac{2\ a\ (\rho\ a)\ U}{(\mu a)}$

where:

a = Drop radius

c = A significant dimension in the flow field

ρa = Air density

ρd = Drop density

U = Free Stream velocity

μa = Air viscosity

The capture rate (lbs/sec) is:

$$W = E_m\ U\ (2\ c)\ L\ w$$

where:

E_m = Fractional catch (see below)

L = Length

w = Liquid water content of air

$E_m = f\ (k, \phi)$

$K = R_u/\psi$ and $\phi = R_u \times \psi$

Using the height of the radome as 2c = 5.92 ft as the smallest dimension presented to the free stream

$$K = \frac{2}{9} \times \frac{1.94 \times (8.53 \times 10^{-5})^2 \times 54}{.23 \times 10^{-6} \times 2.96}$$

(letting a = 26 micron = 8.53×10^{-5} ft)

$$= .24$$

$$\phi = \frac{18 \times 0.00238^2 \times 2.96 \times 54}{.34 \times 10^{-6} \times 1.94}$$

$$= 3.7 \times 10^4$$

E_m then = 0.008

$$W = 0.008 \times 54 \times 5.92 \times 16.67 \times 5.56 \times 10^{-5}$$

(letting: $L = 2\bar{R} = 2 \times 8.337$ ft

and $w = 0.89$ gm/m^3 = 5.56×10^{-5} lbs/ft^3)

$W = 2.36 \times 10^{-3}$ lbs/sec = 8.53 lbs/hr.

8.53 lbs/hr ÷ 478 sq.ft. = .018 lbs/ft^2 - hr

Q_s = .018 lbs/ft^2 - hr x 29.6°F = .527 BTU/ft^2 - hr

Total $Q_s = .527 \times 478 \div 3414 = 0.74$ kW

Q_e = Heat of evaporation

Of the 8.53 lbs of water/hour what portion is flung off and what portion evaporates before it is flung off?

This is a function of the length of time it takes to accelerate the impinged water droplet to tip velocity.

$$T = \sqrt{\frac{2x}{\alpha}}$$

where:

x = Avg. path length
(Assumed 1/2 window ht. x sin avg. window inclination) = 0.663 ft.

α = F x 32.2 fps = 32g fps, where

$F = \frac{\omega^2 R}{g}$; $\omega = 2\pi$ rad/sec; R = Avg radius = 8.337

T = 0.0635 sec

The portion of water which is evaporated is then found from the relationship:

$$T = \frac{\lambda \rho}{2K} \left[\frac{(x_{FF}^2 - x_{IF}^2)}{T_{ow} - T_s} \right] *$$

where:

T = Time

λ = 1,065 BTU/lb (Ht. of Evap.)

ρ = 62.4 lbs/ft^3

K = 1.089 x 10^{-3} BTU/sec °F ft^2 in.

x_{IF} = Initial Film Thickness (Inches)

x_{FF} = Final Film Thickness (Inches)

T_{ow} = Temp of Outside World

T_s = Temp of Skin (rotodome)

The initial film thickness is a function of impinging droplet size.

D = 52 microns (droplet)

R = Radius of hemisphere after impact with radome

$V_s = 4/3\ \pi\ R_s^3$ for sphere

$V_h = 2/3\ \pi\ R_h^3$ for hemisphere

---

* From: Thin Wiped Film Heat Transfer Studies by Jusionis, 1960, Univ. of Cal. L.A. Equation 13.

$$V_s = V_h \therefore R_h = 32.7 \text{ microns}$$

The avg. film thickness $x_{IF} = \frac{4R}{3\pi}$

$$= 13.88 \text{ microns}$$

$$= 5.43 \times 10^{-4} \text{ in.}$$

$$x_{FF} = \sqrt{\frac{.0635 \times 2 \times 1.089 \times 10^{-3} \times (-9)}{1{,}065 \times 62.4} + (5.43 \times 10^{-4})^2}$$

$$x_{FF} = 5.25 \times 10^{-4} \text{ in.}$$

$$\% \text{ Evap} = \frac{5.43 - 5.25}{5.43} \times 100 = 3.31\%$$

Q_e = 8.53 lbs x .331 x 1,065 BTU/hr

= 301 BTU/hr = 0.088 kW

Q_k = The kinetic energy gained from the impinging water droplets.

K.E. = $1/2\ MV^2$

= 0.107 ft-lbs/sec

= 1.94×10^{-4} H.P.

Q_k = 0.2 watts (negligible)

Q_c = The heat loss due to convective heat transfer. This loss is a function of:

Nusselt Number N_{NUL}

Prandtl Number N_{PR}

Reynolds Number N_{REL}

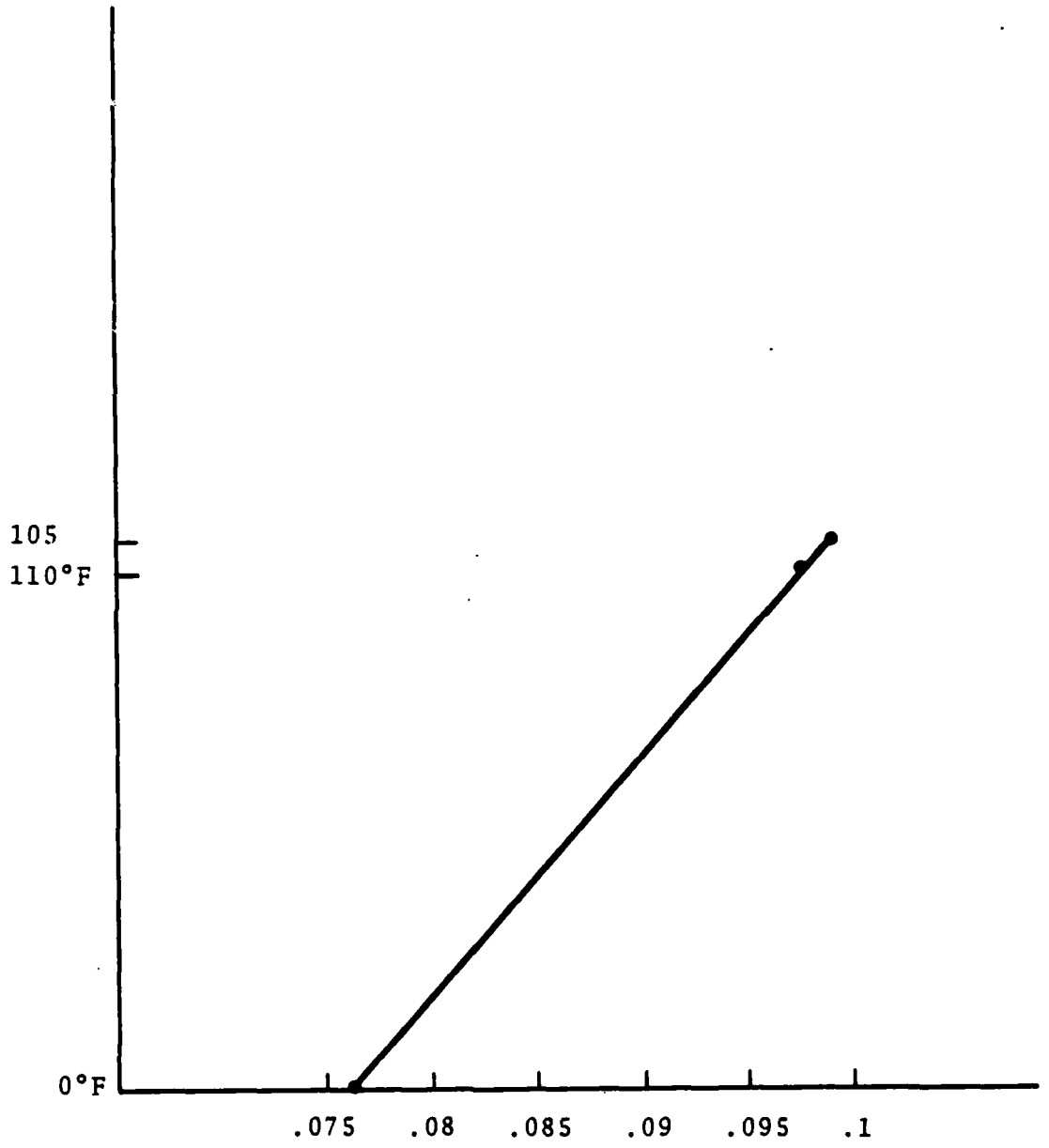

FIGURE 3-9. COEFFICIENT OF THERMAL CONDUCTIVITY FOR FIBERGLASS VS TEMPERATURE

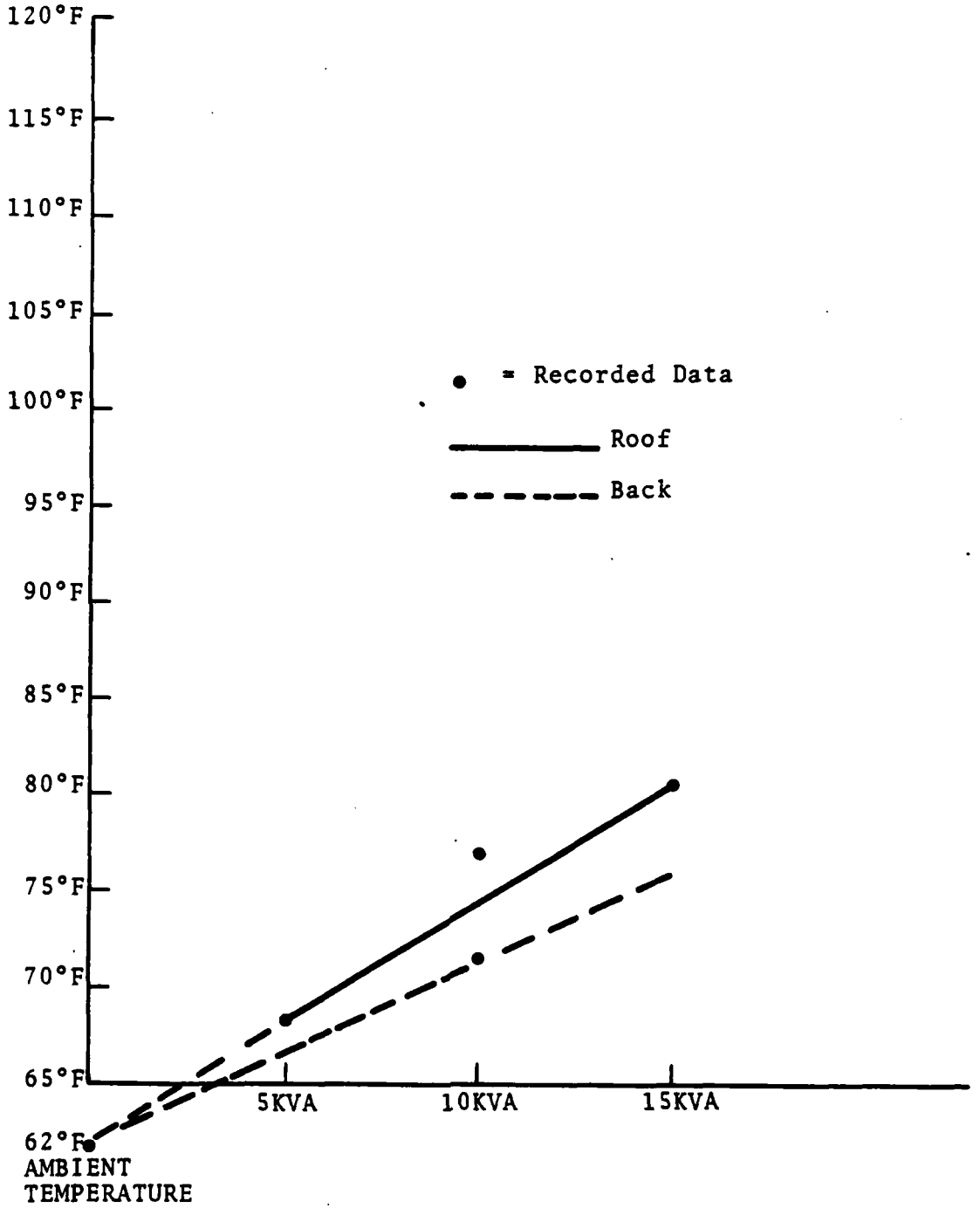

FIGURE 3-10. OUTSIDE BACK TEMPERATURE VS ROOF TEMPERATURE FOR VARIOUS kVA

$$N_{NUL}^{*} = .036\ (N_{PR})^{.33}\left[(N_{REL})^{.8} - 23{,}100\right]$$

Averaged for Laminar & Turbulent Regimes.

Assuming a transition from Laminar to Turbulent Regimes at $N_{REL} = 500{,}000$. For the roof:

$$N_{REL} = \text{Mean Dia} \times V_{fps} \times 3600 \text{ sec/hr} \div .5068 \text{ ft}^2\text{/hr}$$

$$= \frac{16.88^{**} \times 54 \times 3600}{15068}$$

$$= 6.46 \times 10^6$$

The average film coefficient for the radome is a function of mean boundary layer temperature, i.e., $\frac{31^\circ + 1.4^\circ}{2} = 16.2^\circ$.

At 16.2°F

$\nu = 0.498 \text{ ft}^2\text{/hr}$

$K = .0135 \text{ BTU/hr-ft} - {}^\circ\text{F}$

$N_{PR} = 0.722$

$V = 54 \text{ fps}$

$$N_{NUL} = 0.036 \times (0.722)^{.33} \times \left[(6.46 \times 10^6)^{.8} - 23{,}100\right]$$

$$= 8{,}327$$

$$h_{AVG} = N_{NUL} \times \frac{K}{L} \qquad L = \text{Mean Path LN} = 18.23 \text{ ft}^{**}$$

$$= 8{,}327 \times \frac{0.0135}{18.23}$$

$$= 6.17 \text{ BTU/ft}^2 - \text{hr } {}^\circ\text{F}.$$

For the window:

$$N_{REL} = \text{Mean Dia} \times V \times 3{,}600 \div .5068 \text{ ft}^2\text{/hr}$$

$$= \frac{16.45 \times 54 \times 3{,}600}{0.5068} \qquad \bar{R} = 98.71'' = 8.23'$$

$$= 6.31 \times 10^6$$

*From Chapman, Heat Transfer 2nd Ed, equation 8.9
**See para 3.2.4

$$N_{NUL} = 0.036 \times (0.722)^{.33} \left[(6.31 \times 10^6)^{.8} - 23{,}100\right]$$

$$= 8{,}158$$

$$h_{AVG} = N_{NUL} \times \frac{K}{L}$$

$$= 8{,}158 \times \frac{0.0135}{25.86} \qquad L = \pi\bar{R} = 25.86 \text{ ft}$$

$$= 4.26 \text{ BTU/ft}^2 \text{ - hr } ^\circ\text{F.}$$

For the floor:

$$N_{REL} = \frac{9.24 \times 54 \times 3600}{0.5068} = 3.54 \times 10^6$$

$$N_{NUL} = 0.036 \times 0.722^{.33} \left[(3.54 \times 10^6)^{.8} - 23{,}100\right]$$

$$= 4{,}870$$

$$h_{AVG} = 4.87 \times 10^3 \times \frac{0.0135}{9.24}$$

$$= 7.11 \text{ BTU/ft}^2 \text{ - hr } ^\circ\text{F}$$

$$Q_c = \Sigma\, h_i A_i \times \Delta T$$

$$= (6.17 \times 269 + 4.26 \times 209 + 7.11 \times 153) \times 29.6$$

$$= 108{,}000 \text{ BTU/hr} = 31.5 \text{ kW}$$

with the floor insulated

$$Q_c = (6.17 \times 269 + 4.26 \times 209) \times 29.6$$

$$= 75{,}482 \text{ BTU/hr}$$

$$= 24 \text{ kW}$$

The final heat loss to be calculated is the radiant heat loss. From the test data and extrapolations therefrom, as seen on the next page, we can estimate the surface temperatures of the various regions of the rotodome. First several assumptions are made:

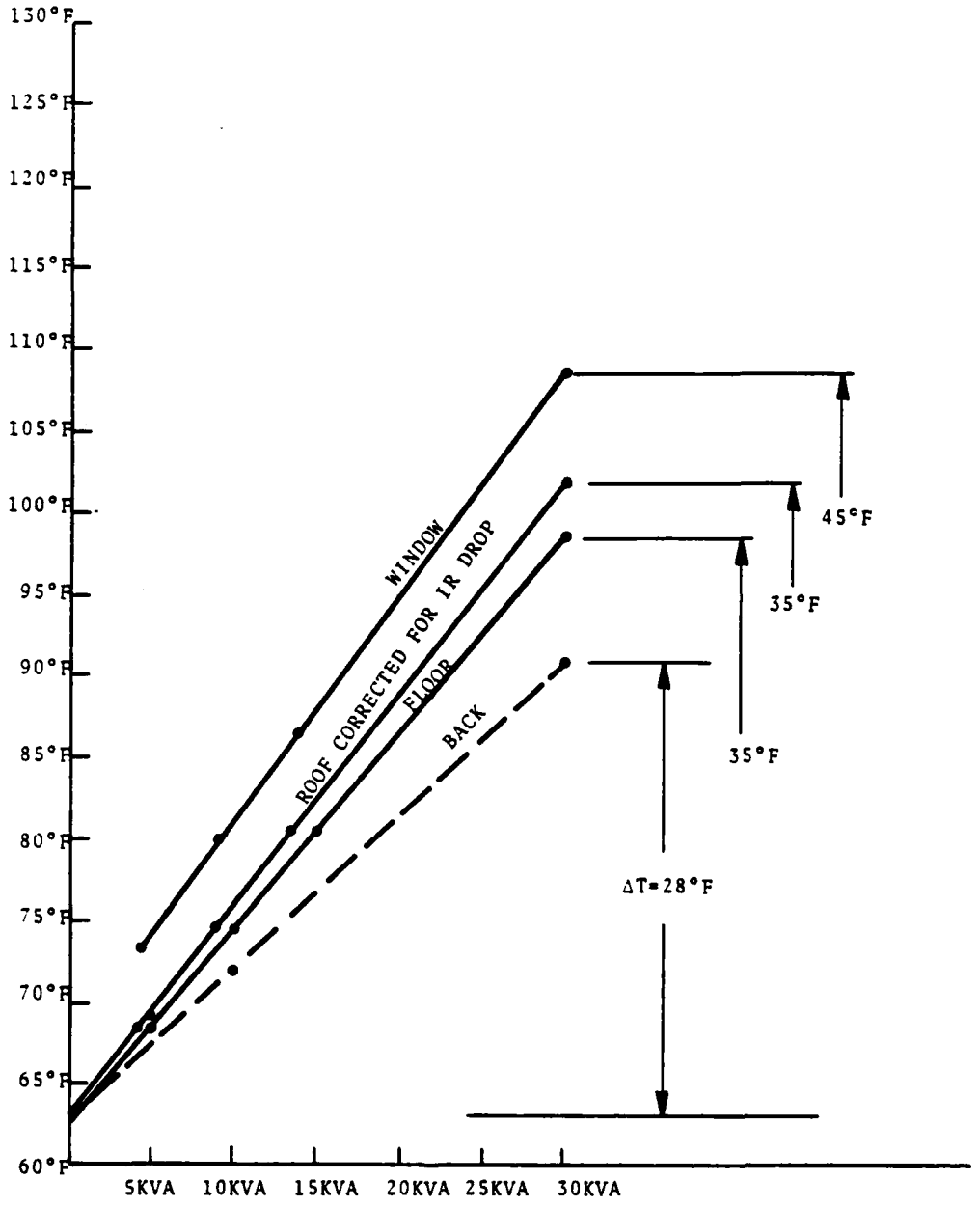

FIGURE 3-11. OUTSIDE SKIN TEMPERATURES EXTRAPOLATED FOR VARIOUS AREAS OF ROTODOME

1) There is a black sky at night for a worst case;

2) There is already snow on the ground so its temperature will be the temperature to which we will radiate on the ground;

3) The snow is at the ambient temperature of 1.4°F;

4) The back of the rotodome = 31°F

5) Emissivity of snow is 0.9.

Again: $Q = 0.171 \times 10^{-8} \Sigma \varepsilon_1 \varepsilon_2 F_{12} A_i (T_s^4 - T_o^4)$

and $Q = 0.171 \times 10^{-8}\ 0.91 \times 0.81 \times 269\ (502^4 - 410^4)$ roof to sky

$+ 0.91 \times 0.9 \times 0.19 \times 269\ (502^4 - 461.4^4)$ roof to ground

$+ 0.91 \times 0.33 \times 104.5\ (508^4 - 410^4)$ window to sky

$+ 0.91 \times 0.9 \times 0.67 \times 104.5\ (508^4 - 461.4^4)$ window to ground

$+ 0.91 \times 0.33 \times 104.5\ (491^4 - 410^4)$ back to sky

$+ 0.91 \times 0.9 \times 0.67 \times 104.5\ (491^4 - 461.4^4)$ back to ground

$+ 0.882 \times 0.9 \times 153\ (498^4 - 461^4)$ floor to ground

$Q = 23{,}385$ BTU/hr

$Q_R = 6.85$ kW

The total energy flow equation then is (for the idealized case above):

$$Q = Q_R + Q_S + Q_E - Q_F - Q_K + Q_{cond} + Q_{conv}$$

$$= (6.85 + 0.074 + 0.088 + 22.1 \cdot 0.330 - 0.0002 + 0.005)\ \text{kW}$$

$Q = 29.45$ kW (required to prevent ice with 37 MPH wind at 1.4°F ambient)

3.2.3.1 De-Icing Capability Conclusions

The analysis indicates that 30 kW of heater power are adequate to perform the de-icing function (30 knotts available versus 29.45 required). De-icing the floor is a potential problem. A .06 inch layer of insulation on the floor, weighing less than 10 pounds would enhance the de-icing balance of the rotodome and would reduce the total power required and thereby provide power cost savings. Calculations of the potential cost savings, for sites with icing climatology are given below for a 15 year period.

Number of alerts per year	46 alerts
Hours per alert	15 hours
Duty cycle during alert (15 MPH wind)	77 percent
Number of years	15 years
Rotodome power	30 kW
Potential reduction in power (*Range 9% to 26%*)	12%
Power cost	$0.057/kWh

Savings per site = 46 x 15 x .77 x 15 x 30 x 0.12 x 0.057

= $1635 per site

Potential reduction in power	= 12%
Cost per kwH	= $0.057
Number of years	= 15 year
Number of alerts per year	= 46 alerts
Duty cycle with 15 MPH winds	= 77%
Rotodome heat	= 30 kW

Savings per site = 0.12 x 0.057 x 15 x 46 x .77 x 30

3.2.4 Calculation of Mean Dia.& Path Length for Roof

Mean Path
Length for Roof:

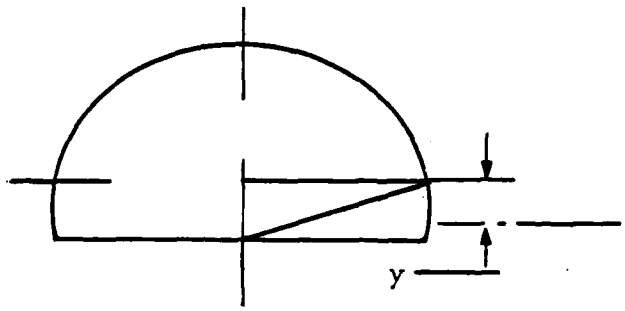

$$y = \frac{4r}{3\pi}$$

$$\frac{4 \times 9}{3 \times \pi} \quad 3.82 \text{ ft}$$

$$1 = 2(9^2 - 3.82^2)^{1/2} = 8.15 \text{ ft} \times 2 = 16.3 \text{ ft}$$

$$16.3 \times \frac{20.13}{18} = 18.23 \text{ ft}$$

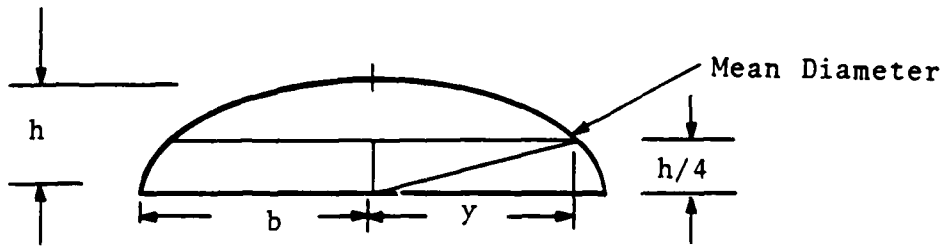

Elevation View

$$\frac{x^2}{a^2} + \frac{y^2}{b^2} = 1$$

$$h = a = 2.21 \text{ ft}$$

$$x = \frac{h}{4} = .55 \text{ ft}$$

8.44 = y

x 2

16.88 Mean Diameter

3.2.5 Raindrop Trajectory Analysis

REF:

MIL-STD-210B
15 Dec. 1973
Para. 5.1.11.2

Drop Dia 0.5 to 1.4 mm.

0.5 mm = 500 micron = 0.0197' Dia.

= 0.0008' Radius

0.5 to 1.4 = 0.95 mm Avg. = 0.0016' Avg. Rad.

$$K = \frac{2}{9} \frac{(82 \times 10^{-5})^2 \times 107}{0.34 \times 10^{-6} \times 2.96} = 15.9 \text{ smallest}$$

$$K = 57 \text{ Average}$$

$$= \frac{18 \times 0.00238^2 \times 2.96 \times 107}{0.34 \times 10^{-6} \times 1.94}$$

$$K = 5 \times 10^4 \text{ maximum}$$

$E_m = 0.605$ Smallest

0.79 Avg.

$W = 0.605 \times 107 \times 5.92 \times 16.67 \times 2.24 \times 10^{-6}$

= 0.0187 lbs/sec (Avg.) = 67.34 lbs/hr

16 mm/hr Specified

31.2 mm/min = 158,624 drops/m^3

From: Fig. LL-7 of Myron Tribus, Mod. Icing Technology, E.R.I. U. of M. 1952.

16 mm/hr = 1,355 drops/m^3/min

= 126 drops/ft^3 min

$V = \frac{4}{3} \pi R^3 = 1.7. \times 10^{-8}$ ft^3

126 drops = 2.156×10^{-6} ft^3 H_2O

= 2.24×10^{-6} lbs/ft^3 sec

= 1×10^{-4} lbs/min

= 0.0081 lbs/hr

$\theta_m = 74°$

β = 89% catch at stagnation zone.

If window is idealized to 90° of a cylinder then 74° is analagous to

$S = R\theta$

$S = 67.7 \times \frac{74}{57.3} = 87.4$

$\frac{74}{90} = 0.822$

$l = R\theta$

$= \frac{92.49 \times 60}{57.3}$

$= 96.8"$

Capture Zone $= \frac{80"}{2}$

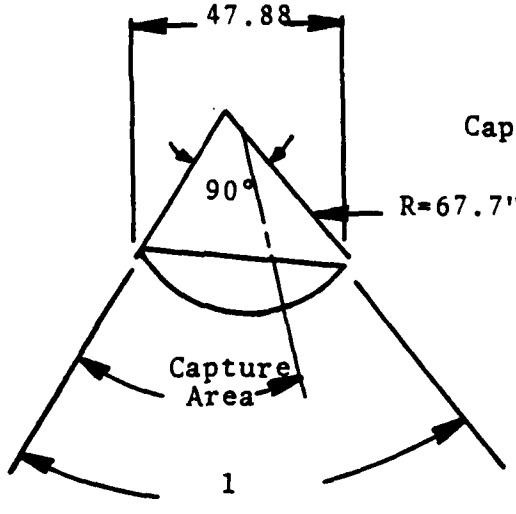

This would be for a horizontal rain.

Using 16.88' as avg. dia.

8.44 as avg. rad.

Then $K = 20.2$

$\phi = 5 \times 10^4 \times 2.85 = 1.4 \times 10^5$

and $E_m = 0.58$

$W = 49.4$ lbs/hr

$\theta_m = 62°$

$\beta = 74\%$

The foregoing analysis is a hypothetical case for raindrops coming at the radome in a horizontal direction. In actuality, the drops are falling at some angle which is a function of:

$$F = Ma$$

where the terminal velocity of the rain drop is in equilibrium between its aerodynamic drag, which is a function of its diameter and density, and the acceleration of gravity. It is assumed that the wind is laminar and that by the time the drop has fallen to the height of the rotodome (above ground) that it has terminal velocity and is moving somewhere near the free stream velocity as regards the horizontal component of velocity, i.e.,

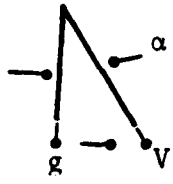

α is a function then of the incident laminar flow regime and the raindrop drag.

It works out that there is an infinitely varying regime of raindrop diameters which typically vary from 52 microns in diameter to 6.4 mm in diameter combined with winds from 0 to 85 MPH that will vary α from 0 to 90 degrees with the smaller diameters approaching 90 degrees in increasing winds.

The writer made one observation with small diameter raindrops in an 8 knot wind where the drops were falling at 35° to the vertical.

For droplets less than 52 microns in diameter, the water content of the air looks like an aerosol and light winds will transport the water content horizontally. This is the case analysed in the de-icing (Thermal) analysis. Then the catch rate of the rotodome window will agree much better with the recorded data of Langmuir and Boldgett cited therein.

Conclusion

The 0.0187 lbs/sec average incident rain found above spread over $\frac{80}{96.8}$ x 209 = 173 sq.ft of window is equal to 10.8 lbs x 10^{5}/ sq.ft/sec which is equal to a layer on the window of 2.08 x 10^{-5} inches of water. It should be noted that this water is constantly being flung off as the average raindrop is spun up to tip velocity within 0.065 seconds. The foregoing analysis is for a 16 mm/hour rainfall rate as specified, thus, the conclusion to be drawn is how much attenuation is experienced by a film of 2.08 x 10^{-5} inches of water spread over the uppermost 40" of the radome window.

3.2.6 Solar Gain

What internal temperature is reached due to solar gain?

Given:

Area of Floor = 153 sq.ft

Area of Roof = 269 sq.ft

Area of Window & Back = 104.5 sq.ft each

$$U_{roof} = \frac{1}{\frac{1}{3.3} + \frac{1}{1.65}} = 1.1 \text{ BTU/hr - °F - ft}^2$$

$$U_{window} = \frac{1}{\frac{1}{1.63} + \frac{0.016}{0.0946} + \frac{1}{1.63}} = 0.716$$

$$U_{back} = \frac{1}{\frac{1}{1.63} + \frac{1}{0.85} + \frac{1}{1.67}} = 0.416$$

$$U_{floor} = \frac{1}{\frac{1}{1.65} + \frac{1}{3.79} + \frac{1}{1.08}} = 0.556$$

Assumptions:

Outside ambient temperature = 120°F

Worst location in U.S.A. for solar incidence. Three hour steady state from 11:00 a.m. to 2:00 p.m. Outside skin temperature = 165°F.

Calculations:

$Q = UA \Delta T$

ΔT = 165°F - 140°F = 25°F (Initial assumption)

Equivalent temperature = 43° + 5° = 48°

(Correction number is 5)

From ASHRAE Fundamental Handbook TETO at 2 p.m. is 53°F, therefore use 53°F.

Roof gain is then:

$Q = UA\ \Delta T$

$= 1.1 \times 269 \times 53°$

$= 15{,}683$ BTUH

The loss through the window simultaneously is:

$Q = UA\ \Delta T$

$\Delta T = 120° - 140°F$ -- first assumption

$Q = 0.716 \times 104.5 \times -20$

$= 1{,}496$ BTUH

The loss through the back would be:

$Q = 0.416 \times 104.5 \times 20 = 869$ BTUH

The loss through the floor would be:

$Q = 0.556 \times 153 \times 20$

$= 1{,}701$ BTUH

Net heat gain is thus:

Q_{net} = Input - Output

$= 15{,}683 - (1496 + 869 + 1701)$

$= 1{,}428$ BTUH

This must either be exhausted or the internal temperature will climb higher. The internal temperature in that case would be:

$$\Delta T = \frac{Q}{AU} = \frac{15{,}683}{104.5 \times 0.716 + 104.5 \times 0.416 + 153 \times 0.556}$$

$\Delta T = 77°F.$

Inside temperature = 120°F + 77°F = 197°F.

The 197°F internal temperature is about equivalent to that reached by a white colored automobile on a very hot day. It

would not be any fun working inside the rotodome under these conditions, so a fan system might be employed to vent the rotodome before entering. Since a 120° day is not a very common occurrence, the condition can probably be tolerated without seriously damaging the rotodome. It should be noted that this temperature analysis is on a "shut down" and sealed up, no wind condition. If the rotodome were spinning, it would be self-cooling as the bounary layer would be thinner. If the wind were blowing, it would be cooler inside for the same reason. If the floor were insulated, it would aggravate the heating due to a hot solar day. The sandwich back on the rotodome acts like an insulator and helped to increase the interior temperature compared to the earlier design calculations.

3.2.7 Melting 4 mm of Ice

Consider 4 mm of ice to be melted from the radome rear window.

4 mm = 0.1576"

1" of ice = 5.256 lbs/ft^2

0.1576" = 0.828 lbs/ft^2

Latent heat of fusion = 144 BTU/lb of ice

0.828 x 144 = 119 BTU/ft^2/hr

This means the outside temperature is 32°F. What inside temperature is required locally to pump 119 BTU/ft^2/hr through the window?

$Q = UA\Delta T \qquad \Delta T = ?$

$Q = 119$ BTU/ft^2/hr

$$U = \frac{1}{1/h_w + 1/h_t}$$

$h_w = 0.85$ BTU/ft^2/hr for rear window (from test experience)

h_t = 3.0 BTU/ft^2/hr for forced convection (from test experience)

$$U = \frac{1}{1.176 + 0.333}$$

$$U = 0.663 \text{ BTU/hr/ft}^2 \text{ °F}$$

$$\Delta T = \frac{119}{0.663} = 179°F$$

T inside = 211°F

Extrapolating Test Data (Assumed)

ΔT = (157°F - 74°F) @ 13.5 kVA = 83°F (As tested)
ins. outside

ΔT = (216°F - 32°F) @ 30 kVA = 184°F (Extrapolated)
ins. outside

Obviously, it is not desirable to heat the inside of the radome to 211-216°F. However, experience has shown with the TACAN rotodome that ice falls off after 1 mm melts; therefore, if the difference in temperature from inside to outside is 1/4 as much (184/4) or only 46° the ice would be removed in 1 hour by the heaters with an inside temperature of only 46 + 32 ≈ 78°F. If the cut-off on the temperature control is set at approximately 140°F, then approximately 2-1/3 mm of ice could be melted in one hour or it would take only about 26 minutes to clear the window and back of 1 mm of ice. The roof would melt ice a little faster, but it would not drop off, due to the effect of gravity, quite so rapidly.

APPENDIX A

LIQUID WATER CONTENT OF AIR VS MEDIAN DROPLET DIAMETER

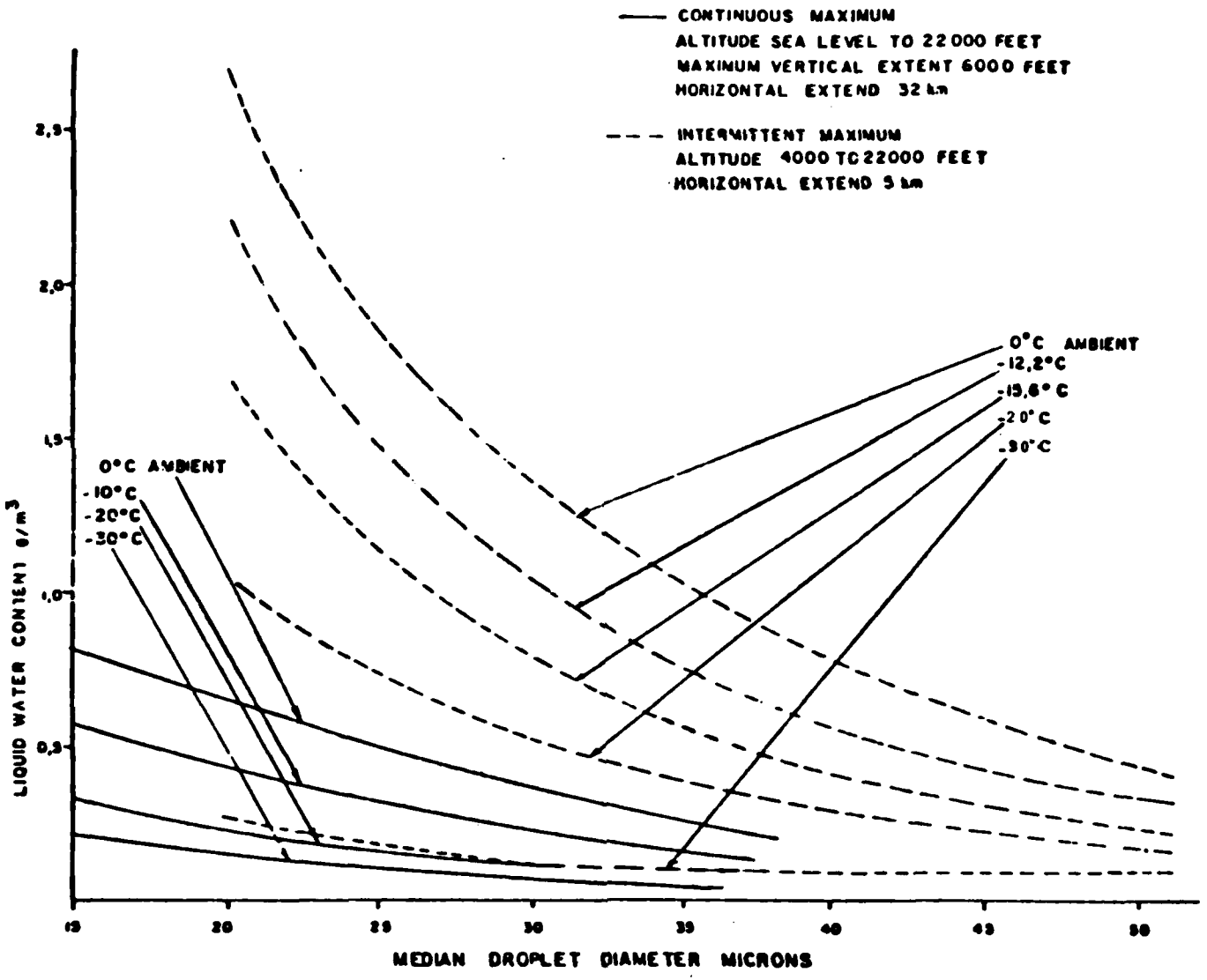

FIGURE A-1. LIQUID WATER CONTENT

APPENDIX B

ICING ENVELOPE TEMPERATURE VS ALTITUDE

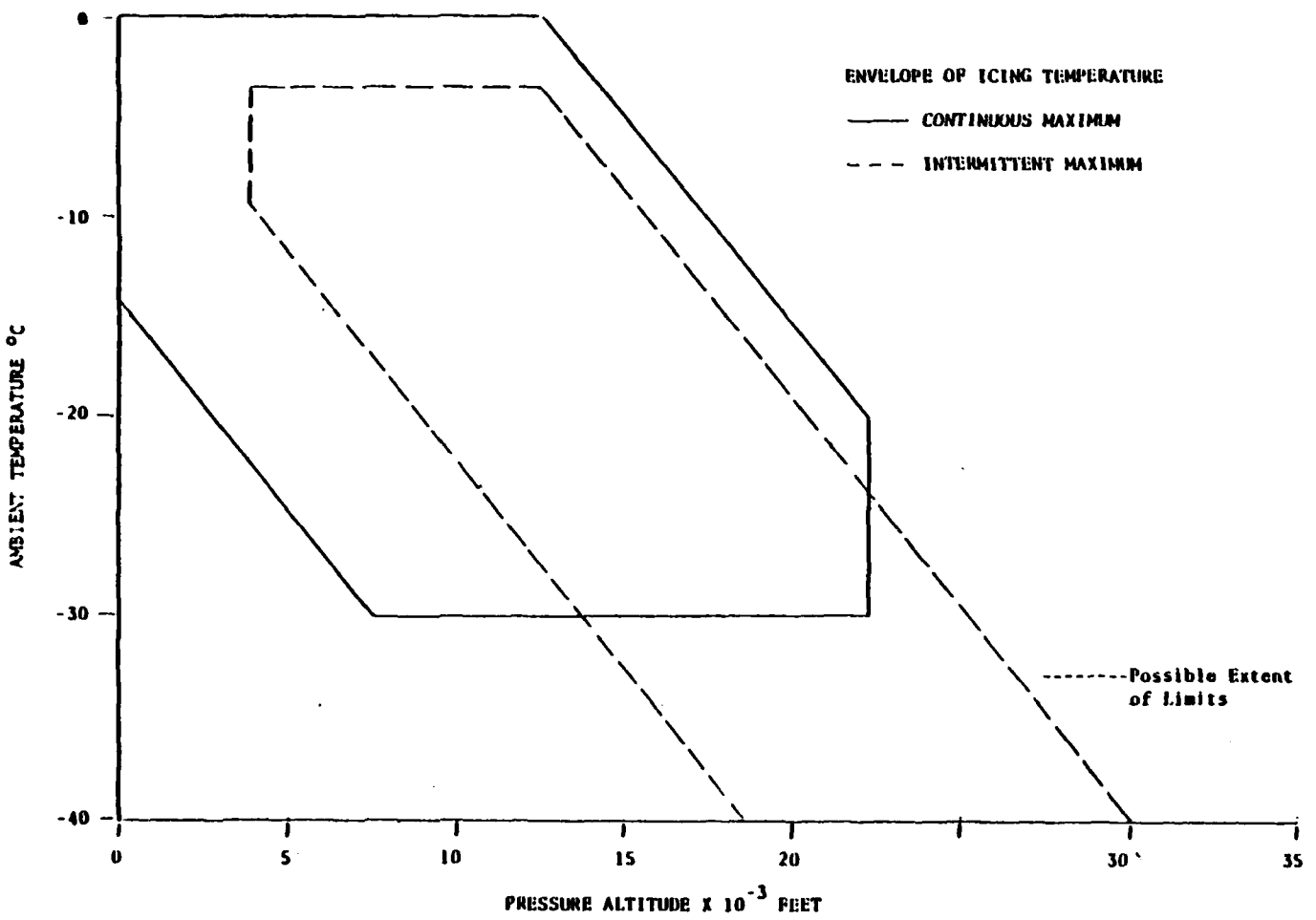

FIGURE B-1. ENVELOPE OF ICING CONDITIONS

APPENDIX C

SOME ACTUAL TEST SAMPLES OF METEROLOGICAL ICING CONDITIONS ON MT. WASHINGTON

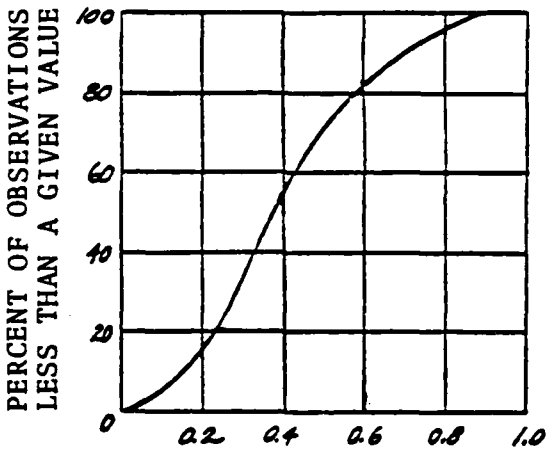

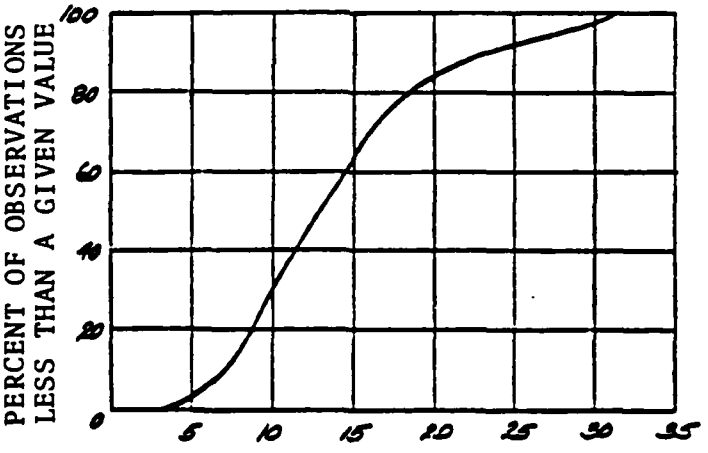

FIGURE C-1. CUMULATIVE FREQUENCY CURVES FOR LIQUID WATER AND DROPLET SIZE

APPENDIX D

RADOME INSTALLED FOR TESTS ON MT. WASHINGTON IN 1954-55

AVERAGE HOURS OF FREEZING RAIN AND DRIZZLE PER YEAR

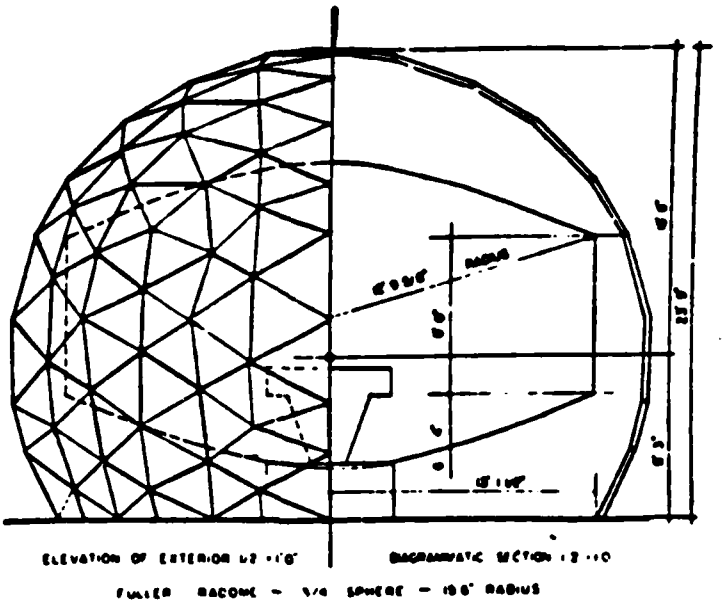

FIGURE D-1. RADOME, MT. WASHINGTON, 1954-55

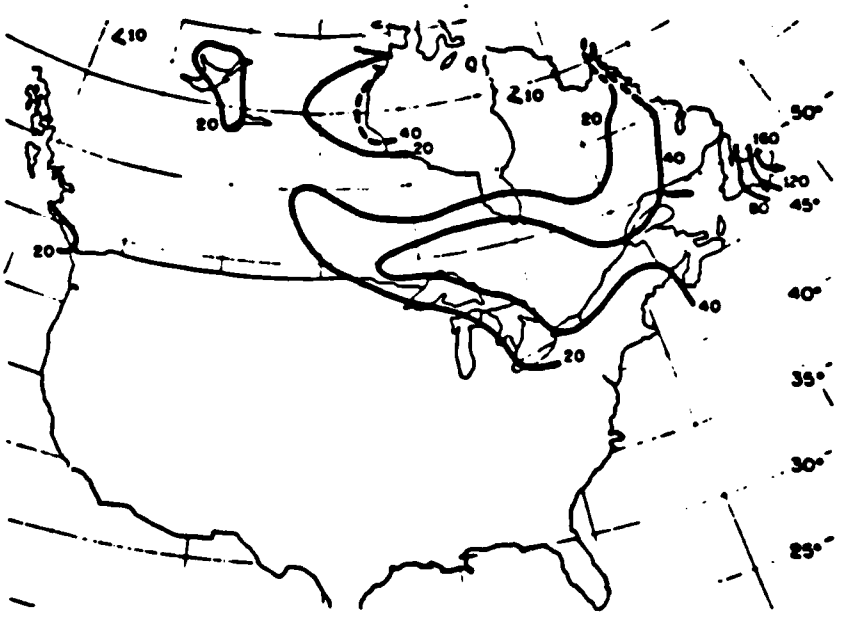

FIGURE D-2. AVERAGE HOURS OF FREEZING RAIN AND DRIZZLE (PER YEAR)

APPENDIX E

STATISTICAL GRAPHS OF METEROLOGICAL ICING CONDITIONS FROM UCLA DEPARTMENT OF ENGINEERING

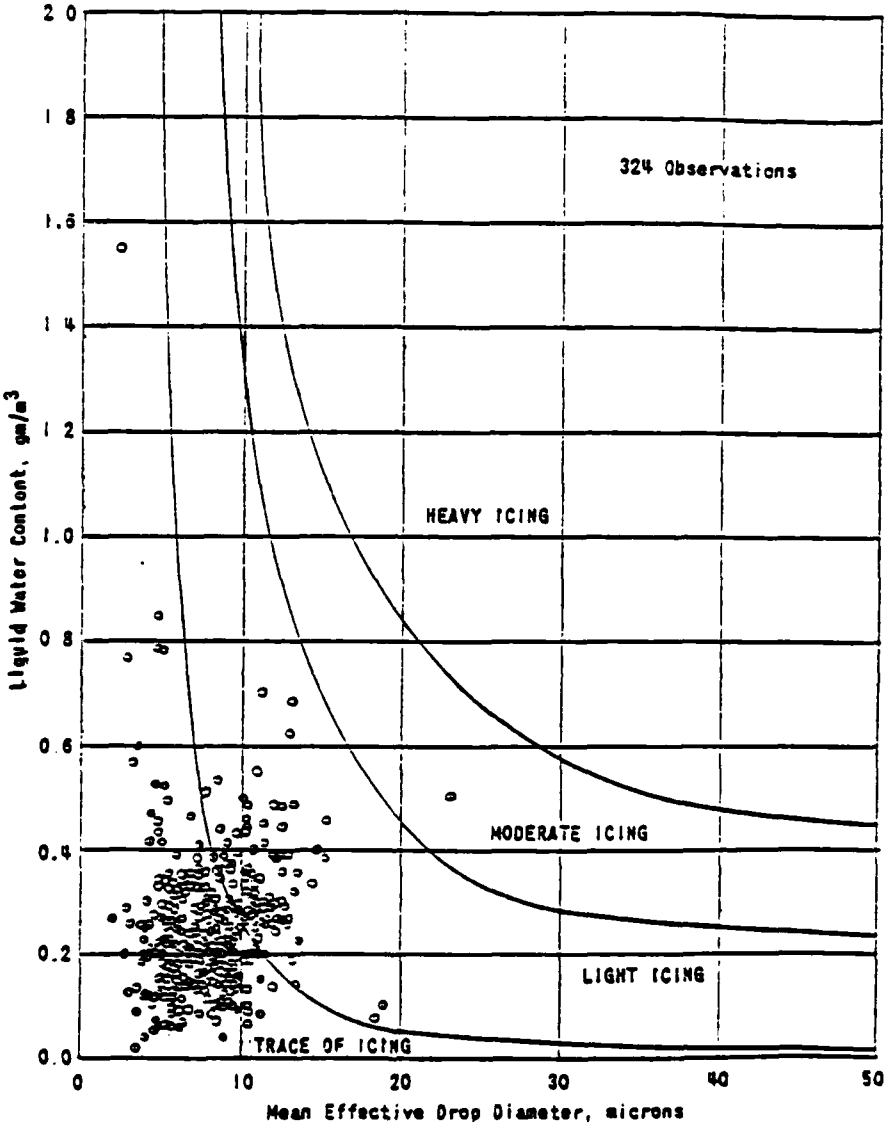

LIQUID WATER CONTENT AS RELATED TO MEAN EFFECTIVE DROP DIAMETER FOR MOUNTAIN OBSERVATIONS IN THE TEMPERATURE RANGE -10° TO 0°F.

FIGURE E-1. MOUNTAIN TOP ICING CONDITIONS (-10°F to 0°F)

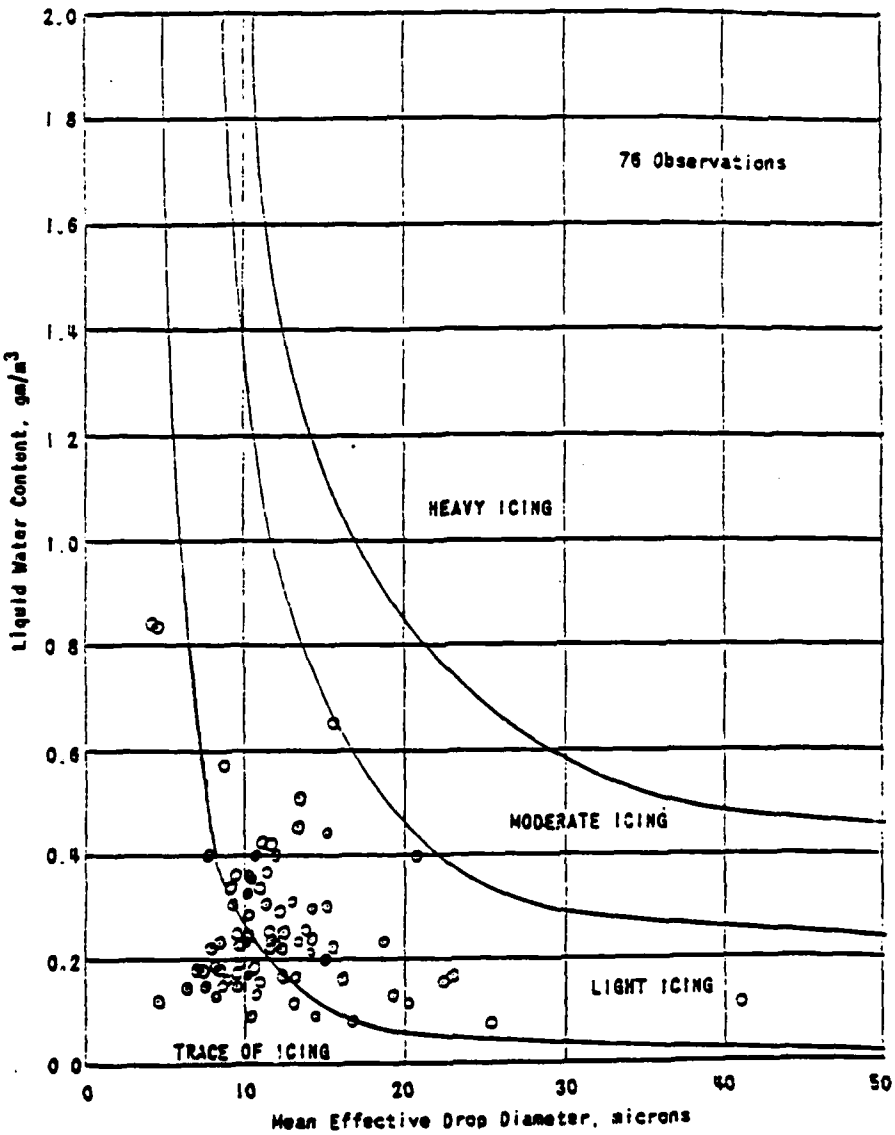

LIQUID WATER CONTENT AS RELATED TO MEAN EFFECTIVE DROP DIAMETER FOR FLIGHT OBSERVATIONS BETWEEN SEA LEVEL AND 5,000 FEET PRESSURE ALTITUDE IN THE TEMPERATURE RANGE 20° TO 25°F.

FIGURE E-2. IN-FLIGHT ICING CONDITIONS

(5-10,000 FT, 20°F TO 25°F)

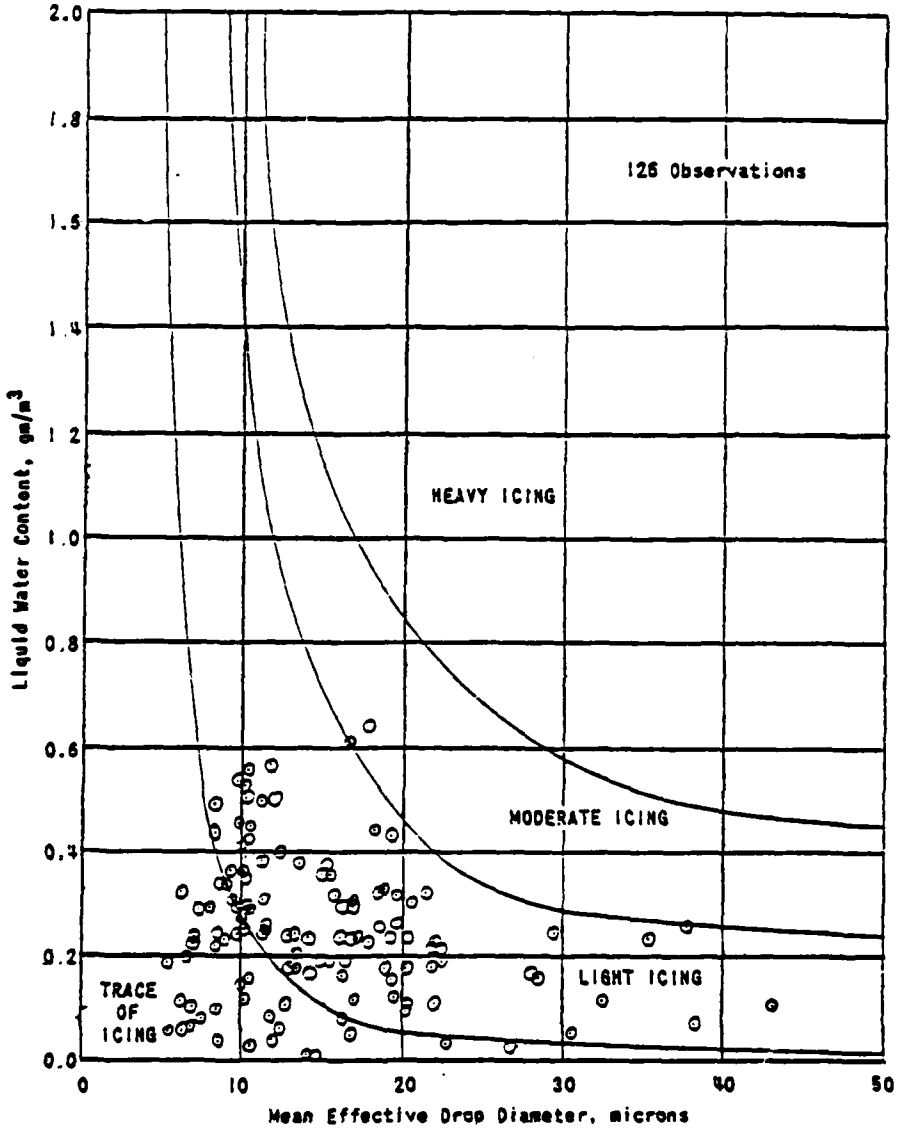

LIQUID WATER CONTENT AS RELATED TO MEAN EFFECTIVE DROP DIAMETER FOR FLIGHT OBSERVATIONS BETWEEN 5,000 AND 10,000 FEET PRESSURE ALTITUDE IN THE TEMPERATURE RANGE 20° TO 25°F.

FIGURE E-3. IN-FLIGHT ICING CONDITIONS
(SEA LEVEL TO 5000 FT, 20°F to 25°F)

APPENDIX F

METEROLOGICAL ICING DATA FROM UNIVERSITY OF MICHIGAN ENGINEERING RESEARCH INSTITUTE

RECOMMENDED VALUES OF METEOROLOGICAL FACTORS FOR
CONSIDERATION IN THE DESIGN OF AIRCRAFT ICE-PREVENTING EQUIPMENT

Class	Item	Air temp. (°F)	Liquid water content (g/m³)	Drop diameter (microns)	Pressure altitude (ft)	Remarks
I - M Intermittent, Maximum	1	32	3.0	25	10,000 to 20,000	Horizontal extent: 1/2 mile. Duration at 180 mph: 10 seconds. Characteristic: Very high liquid water content. Applicable to: Any part of the airplane, such as guide vanes in inlet ducts, where a sudden large mass of supercooled water would be critical, even though of short duration. Example: Induction systems, particularly turbine-engine inlets.
	2	14	4.0	25	20,000 to 25,000	
	3	-4	3.0	25	25,000 to 30,000	
	4	-22	2.0	20	30,000 to 35,000	
	5	-40	.5	15	30,000 to 35,000	
I - N Intermittent, Normal	6	32	1.0	20	10,000 to 20,000	
	7	14	1.0	20	10,000 to 25,000	
	8	-4	.6	18	12,000 to 30,000	
	9	-22	.2	15	15,000 to 30,000	
	10	-40	<.1	13	15,000 to 30,000	
II - M Intermittent, Maximum	11	32	2.5	20	10,000 to 15,000	Horizontal extent: 3 miles. Duration at 180 mph: 1 minute. Characteristic: High liquid water content. Applicable to: Any critical component of the airplane where ice accretions, even though slight and of short duration would not be tolerated. Example: Induction systems, windshields when continuous visibility is required.
	12	14	2.2		10,000 to 20,000	
	13	-4	1.7		10,000 to 30,000	
	14	-22	1.0		15,000 to 30,000	
	15	-40	.2		15,000 to 30,000	
	16	32	1.3	35	5,000 to 15,000	
	17	14	1.0		5,000 to 20,000	
	18	-4	.8		10,000 to 30,000	
	19	-22	.5		15,000 to 30,000	
	20	-40	.1		15,000 to 30,000	
	21	32	.6	50	5,000 to 15,000	
	22	14	.3		5,000 to 20,000	
	23	-4	.2		10,000 to 30,000	
	24	-22	.1		15,000 to 30,000	
	25	-40	<.1		15,000 to 30,000	
II - N Intermittent, Normal	26	32	.8	20	5,000 to 12,000	
	27	14	.6	20	5,000 to 15,000	
	28	-4	.4	18	10,000 to 20,000	
	29	-22	.1	15	15,000 to 25,000	
	30	-40	<.1	13	15,000 to 25,000	
III - M Continuous, Maximum	31	32	.8	15	1,000 to 20,000	Horizontal extent and duration: Continuous. Characteristic: Moderate to low liquid water content for an indefinite period of time. Applicable to: All components of the airplane that is, every part of the airplane should be examined with the question in mind, "Will this part be affected seriously by accretions during continuous flight in icing conditions?" Example: Wings and tail surfaces.
	32	14	.6			
	33	-4	.3			
	34	-22	.2			
	35	-40	<.05			
	36	32	.5	25		
	37	14	.3			
	38	-4	.15			
	39	-22	.10			
	40	-40	.05			
	41	32	.15	40		
	42	14	.10			
	43	-4	.06			
	44	-22	.05			
	45	-40	.02			
III - N Continuous, Normal	46	32	.3	15		
	47	14	.2			
	48	-4	.1			
	49	-22	<.1			
IV - M Freezing Rain	50	25 to 32	.15	1000	0 to 5,000	Horizontal extent: 100 miles. Duration at 180 mph: 30 minutes. Characteristic: Very large drops at near-freezing temperatures and low values of liquid water content. Applicable to: Components of the airplane for which no protection would be supplied after considering classes I, II, and III. Example: Fuselage static pressure airspeed vents.

COMPARISON OF EXPERIMENTS AND COMPUTED DATA

Run	Measured: Drop Diam. Micron	Measured: Liq.Wat. Content g/m³	Measured: Air Temp °F	Measured: Air Speed mph	Measured: Heat Loss Dry	Measured: Heat Loss Moist	Computed: E_M	Computed: β_o	Computed: $h_{c,o}$	Computed: t_o °F	Computed: $h_{c,av}$	Heat Lost/Frontal Area, Btu/hr ft²: Convect.	Evap'n	Radiant	Sensible	Total Watts/cm²	Comment
1	5.8	0.29	7	41	1.7	1.3	0.14	0.70	50.0	60	27.4	4570	577	167	28	1.68	Light Snow
2	6.6	0.38	7	64	2.2	1.9	0.30	0.48	62.2	62	36.1	6350	2450	176	137	2.86	Very Light Snow
3	6.9	0.31	- 2	62	2.8	2.2	0.33	0.51	61.2	57	35.6	6600	2170	185	121	2.91	Light Snow
4	7.6	0.37	- 2	56	3.1	2.8	0.36	0.53	58.2	63	33.1	6760	2590	204	166	3.05	Very Light Snow
5	7.6	0.37	- 6	59	3.3	3.0	0.36	0.55	60.0	64	34.4	7570	2690	220	178	3.34	Very Light Snow
6	8.2	0.38	3	70	3.7	3.2	0.44	0.60	65.1	70	38.0	8010	4020	211	255	3.92	Trace of Snow
7	8.2	0.39	8.5	60	3.2	2.6	0.41	0.57	60.2	66	34.8	6290	3540	180	182	3.14	Light to Moderate Snow
8	8.6	0.26	- 6	77	3.3	2.8	0.47	0.62	68.5	64	40.4	9050	3520	220	246	4.10	Light Snow
9	8.9	0.25	- 0	64	3.1	2.5	0.44	0.60	62.2	56	36.2	6360	2450	176	130	2.87	Heavy Snow
10	10.2	0.38	3	64	4.0	3.4	0.52	0.66	62.2	71	36.2	7740	4350	214	280	3.94	Trace of Snow
11	10.2	0.44	1	67	4.6	3.9	0.53	0.66	63.6	76	37.1	8750	5390	236	383	4.64	Light Snow
12	12.7	0.13	0	56	4.7	4.1	0.60	0.72	58.2	43	33.4	4620	1520	284	67	2.03	Moderate Snow
13	8.3	0.32	3	80	5.5	5.2	0.47	0.62	69.9	68	41.3	8560	4180	208	280	4.18	Very Light Snow
14	9.0	0.50	14	61	5.4	5.0	0.45	0.60	61.1	76	35.2	6960	4770	198	290	3.85	Heavy Snow
15	9.6	0.42	7	76	7.5	4.3	0.53	0.66	68.0	77	40.1	8810	5880	219	390	4.80	Very Light Snow
16	11.7	0.62	12	80	7.0	6.9	0.62	0.74	69.8	93	41.3	10500	10700	279	820	7.00	Light to Moderate Snow
17	15.0	0.43	1	88	5.8	6.5	0.73	0.83	73.1	89	43.6	11900	9700	273	650	7.14	No Snow
18	17.1	0.75	12	57	5.2	4.5	0.72	0.82	58.8	98	33.7	9000	10700	267	910	6.55	Light Snow
19	16.3	0.65	30	62	5.8	5.1	0.71	0.81	61.2	94	35.6	7160	9940	201	572	5.60	Light Snow
20	17.7	1.12	25	48	5.6	5.1	0.71	0.81	54.0	109	30.4	7650	13200	251	1050	6.95	No Snow
21	5.7	0.12	28	71	0.7	0.4	0.24	0.43	65.8	43	38.6	2170	710	57	30	0.93	No Snow
22	8.8	0.10	-18	75	3.6	2.1	0.26	0.77	67.5	40	39.8	7250	677	182	37	2.55	Light Snow
					Watt/cm²								Btu/hr, ft²			Watt/cm²	

APPENDIX G

TRAJECTORY OF WATER DROPLETS AROUND STREAMLINED BODIES

TRAJECTORIES OF WATER DROPS AROUND STREAMLINED BODIES

The Icing of a Cylinder

The first step in an attack upon the icing problem is the analysis of the icing rates to be expected upon a particular surface.

Consider first the icing of right circular cylinder placed transverse to the air stream. Figure II-1 shows the streamlines for an incompressible non-viscous fluid flowing past a cylinder. A spherical water drop in the fluid stream will not follow the stream lines, but due to its inertia will follow a trajectory which is less curved. Figure II-2 shows a typical water-drop trajectory.

The drop trajectory shown in Figure II-2 was calculated as follows: Consider a drop in air, let

u_a, v_a = components of air velocity

u_d, v_d = components of drop velocity.

Then let

$(u_a - u_d)$, $(v_a - v_d)$ = components of P , the relative drop velocity.

The relative velocity of the droplet gives rise to a drag force

AD-A115 445 GOULDING (MERRILL K) AND ASSOCIATES GLENDALE CA F/G 1/5
STUDY OF THE DE-ICING PROPERTIES OF THE ASDE-3 ROTODOME.(U)
APR 82 M K GOULDING DOT-TS-15950

UNCLASSIFIED DOT-FAA/RD-81-112 NL

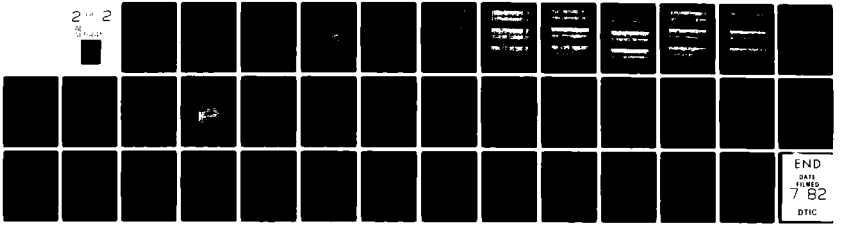

END
DATE FILMED
7 82
DTIC

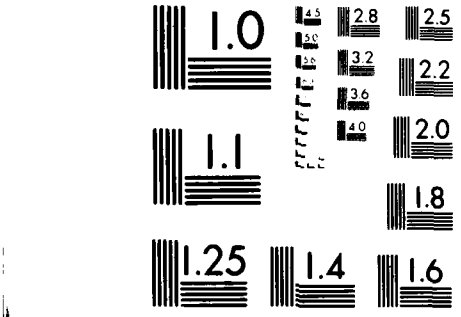

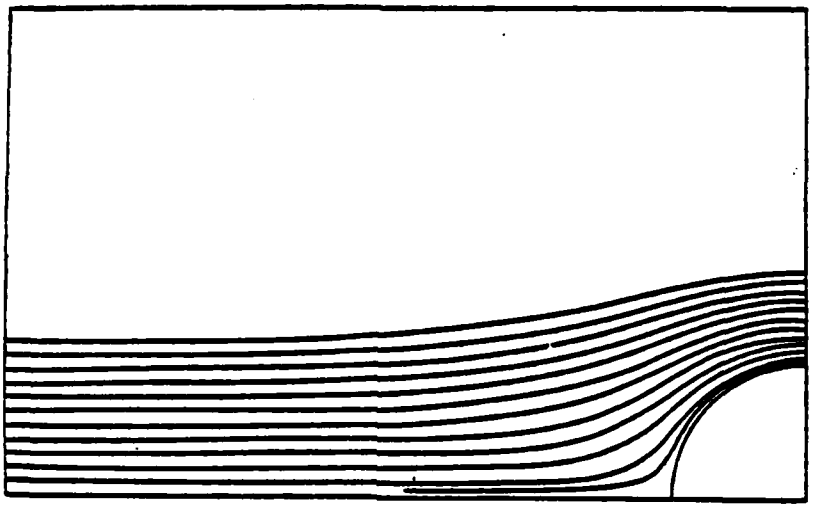

Figure II-1. Flow field ahead of a cylinder.

$$F_x = \frac{1}{2}\rho_a \pi a^2 C_D P (u_a - u_d)$$

$$F_y = \frac{1}{2}\rho_a \pi a^2 C_D P (v_a - v_d) \quad ,$$

a = drop radius

C_D = drag coefficient

ρ_a = air density

Components of drag give rise to accelerations according to Newton's
n.

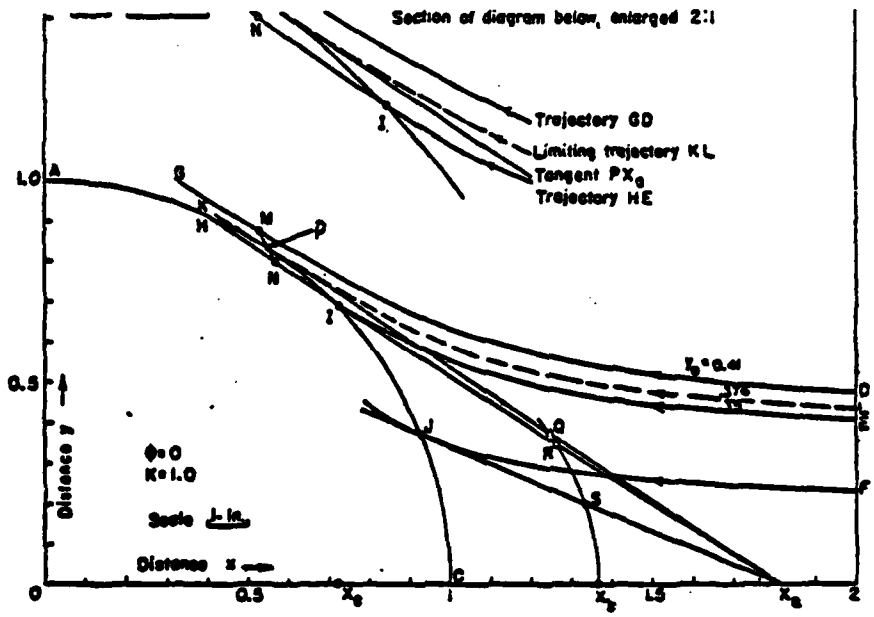

Figure II-2. Typical water drop trajectory drawn by Differential Analyzer (Reference 2).

$$F_x = m a_x = \frac{4}{3} \pi a^3 \rho_d \frac{d u_d}{dt}$$

$$F_y = m a_y = \frac{4}{3} \pi a^3 \rho_d \frac{d v_d}{dt} ,$$

where

ρ_d = drop density.

Equating the forces yields:

$$\frac{d u_d}{dt} = \frac{3}{8} \frac{\rho_a}{\rho_d} \frac{P(u_a - u_d)}{a} C_D$$

$$\frac{d v_a}{dt} = \frac{3}{8} \frac{\rho_a}{\rho_d} \frac{P(v_a - v_d)}{a} C_D ,$$

The trajectory of the drop is obtained by integrating the following equations simultaneously:

$$(x - x_o) = \int \left\{ \int \frac{3}{8} \frac{\rho_a}{\rho_d} (u_a - u_d) \frac{P\, C_D}{a}\, dt \right\} dt$$

$$(y - y_o) = \int \left\{ \int \frac{3}{8} \frac{\rho_a}{\rho_d} (v_a - v_d) \frac{P\, C_D}{a}\, dt \right\} dt \quad .$$

The first integration yields the drop velocity and the second integration the drop displacement. To lessen the number of calculations required the equations are rendered dimensionless as follows:

$$\frac{x}{C} = \frac{x_o}{C} + \int \left\{ \int \left(\frac{9\, \rho_a\, C}{\rho_d\, a} \right) \left(\frac{C_D\, P}{24\, U} \right) \left(\frac{u_a - \dot{x}}{U} \right) d\left(\frac{Ut}{C} \right) \right\} d\left(\frac{Ut}{C} \right)$$

$$\frac{y}{C} = \frac{y_o}{C} + \int \left\{ \int \left(\frac{9\, \rho_a\, C}{\rho_d\, a} \right) \left(\frac{C_D\, P}{24\, U} \right) \left(\frac{v_a - \dot{y}}{U} \right) d\left(\frac{Ut}{C} \right) \right\} d\left(\frac{Ut}{C} \right) \quad .$$

Now let

$$\psi = \frac{9\, \rho_a\, C}{\rho_d\, a} \quad , \quad R_p = \frac{2a\, \rho_a\, P}{\mu_a} \quad , \quad R_u = \frac{2a\, \rho_a\, U}{\mu_a} \quad .$$

μ_a = air viscosity

C = a significant dimension in the flow field

U = free stream velocity

$$\frac{x}{C} = \frac{x_o}{C} + \int \left\{ \frac{\psi}{R_u} \int \left(\frac{C_D\, R_p}{24} \right) \left(\frac{u_a - \dot{x}}{U} \right) d\left(\frac{Ut}{C} \right) \right\} d\left(\frac{Ut}{C} \right)$$

$$\frac{y}{C} = \frac{y_o}{C} + \int \left\{ \frac{\psi}{R_u} \int \left(\frac{C_D\, R_p}{24} \right) \left(\frac{v_a - \dot{y}}{U} \right) d\left(\frac{Ut}{C} \right) \right\} d\left(\frac{Ut}{C} \right) \quad .$$

The integration of these equations must be accomplished step-wise, graphically, or via a differential analyzer, since C_D is a function of R_p and, except for very simple cases, $\frac{u_a}{U}$ and $\frac{v_a}{U}$ are rather complicated functions of $\frac{x}{C}$ and $\frac{y}{C}$.

For the cylinder, then, it follows that the trajectories, i.e., the loci of $\frac{x}{C}$, $\frac{y}{C}$ from these equations, are functions of ψ and R_p .

In the special case that $(C_D R_p/24) = 1$, the region of Stokes' law, the term in $R_u = R_p(U/P)$ does not appear inside the integral and the trajectories are functions of one parameter only, i.e., ψ/R_u .

Albrecht[1] was the first to calculate the trajectories around a cylinder for the case of the Stokes' law regime. Later Langmuir and Blodgett, using a differential analyzer, calculated trajectories for the case where C_D varies with R_p as determined experimentally for large spheres.[2] In this same report they calculated trajectories past ribbons and spheres, the results of which will be considered later.

From these trajectories certain specific items of information emerge. The first is known as the "percentage catch" and sometimes the "collection efficiency". Figure II-3 illustrates the physical significance of this term. All the

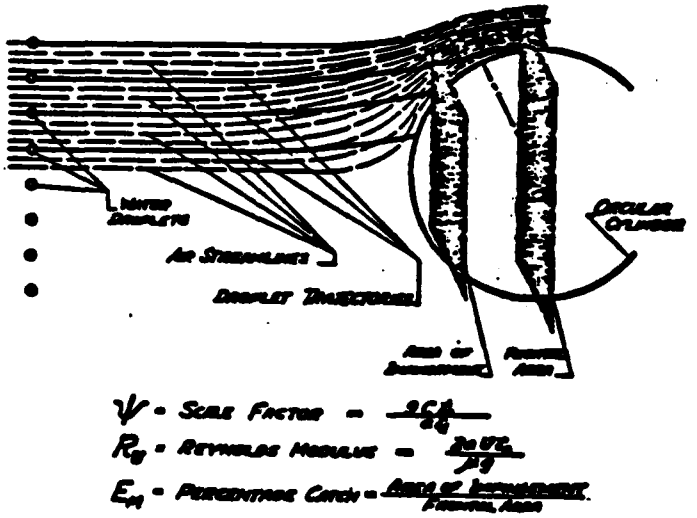

Figure II-3. Graphical representation of parameters used in trajectory work.

drops which lie within the limiting trajectories strike the cylinder. Those drops which lie outside these trajectories do not strike the cylinder but are blown around it. The ratio of the original y coordinate of the "tangent trajectory" to the cylinder radius defines the "percentage catch" which, expressed as a fraction, is given the symbol E_M.

Another property of interest is the area over which the cylinder is wetted. The angle measured from the stagnation line to the tangent trajectory is given the symbol θ_m. All drops which strike the cylinder do so within $\pm \theta_m$.

A third property of trajectories is the intensity of catch at the stagnation line, β_o. (The symbols are all from Langmuir and Blodgett.)

The catch rate may be computed from the percentage catch by

$$W = E_M U (2C) L w ,$$

where

W = catch rate (lbs/sec)

E_M = "fractional catch"

U = velocity (ft/sec)

C = cylinder radius (ft)

L = cylinder axial length (ft)

w = liquid water content of atmosphere (lbs/ft^3)

The intensity of catch along the stagnation line is given by

$$\frac{dW}{dA} = \beta_o U w$$

dW/dA = intensity of catch, $lbs/sec\ ft^2$.

Because of certain end uses for their data, Langmuir and Blodgett plotted the quantities E_M, θ_m, and β_o versus two parameters defined as follows:

$$K = Ru/\psi \qquad \phi = Ru \cdot \psi$$

Figures II-4a to II-6b show graphs of E_M, θ_m, β_o, and relative velocity V_1 versus K and ϕ. The relative velocity is the fraction of free stream velocity possessed by the drops as they strike the stagnation point, $\theta = 0$.

For values of $K \leq 1/8$, $E_M = 0$ on a cylinder. Since K contains the cylinder radius C in the denominator, it follows that for a given icing condition there is a maximum size of cylinder which will collect ice! This effect of size was not always appreciated. The author once participated in a test flight where the heat supply to the wings was being continuously diminished to find the

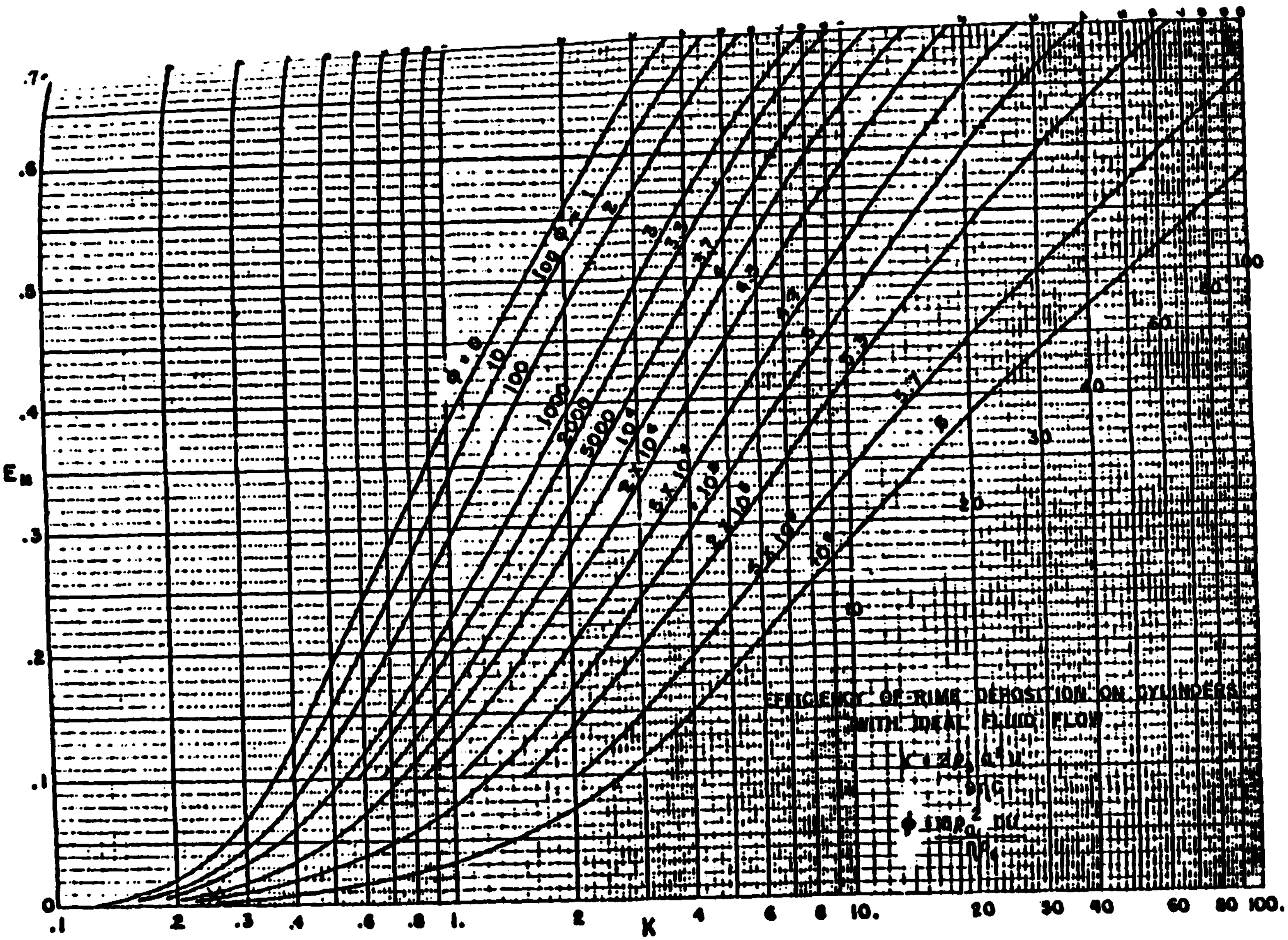
EFFICIENCY OF RIME DEPOSITION ON CYLINDERS
WITH IDEAL FLUID FLOW
K
E
.1
.2
.3
.4
.6
.8
1.
2
4
6
8
10.
20
30
40
60
80
100.
0
.7
.6
.5

Figure II-4a

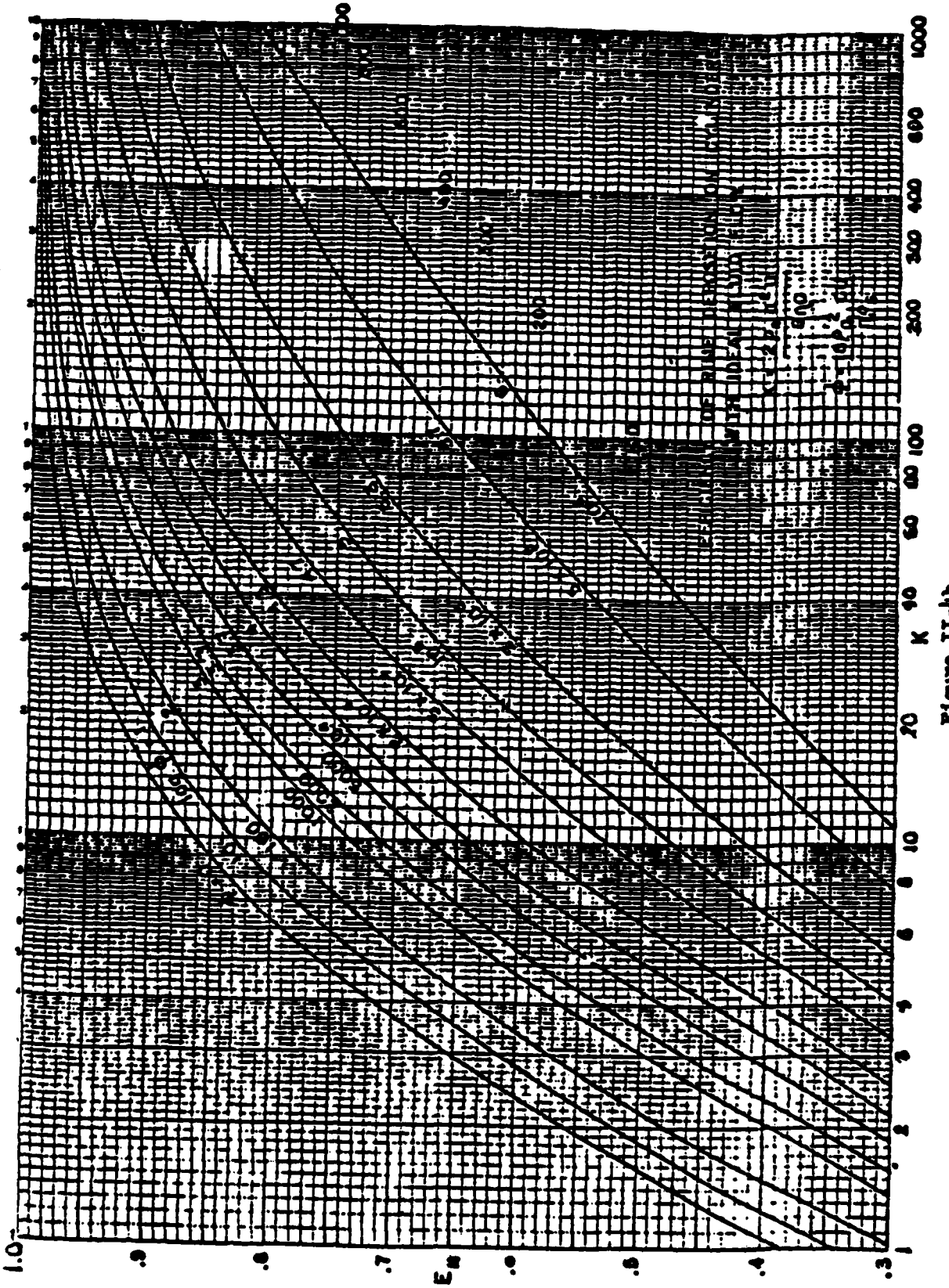

Figure II-4b

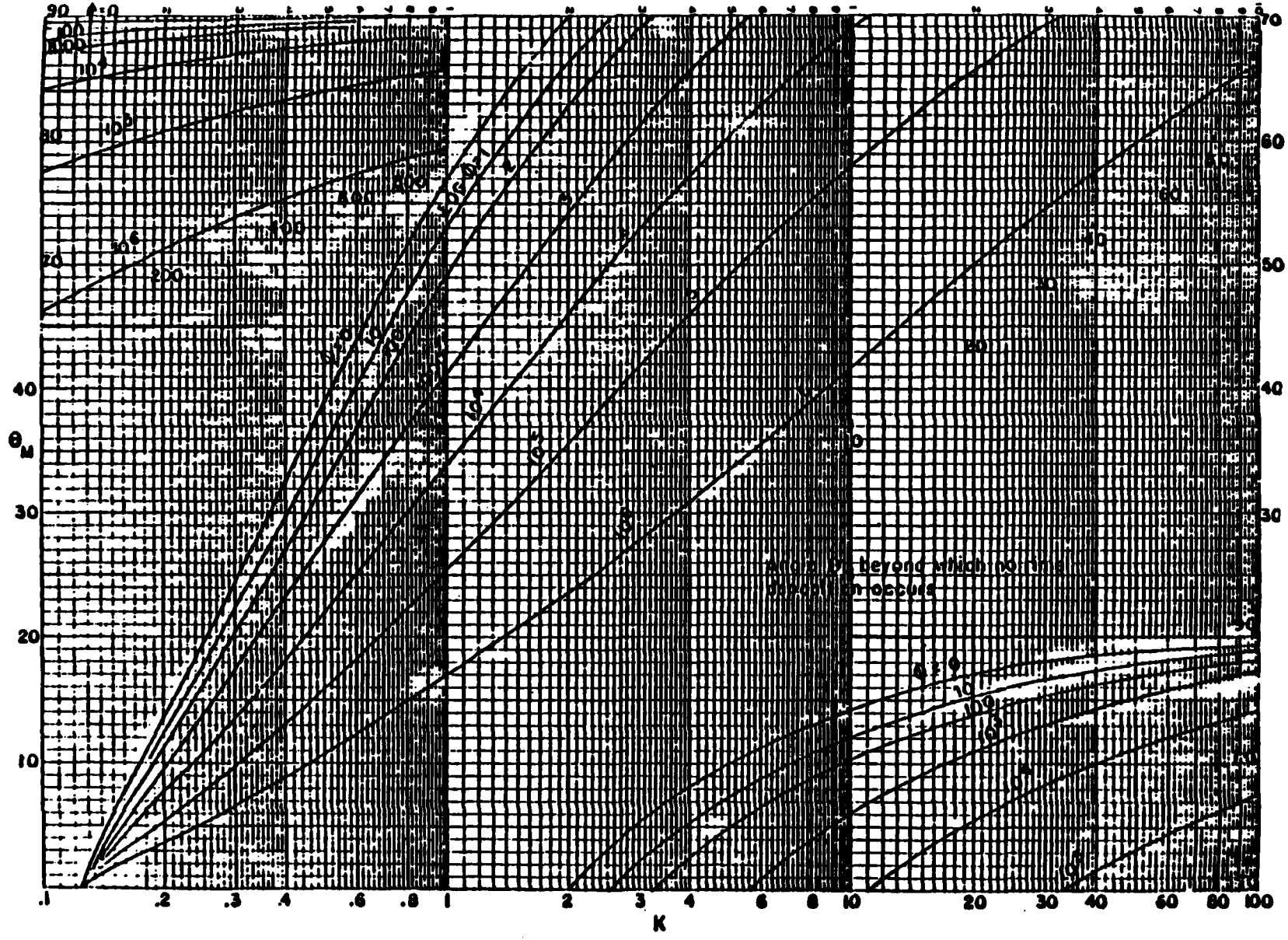

Figure II-5

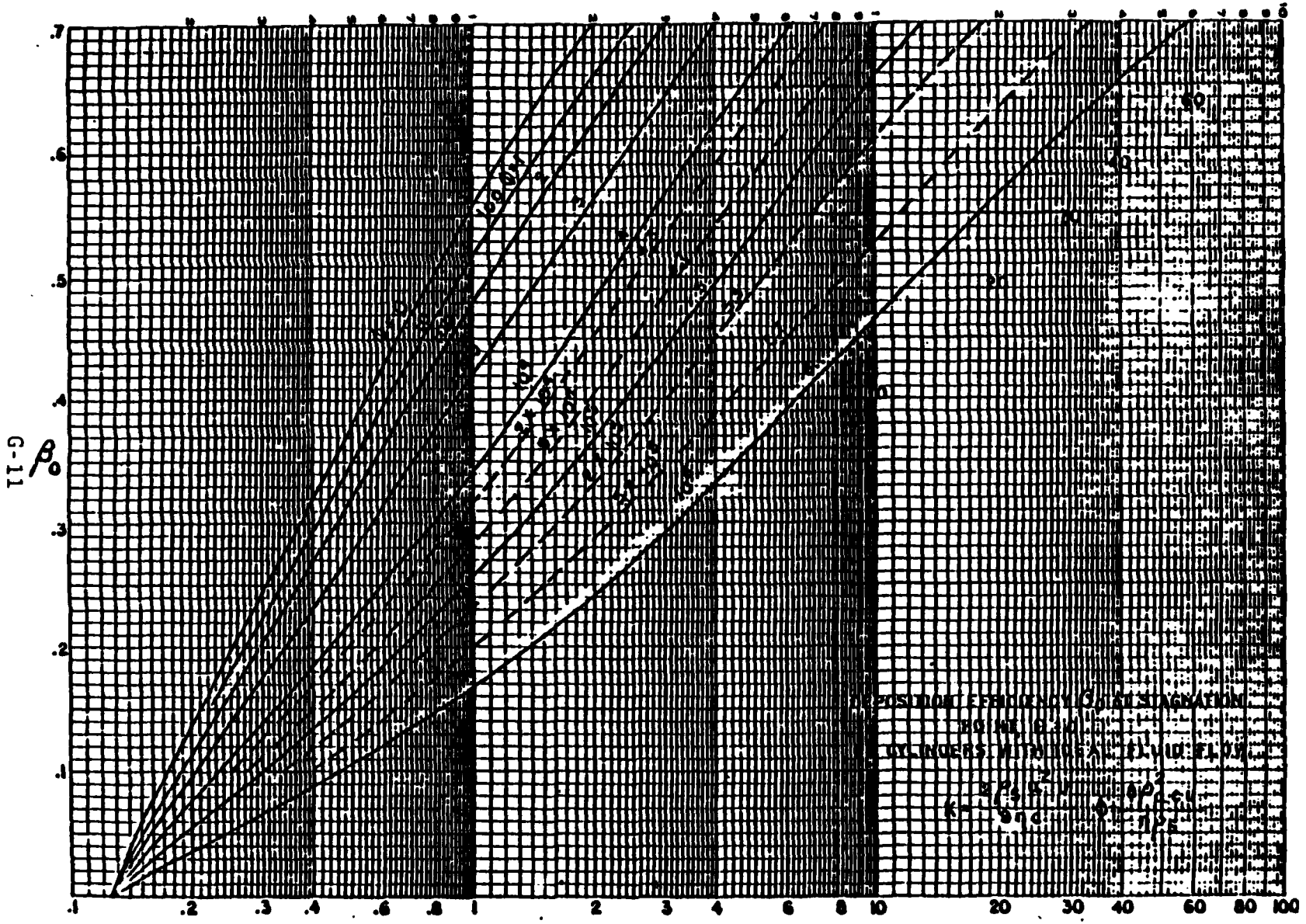

Figure II-6a

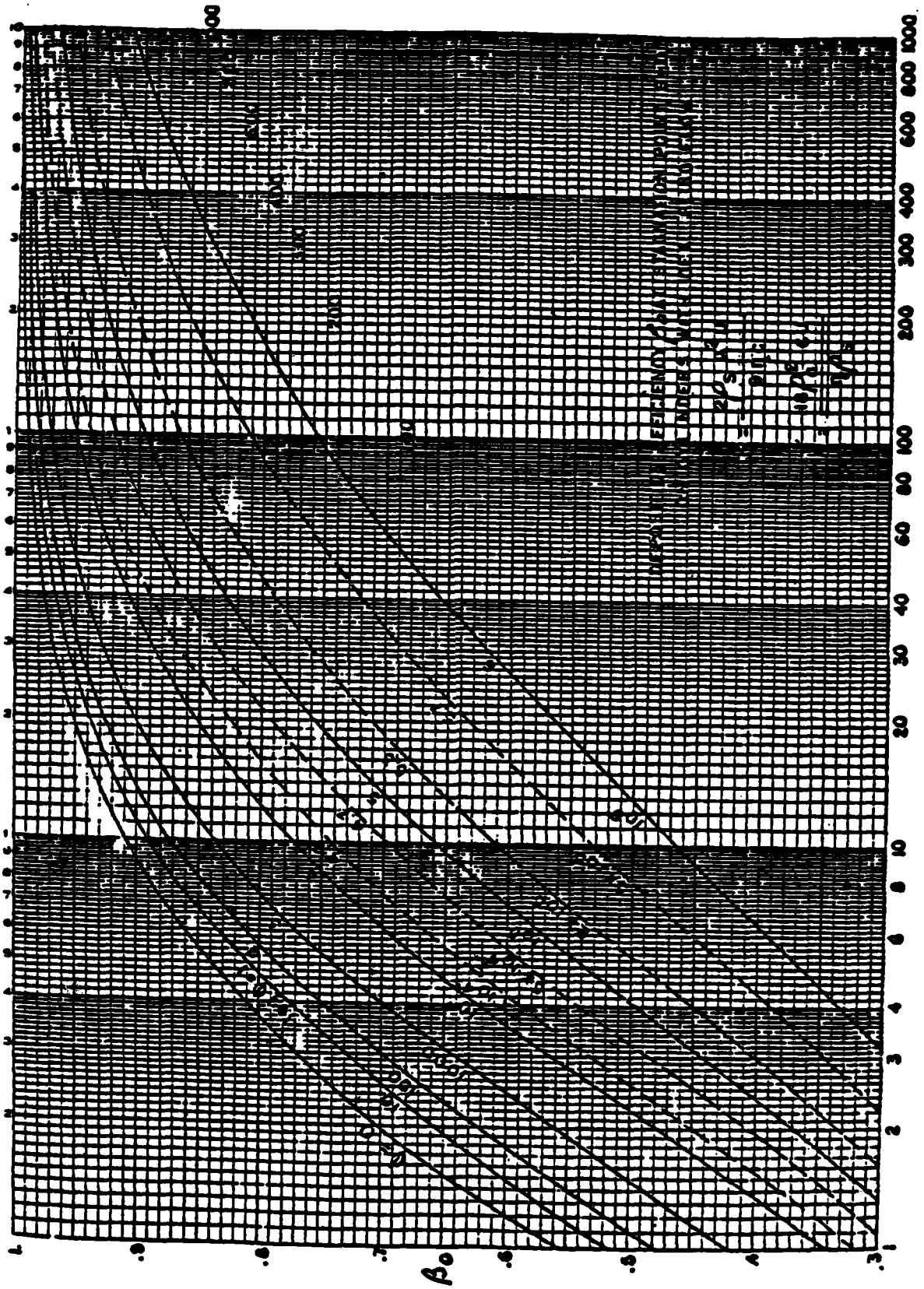

Figure II-6b

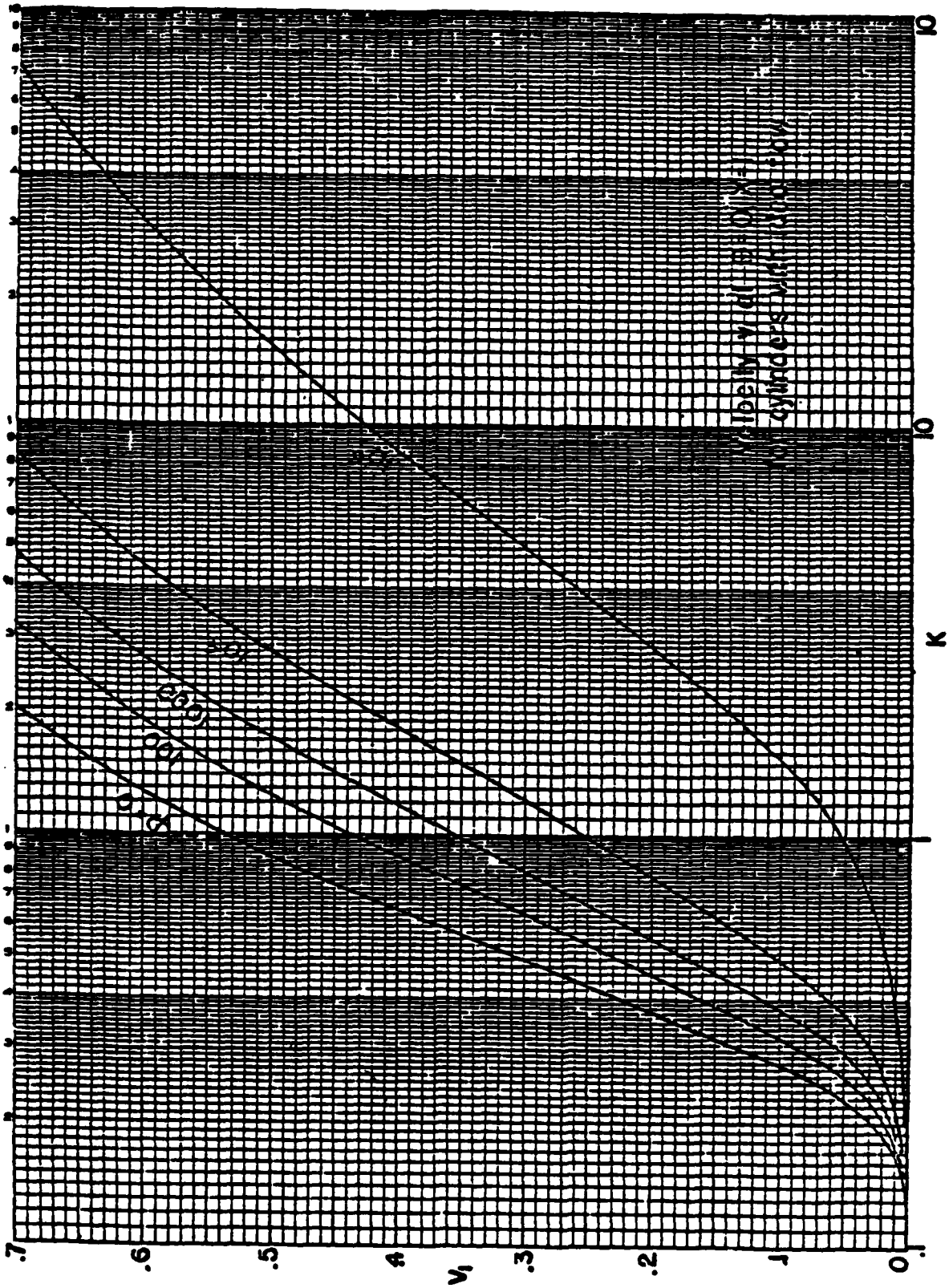

Figure II-7a

minimum heat required to prevent ice. When the heat supply was reduced to zero, the wings still remained ice-free. Meanwhile the antenna wires and mast were icing rapidly. It is now known that this effect may occur when the drops are small. The wing, having a large radius of curvature tended to deflect the drops while the antenna mast had, in effect, a high value of K and therefore a high collection efficiency.

Experimental Verification

Figures II-8a and II-8b show ice accretions on cylinders and spheres which verify qualitatively the trajectory data given by Langmuir and Blodgett. The best check of the calculations may be made using a cylinder, since the cylinder may be rotated and will remain cylindrical while icing.

A quantitative verification of the trajectory data has been obtained by mounting cylinders on a common axis and exposing them to the icing windstream. These cylinders are of different sizes and are rotated to preserve the cylindrical shape during the icing. The unknown properties of the windstream are the liquid-water content (w) and the drop diameter (2a). If the weight of ice catch on each cylinder is divided by the cylinder frontal area, wind velocity and exposure duration and the quotient plotted versus cylinder radius, C, using logarithmic coordinates, we get the results shown in Figure II-9. A graph of E_M versus 1/K with ϕ as a parameter is shown in Figure II-10. An attempt is then made to fit the points of Figure II-9 to the curves of Figure II-10. Since a shift along either logarithmic coordinate corresponds to multiplication by a constant, it is not necessary to know the liquid-water content or drop diameter to do the curve fitting. Figure II-11 shows an example of the "fit". The amount of vertical and horizontal shift permits calculation of the unknown liquid water content and of the drop radius.

Various modifications of the above curve-fitting process have been used, all representing the same basic method. Charts have been prepared in which the curves of E_M versus 1/K have two parameters, one the droplet Reynolds Modulus, Ru, and the other a characterization of the droplet-size distribution. Such curves are given in Reference 3. By matching experimental points to these curves, one obtains not only the liquid-water content and mean drop size but also the approximate drop-size distribution.* Figure II-12 shows an example of such a

* Lewis and Hocker, NACA TN 1904 "Observations of Icing Conditions Encountered in Flight During 1948" comment that the rotating-cylinder method when used in the manner described yields "indications of drop-size distribution (that) are so unreliable that they are of little or no value". However, the Lewis data under discussion was obtained partly from two-cylinder and partly from four-cylinder apparatus. Such data can often be fitted to any of several curves. Data taken, using six or more cylinders at Mt. Washington, generally can be fitted to one curve only. It seems evident that, if one is attempting to measure three variables, more than two measurements should be made.

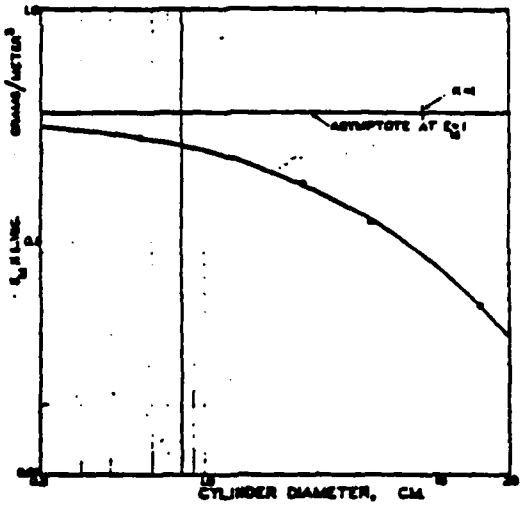

Figure II-12. Comparison between data of Reference 2 and flight measurement (Reference 3).

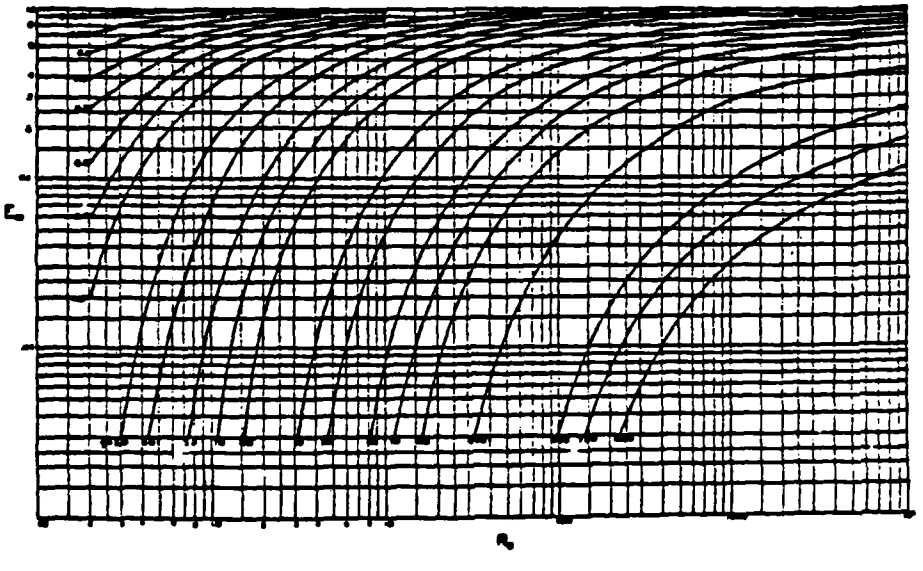

Figure II-13. Replot of data from Reference 2 to show effect of velocity on catch (Reference 4).

APPENDIX H

HEXCELL PUBLISHED DATA ON THERMAL CONDUCTIVITY OF SANDWICH MATERIAL

6. Thermal

Thermal conductivity through sandwich panels can be isolated into the contribution of each component: facings, core and adhesive. The resistances (or reciprocal of conductivity) can simply be added — including the effect of boundry layer conditions. The thermal properties of typical facing materials may be found in handbooks. Thermal resistance values for typical core to facing adhesives are 0.03 for film adhesives with a scrim cloth support and 0.01 for unsupported adhesives. Figure IX-4 and IX-5 give the resistance for aluminum and non-metallic honeycomb at a mean temperature of 75°F. Note that for non-metal'ic honeycomb it has been found that the cell size is more critical than core density. The reverse is true with aluminum honeycomb. To correct for mean temperature divide the resistance at 75°F by K using Figure IX-6.

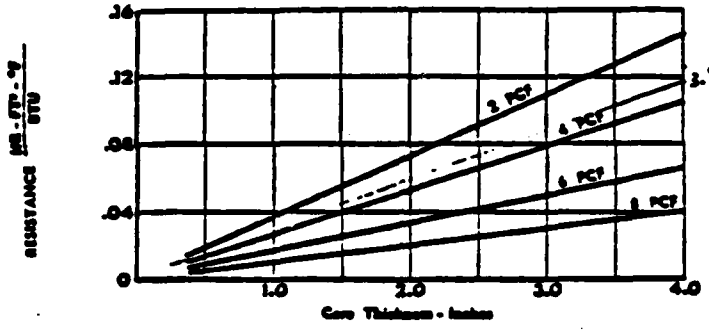

Figure IX-4
Thermal Resistance
Aluminum Honeycomb

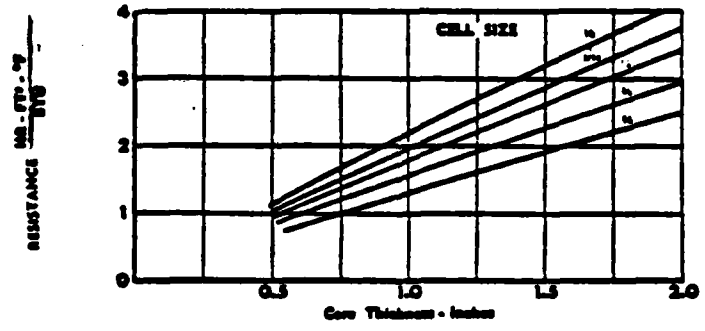

Figure IX-5
Thermal Resistance
Non-Metallic Honeycomb

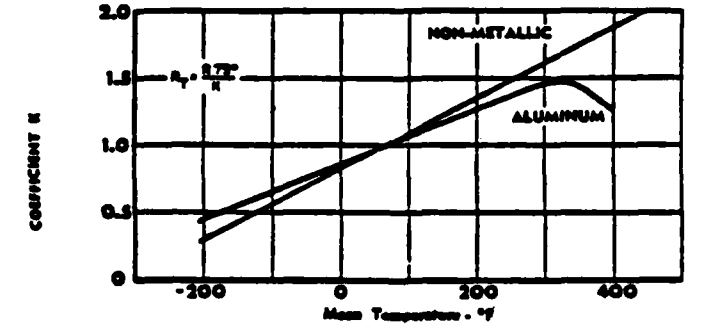

Figure IX-6
Effect of Mean
Temperature

TYPICAL HEAT TRANSFER PROPERTIES OF HONEYCOMB SANDWICH STRUCTURES

Figure 9 offers a synopsis of the typical heat transfer properties of various honeycomb sandwich configurations. The following references have been used in developing the curves:

"Measurement of the Thermal Properties of Various Aircraft Structural Materials" WADC Technical Report 57-10

"Analysis of Effective Thermal Conductivities of Honeycomb Core and Corrugated Core Sandwich Panels" NASA TN-714

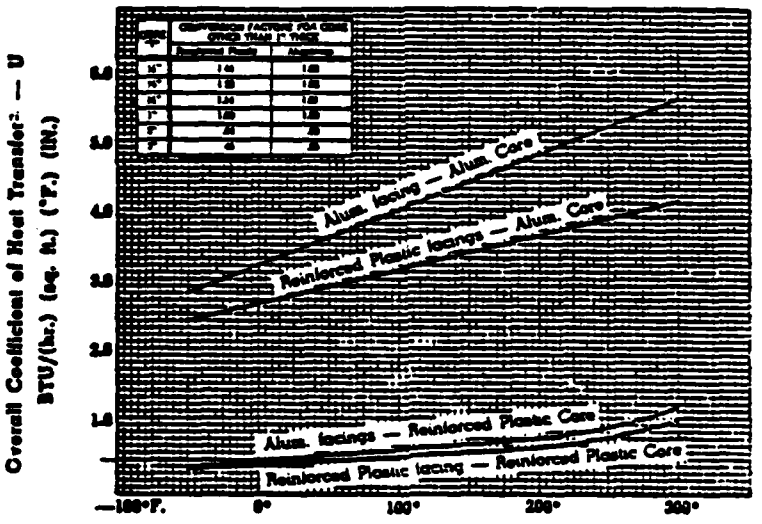

Figure 9.

[1] Less Tangent tests for NP ¼-21-4.0 only because of required T dim (17")
Values were: for parallel polarization 0.002
for perpendicular polarization 0.001

[2] Values of U do not include coefficients for inside and outside surface conditions.

APPENDIX I

DESCRIPTION OF HEATING SYSTEM

Radome Heating and De-Icing

Heaters located in the rotating antenna/radome (See figure 1 and 2) provide heating of the rotodome/antenna to prevent ice formation. The heating system used is hot air supplied by heater/fan assemblies. The required 30 kw of heater power is supplied by slip rings located in the pedestal.

The de-icing heating system (See figure 3) is controlled by an ice sensor located atop the roof. Operation of the de-icing heating cycle is as follows:

a. The ice sensor, located outside in the vicinity of the rotodome, indicates the presence of icing conditions. The sensor provides a contact closure signal to the sensor's controller located in the equipment room. This signal sets a 15 minute timer that is used to control the power level to the heaters. The controller sends a signal to the Contactor Box located below the rotodome near the prime power interface. A brush lifter signal is sent to the pedestal.

b. The brush lifter solenoid is energized, closing the heater power slip ring paths. When the brushes are in contact with the slip rings, a microswitch closure is made to signal the Contactor Box to turn heater power on.

c. The Contactor Box 7.5 K watts relays are turned on. Each heater/blower in the rotodome comes on, providing a total of 15 KW of power to heat the rotodome air. Each heater can operate at 7.5 or 15 KW.

d. If after 15 minutes the icing signal persists, and the thermostat (actually two thermostats in series for redundancy) has not opened at 135°F, the Contactor Box 15 KW relays are actuated, and the heater/blowers operate at 15 KW each (30 KW total). As long as the icing signal persists, the heaters are controlled by the thermostats at the KW level required to cycle the thermostats in the prescribed time. An alarm thermostat, set at 165°F, is located on each heater/blower at the blower intake. These thermostats are wired in series with the control thermostats, and cut off heater power. An alarm signal is also sent to the maintenance room.

e. The heater power down cycle is the reverse of the up cycle. Heater power is removed from the brushes before they are lifted off the slip ring to preclude arcing. If the drive motor for the antenna is powered up during the heating-on cycle, then the heating is interrupted for 30 seconds (adjustable) to allow the motor's starting surge to pass.

The ice sensor, manufactured by Rosemount Engineering, detects the formation of ice on a small half spherical rod end by sensing the change in resonance frequency of the rod structure. The ice sensor is located in the vicinity of the rotodome and since ice forms more rapidly on a small spherical surface (the sensor-rod end) than on the large rotodome (spherical) surface, sufficient time exists to turn on the rotodome's heaters to preclude any possibility of ice build up. If the rotodome is spinning, there is little likelihood that ice will form even without heat. The shape of the roof, the smoothness of the surface and the centrifugal force tend to keep the roof clean. The smooth surface windows of the rotodome curve inwards, seeing direct rain only in heavy winds.

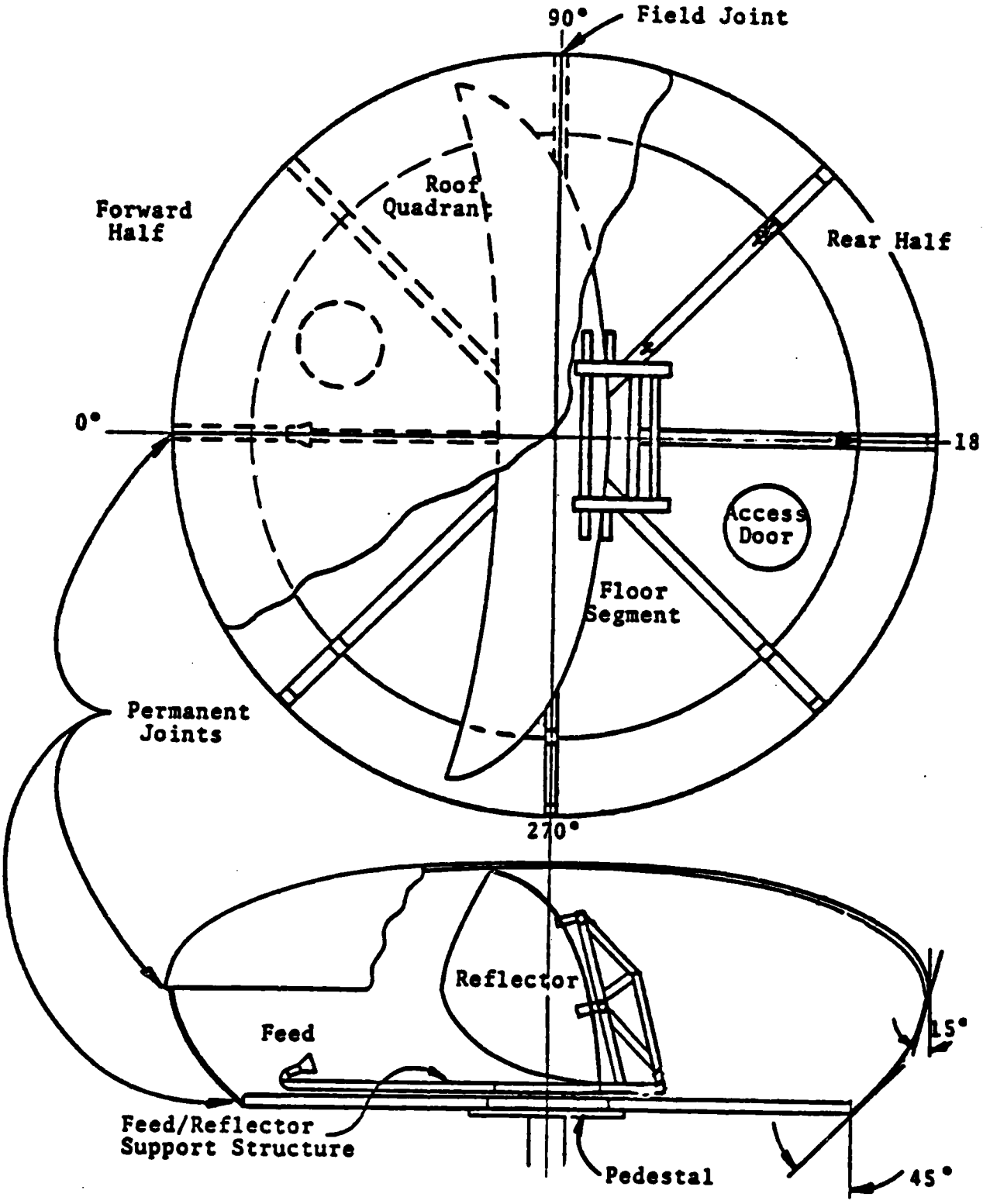

FIGURE I ROTODOME CONFIGURATION

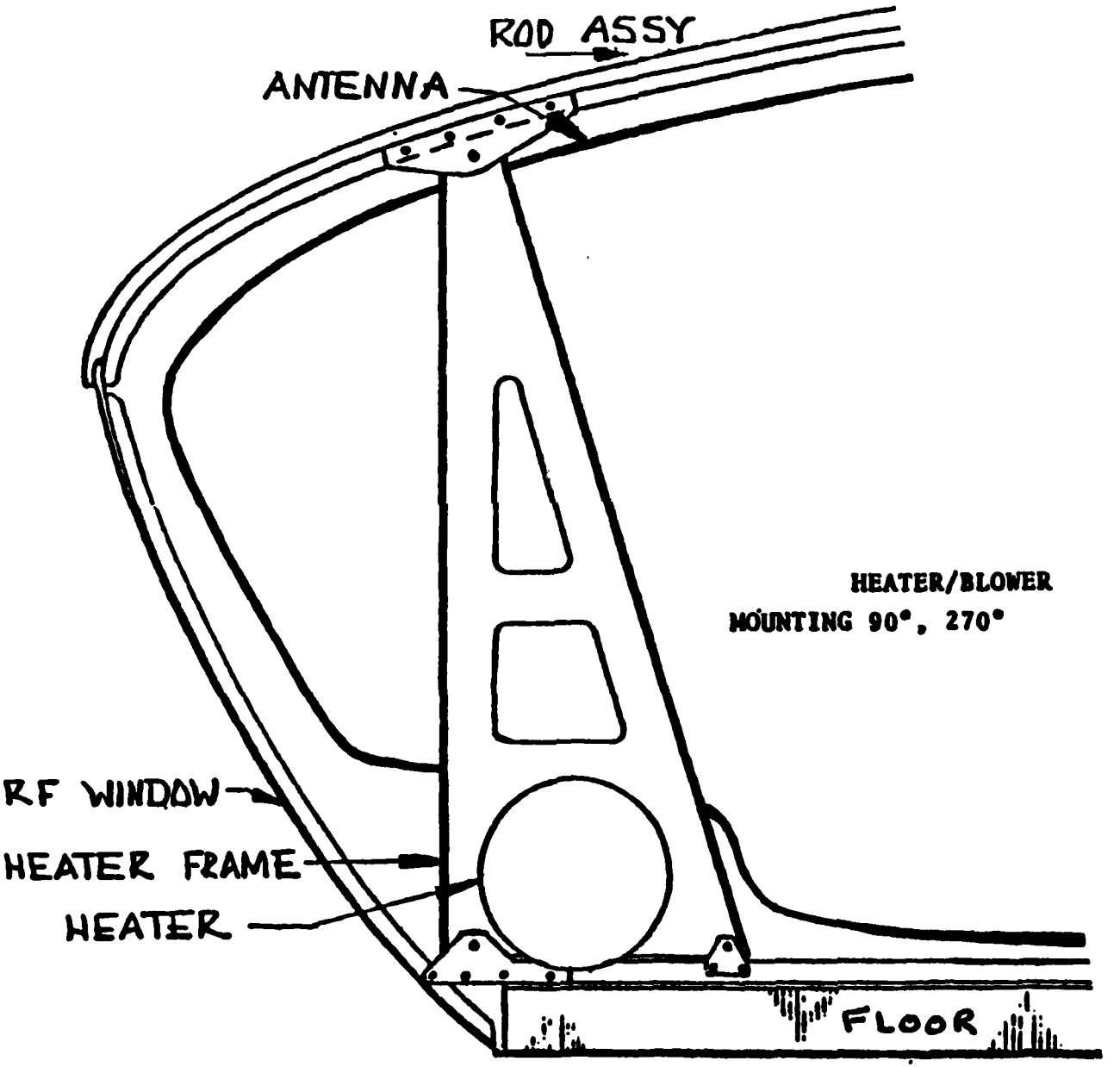
ROD ASSY
ANTENNA
HEATER/BLOWER
MOUNTING 90°, 270°
RF WINDOW
HEATER FRAME
HEATER
FLOOR

FIGURE 2.

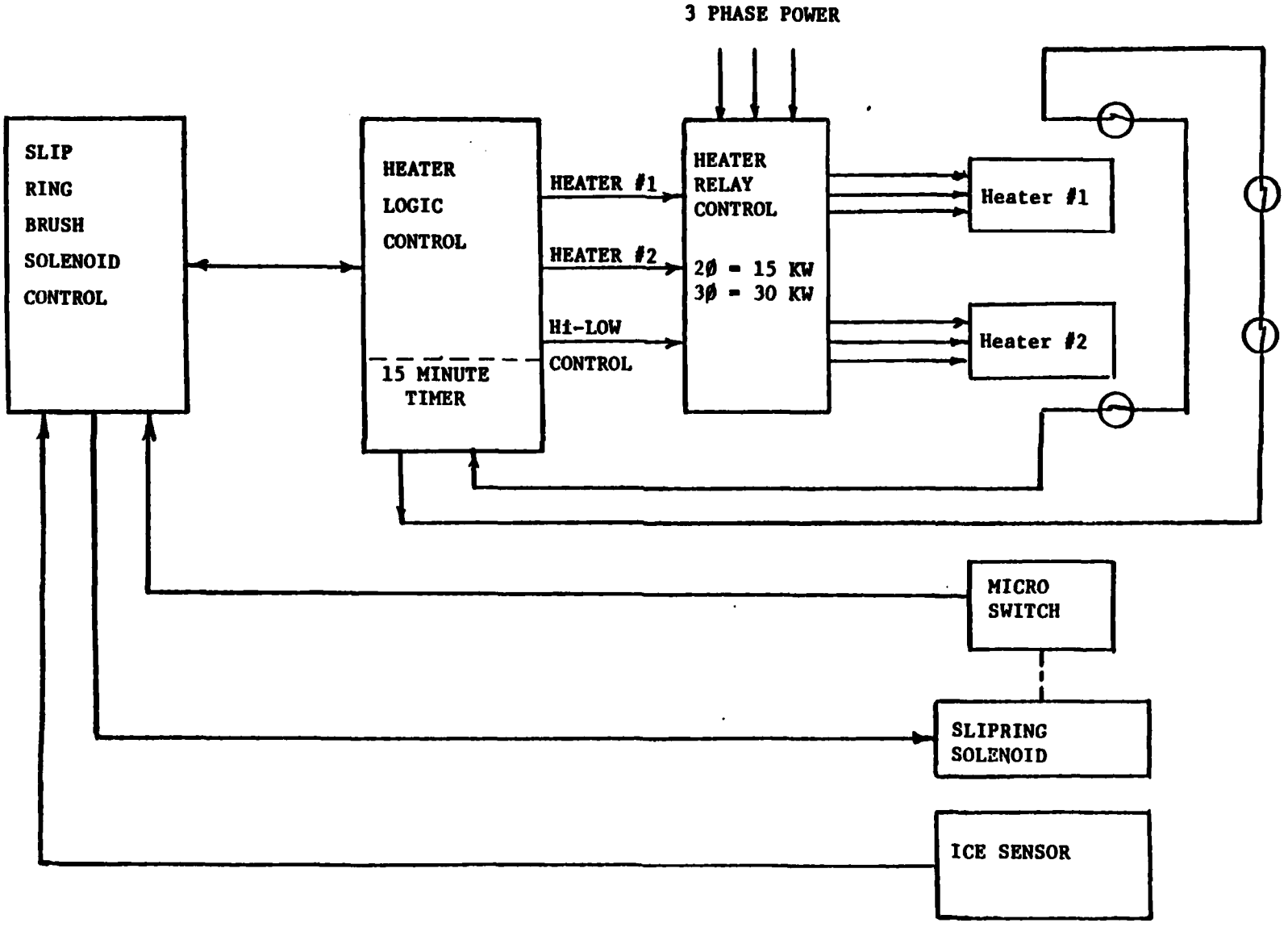

FIGURE 3. HEATER CONTROL BLOCK DIAGRAM

APPENDIX J

TEST REPORT #1 OF THE ORIGINAL ASDE-3 ROTODOME

APPENDIX J

CHRONOLOGICAL HISTORY OF PRELIMINARY ASDE-3 THERMAL TESTS MADE AT SAN DIEGO, CALIFORNIA, January 10, 1979

Outside Temperature = 60°F

Window (in sunlight) in front of heater at AZ* = 135°
1 ft from bottom, Temp. = 90°F
(at heater exhaust port)

Window (in shade) in between heaters at AZ = 180° 6" from top temp. = 79.5°F

Heaters just shut off	4:18 p.m.
	4:23 p.m. = 75°F
	4:24 p.m. = 72°F
Roof 9" above edge at 175° AZ	68°F
Floor 1" from edge at 175° AZ	65°F
	4:30 p.m.

Thermostat set @ 80°F (turns back on at 79°F)

Air temp. outside = 58°F

Thermostat physically 6-8" off bottom by rear door (suspended)

4:45 p.m. 56°F outside

Roof temp. 175°F, 5" up from edge	59°F
Heaters on @	4:47 p.m.

(Off 29 min with (1) door open)

Thermostat now @ mid-height of radome last 5 min.

*Azimuth location on rotodome as viewed from top. Plus is clockwise from boresight.

AT	4:50 p.m. roof (same spot)	66°F
	4:52 p.m. roof (same spot)	72°F
Cut off	4:53 p.m. roof (same spot)	75°F
	4:54 p.m. window 175°F AZ	77°F
	4:55 p.m. floor 175° AZ 1' from edge	70°F
	4:56 p.m. floor 175° AZ 2' from edge	64°F
	4:57 p.m. floor 175° AZ 3' from edge	64°F
	4:57 p.m. floor 175° AZ 4' from edge	64°F
	4:58 p.m. window 175°F from top	67°F
	5:00 p.m. window half way up	66°F
	5:01 p.m. window 4" from bottom	64°F
	--No wind--	
Cut on	5:04 p.m. from bottom	64°F
	window 4" from top	64°F
	roof	64°F
	floor	62°F
	Ambient 56°F	
	5:08 p.m. window 175° AZ 6" from top	65°F
Cut off	5:08-1/2 p.m. window 175° AZ 6" from top	68°F
	5:08:40 p.m. window 175°F AZ 6" from top	70°F
	roof 175° 6" from edge	71°F
	5:09 p.m. floor 175°F 1' from edge	64°F
	5:10 p.m. floor 175°F	63°F
	5:13 p.m. window 175° 4" from top	70°F
	5:15 p.m. ambient	55°F
	5:18 p.m. window 4" from top	68°F
Cut on	5:19 p.m. window 4" from top	65°F
	5:20 p.m. window 4" from top	67°F
	5:21 p.m. window 4" from top 175° AZ	65°F
	5:22 p.m. window 4" from top 175° AZ	70°F
	5:22-1/2 p.m. window 4" from top 175° AZ	71°F
	55° Ambient	

	5:23 p.m. window 4" from top 175°F	71.5°F
Cut off	5:23-1/2 p.m. window	72°F
	5:25 p.m. window 185° AZ 4" top	68°F
	5:25 p.m. window 225° AZ 4" top	67°F
	260° AZ 4" half way	65°F
	5:27 p.m. window 260°F half way	67°F

Rated Heater V = 208

Actual Heater V = 180

COMMENTS ON DATA

1. The Leeds and Northrop Mod 8693 temperature potentiometer was difficult to read in less than 1° increments.
2. The ambient temperature may have been dropping exponentially as the sun was setting.
3. The roof and window behaved very much alike.
4. The floor was a fairly constant temperature along its 180° azimuth radius from $\underline{\mathcal{C}}$ to edge.
5. The floor did not fluctuate as greatly as the other parts, perhaps due to the volume of air trapped in its cells.
6. The first bounce on the Robert-Shaw thermostat seemed quite high both days, probably due to the necessity of warming up its housing. Subsequent bounces became less.

HEAT LOSS CALCULATION

$$\text{Duty Cycle} = \frac{4.5 \text{ min on}}{4.5 + 10.5 \text{ min off}}$$

$$= 30\%$$

$$30 \text{ kW Heaters} \times \frac{180}{208} \text{ (I x R drop)} = 26 \text{ kW}$$

$$.3 \times 26 \text{ kW} = 7.8 \text{ kW hours/hours}$$

$$\text{Average inside temp} = \frac{83^\circ + 79^\circ}{2} = 81^\circ F$$

$$\text{Average outside temp. (from 4:53 p.m. to 5:22 p.m.)} = \frac{57^\circ + 55^\circ}{2} = 56^\circ F$$

Average $\Delta T = 81^\circ - 56^\circ = 25^\circ F$

This is for a "No-Wind" condition

For 100% Duty Cycle:

$$\frac{100}{30} \times 25^\circ F = 83.3^\circ F \text{ (if linear)}$$

$$Q = h A \Delta T$$

However, radiant heat loss in this case was not to a black sky, but towards the ground and the sunset.

The ΔT (lowest value) between window and roof versus ambient was $64 - 56 = 8^\circ F$.

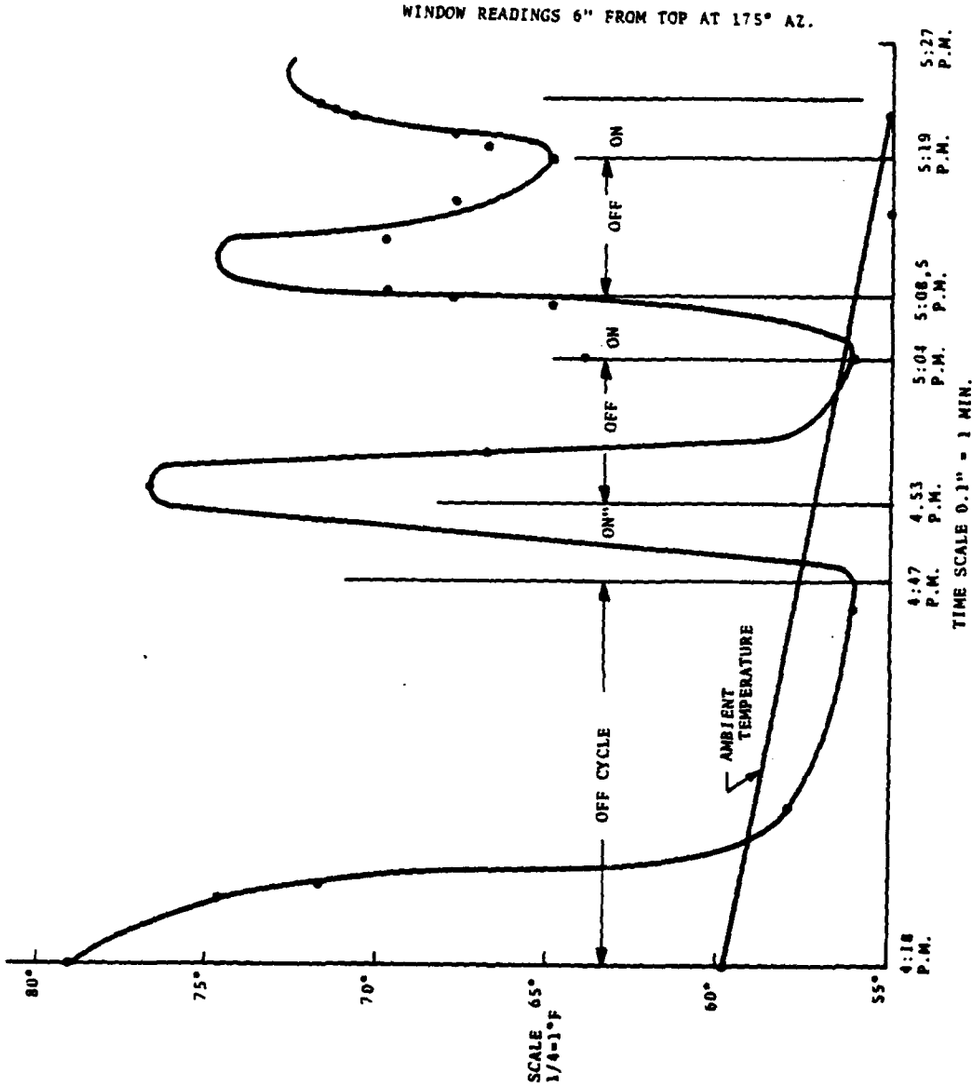

FIGURE G-1. PRELIMINARY TEMPERATURE TESTS

FOR A 100% DUTY CYCLE

The window/ambient temperature could be:

$$\frac{100}{30} \times 8 = 26°F$$

To maintain the radome at 33°F outside skin temperature with no ice and no wind and no insulation on the floor, then the static (non-rotating) ambient temperature could be:

$$33°F - 26°F = 7°F$$

This is a cursory calculation which does not take into account:

1) Density of moisture in atmosphere
2) Water droplet size
3) Barometric pressure
4) Night sky
5) Wind or rotation effects
6) Correct orientation of radome

APPENDIX K

REPORT ON NEW TECHNOLOGY

APPENDIX K

REPORT ON NEW TECHNOLOGY

The work accomplished under this contract as reported herein provides data that could be used to establish the heat required to prevent icing on a spheri-elipsoidal radome. This report contains data on the engineering model ASDE-3 radome, and it represents the only data of its kind.

APPENDIX L

DEFINITION OF TERMS AND SYMBOLS

Terms

Coefficient of Scope:	Percent of Frontal area presented to the wind covered by ice.
Outages:	The period of time during which a radar is non-operational due to ice or snow on the radome covering it.
R-F:	Radio Frequency, i.e., microwave signal energy.
Rate of Catch:	The amount of water impinging upon an object in lbs/hours.
Rotodome:	A rotating radome, in this instance the ASDE-3 Radome.
TACAN:	Tactical Air Navigation Aid.
VOR:	Very High Frequency Omnirange Facility or Antenna.
VORTAC:	Very High Frequency Omnirange/TACAN.

Symbols

a = radius of a water droplet

C_f = drag coefficient (skin friction)

C = a significant dimension in the flow field

D = diameter

E_m = fractional catch of incipient moisture

g = acceleration of gravity

h = unit surface conductance

HP = horse power

k = R_u/ψ

K = coefficient of heat transfer

K.e. = kinetic energy

Symbols (cont.)

kw = Kilo watt

L = length of path

M = mass

m = meter

N_{PR} = Prandtl Number

N_{NUL} = Nusselt Number

$q = 1/2\rho V^2$

Q = heat energy

R = radius

R_u = Reynolds Modulus = $\frac{2a\rho aV}{ua}$

R_e = Reynolds Number = $\frac{DV}{\nu}$

T = temperature

S = surface area

T = time

V_s = volume sphere

V = velocity

W = capture rate (lbs/sec)

w = watt

w = liquid water content air

x = distance

Greek Symbols

α = acceleration

ψ = $qC_{\rho}a/a_{\rho_d}$ a scale factor

ϕ = $R_u \times \psi$

μa = air viscosity

ρ_a = density air

ρ_d = droplet density

ω = rotation rate radians/sec

λ = heat of evaporation

ν = dynamic viscosity Ft^2/sec

Miscellaneous Symbols

$\int$ = integral

Σ = sum

$\sqrt{}$ = square root

$>$ = greater than

$<$ = less then

∞ = infinite

$!$ = factorial

lim = limit

n = 1,2,3

APPENDIX M

BIBLIOGRAPHY

1. Books

ASHRAE Handbook of Fundamentals, American Society of Heating, Refrigerating and Air Conditioning Engineers, 1972.

ASHRAE Handbook of Product Directory Systems, American Society of Heating, Refrigerating and Air Conditioning Engineers, 1976

Handbook of Tables for Applied Engineering Science, The Chemical Rubber Co., 1970.

Cornwall, K. The Flow of Heat, Van Nostrand Reinhold, N.Y., 1977.

Eshbach, Handbook of Engineering Fundamentals, Wiley, Publ., N.Y. 1975.

Faires, Thermodynamics, McGraw Hill, N.Y. 1957.

Hoerner, Fluid Dynamic Drag, Hoerner Press, 1969.

Rohsenow, Warren M. and Hartnett, James P., Handbook of Heat Transfer

Rothbart, Mechanical Design and Systems Handbook, McGraw Hill, N.Y., 1964.

2. Govt. Publications

AD-777-947 An Evaluation of Passive De-Icing Mechanical De-Icing and Ice Detection. FAA 1973.

FAA-RD-76-130 Postel, H. Test & Evaluation of 6 Wire-Wound Tactical Air Navigation Aid (TACAN) Heated Radomes With Weather Sensors. Aug. 1976.

FSTC-HT-23-486-69 Calculation of Glaze Wind Loads Upon High Installations Country USSR, Technical Translation

SF 013-99-02, Task 0519 Ice Adhesion and a De-Icing Coating Naval Applied Science Laboratory, N.Y. 1969

Lewis and Hocker, Observations of Icing Conditions During Flight, NACA TN 1904.

MIL-STD-210, Environmental Data, 15 Dec. '73.

NACA, Recommended Values of Meterological Factors for Consideration in the Design of Aircraft Ice Prevention Equipment.

Report No. FAA-RD-71-56 Minimize Snow & Weather Effects-Vortak Task II TACAN Antenna Sept. 1977 D.O.T.

TL 422 Korzhavin, K.N. Influence of Ice Upon Construction, and Methods of Combating Ice Problems Translated from Russian Oct. 74.

WADC Technical Note 55-520, Icing Intensity Data for the 1954-55 Season October 1955.

3. Papers

Ambrosio, Alfonso, Statistical Analysis of Meterological Icing Conditions, UCLA Engineering Dept., 1950.

California Institute of Technology, Wind Tunnel Report, No. 997.

Chapman-Rubesin, Heat Transfer from a Flat Plate in Laminar Flow.

Fein, N.A. Survey of the Literature on Shipboard Ice Formation Naval Engineers Journal Dec. 1965.

Tabata, Tadashi Research on Prevention of Ship Icing Defense Research Board, Canada July 1968.

Teledyne Micronetics, Wind Tunnel Report. No. R17-77.

Tribus, Myron, Modern Icing Technology Project M992-E Air Research and Development Command, USAF.

University of Michigan, Energy Transfer at an Icing Surface, Engineering Research Institute.

University of Michigan, Some Actual Test Runs of Icing/De-Icing Conditions in a Wind Tunnel, Engineering Research Institute.

Vitale, J.A., Climatic Tests of a Rigid Radome for Ground Systems Radome Symposium, Columbus, Ohio June 28, 1955.

150 copies


DATE
FILME
8